Gláucia Regina Medeiros

IMPREGNAÇÃO DE ÓLEO ESSENCIAL DE CRAVO DA ÍNDIA (*Eugenia caryophyllus*) EM FILMES DE POLIETILENO LINEAR DE BAIXA DENSIDADE UTILIZANDO DIÓXIDO DE CARBONO EM ALTAS PRESSÕES

Tese submetida ao Programa de Pós-Graduação em Engenharia de Alimentos da Universidade Federal de Santa Catarina para a obtenção do título de Doutor em Engenharia de Alimentos.

Orientador: Prof. Dr. Bruno Augusto Mattar Carciofi
Coorientadora: Prof.ª Dr.ª Sandra Regina Salvador Ferreira

Florianópolis
2017

Ficha de identificação da obra elaborada pelo autor,
através do Programa de Geração Automática da Biblioteca Universitária da UFSC.

Medeiros, Glaucia Regina
Impregnação de óleo essencial de cravo da Índia (Eugenia caryophyllus) em filmes de polietileno linear de baixa densidade utilizando dióxido de carbono em altas pressões / Glaucia Regina Medeiros ; orientador, Bruno Augusto Mattar Carciofi, coorientadora, Sandra Regina Salvador Ferreira, 2017.
173 p.

Tese (doutorado) - Universidade Federal de Santa Catarina, Centro Tecnológico, Programa de Pós Graduação em Engenharia de Alimentos, Florianópolis, 2017.

Inclui referências.

1. Engenharia de Alimentos. 2. Embalagem ativa. 3. Fluido supercrítico. 4. Propriedades termomecânicas. 5. Coeficiente de difusão efetivo. I. Carciofi, Bruno Augusto Mattar. II. Ferreira, Sandra Regina Salvador. III. Universidade Federal de Santa Catarina. Programa de Pós-Graduação em Engenharia de Alimentos. IV. Título.

Gláucia Regina Medeiros

IMPREGNAÇÃO DE ÓLEO ESSENCIAL DE CRAVO DA ÍNDIA (*Eugenia caryophyllus*) EM FILMES DE POLIETILENO LINEAR DE BAIXA DENSIDADE UTILIZANDO DIÓXIDO DE CARBONO EM ALTAS PRESSÕES

Esta tese foi julgada adequada para obtenção do Título de Doutor em Engenharia de Alimentos e aprovada em sua forma final pelo Programa de Pós-Graduação em Engenharia de Alimentos.

Florianópolis, 27 de novembro de 2017.

_____
Prof. Dr. Bruno Augusto Mattar Carciofi
Coordenador do Curso

Banca Examinadora:

_____
Prof. Dr. Bruno Augusto Mattar Carciofi
Orientador

_____
Prof.ª Dr.ª Mathilde Julienne Gisèle Champeau Ferreira
Universidade Federal do ABC

_____
Prof. Dr. Guilherme Mariz de Oliveira Barra
Departamento de Engenharia Mecânica, UFSC

_____
Prof.ª Dr.ª Cláudia Sayer
Programa de Pós-Graduação em Engenharia Química, UFSC

_____
Prof. Dr. João Borges Laurindo
Programa de Pós-Graduação em Engenharia de Alimentos, UFSC

Dedico este trabalho à minha mãe,
Elenira.

AGRADECIMENTOS

Aos meus orientadores, professor Bruno Carciofi e professora Sandra Ferreira, pela dedicação, amizade e orientação. Obrigada pela confiança e incentivo durante a realização deste trabalho.

Aos professores membros das bancas de qualificação, Pedro Henrique de Araújo, Guilherme Barra e João Borges Laurindo, e de defesa, Mathilde Champeau Ferreira, Guilherme Barra e Cláudia Sayer, pela disponibilidade e contribuições para a tese.

Ao Programa de Pós-Graduação em Engenharia de Alimentos (PGEAL) da Universidade Federal de Santa Catarina (UFSC), pela oportunidade e viabilização deste trabalho. Aos professores do PGEAL pela convivência e ensinamentos repassados. À CAPES pelo apoio financeiro.

À minha mãe, Elenira, e ao Mauro, pela educação, carinho e apoio em cada etapa da minha caminhada. À Andressa e ao Ayslans pelo grande incentivo. Aos meus familiares, em especial aos meus avós Helena, Pedro e Clara.

Ao Eduardo, pelo companheirismo, compreensão e carinho.

Ao Laboratório de Propriedades Físicas de Alimentos (PROFI) e Laboratório de Termodinâmica e Tecnologia Supercrítica (LATESC) pelo acolhimento e viabilização dos estudos. À Carolina Guimarães pela dedicação nos trabalhos e ensaios. Aos demais laboratórios e funcionários da UFSC pela disponibilidade e suporte técnico, em especial ao Leandro Guarezi e ao Américo Cruz.

Ao professor Edmar Clemente (*in memoriam*) da Universidade Estadual de Maringá (UEM) pelas primeiras indicações no caminho da pesquisa.

Aos grandes amigos Camila, Eto, Jaque, Jhony, Kátia, Sara e Simone pela amizade, conselhos e bons momentos partilhados. À Manu e ao Iaça pela agradável convivência na etapa final do trabalho. Aos amigos feitos durante o mestrado e doutorado, em especial Denise, Gean, Gustavo, Jade, Juca, Leidi, Leno e Ricardo. Aos amigos da graduação e aos que permanecem sempre presentes, especialmente Jéssica, Karina, Murilo, Flávia e Thaila.

À Deus pela vida e coragem para seguir em frente.

A todos que de alguma forma contribuíram para a realização deste trabalho.

A vida é como andar de bicicleta.
É preciso se manter em movimento para não perder o equilíbrio.

Albert Einstein

RESUMO

Embalagens ativas para alimentos contribuem para a conservação dos alimentos, além de proporcionarem uma barreira inerte às condições externas, prolongando a vida de prateleira e a qualidade dos produtos embalados. A impregnação assistida por dióxido de carbono (CO_2) em altas pressões é uma tecnologia inovadora para incorporar agentes ativos em materiais poliméricos. Sua principal vantagem é a operação em temperaturas baixas, permitindo o processamento de compostos termossensíveis. Agentes ativos naturais, como os óleos essenciais, apresentam reconhecida atividade antimicrobiana e antioxidante, além de serem classificados como compostos de baixo risco à saúde. Desta forma, o óleo essencial de cravo da Índia (OEC) (*Eugenia caryophyllus*), um agente ativo multicomponente naturalmente rico em eugenol, foi incorporado em filmes de polietileno linear de baixa densidade (PELBD) por meio da impregnação assistida por CO_2 em alta pressão. Os parâmetros operacionais de temperatura, pressão, fração mássica OEC:CO_2, tempo e taxa de despressurização foram avaliados em uma célula de alta pressão com volume variável. A impregnação do OEC em filmes de PELBD foi mais eficiente com o aumento da fração mássica OEC:CO_2 e da temperatura, mas com a redução da pressão e da taxa de despressurização. A quantidade máxima de OEC foi impregnada em 2 horas de processamento. Os filmes processados com CO_2 puro em alta pressão mantiveram suas propriedades térmicas e mecânicas. A incorporação do OEC aumentou a mobilidade das cadeias poliméricas, reduzindo a resistência à tração dos filmes. Filmes impregnados na máxima taxa de despressurização foram mais suscetíveis às variações na topografia da superfície e na morfologia. A migração do OEC em fluidos simuladores de alimentos aquosos e oleosos foi governada pela transferência de massa por difusão. O coeficiente de difusão efetivo do OEC no PELBD variou de $5{,}4 \times 10^{-13}$ a $1{,}0 \times 10^{-12}$ $m^2\ s^{-1}$. Os parâmetros operacionais podem ser ajustados para aumentar a incorporação do OEC, mas apresentam efeito desprezível na difusividade do OEC no PELBD e nas propriedades termomecânicas dos filmes. A impregnação assistida por CO_2-SC é uma tecnologia alternativa e inovadora para os processos convencionais de incorporação de compostos ativos em matrizes poliméricas. Os filmes de PELBD impregnados com OEC apresentam potencial aplicação para embalagens ativas para alimentos.

Palavras-chave: embalagem ativa, fluido supercrítico, eugenol, propriedades termomecânicas, coeficiente de difusão efetivo.

ABSTRACT

Active food packaging contributes to food preservation, besides providing an inert barrier to external conditions, extending shelf life and quality of packaged products. High-pressure carbon dioxide (CO_2) impregnation is an innovative technology to incorporate active agents in polymer materials. Its major advantage rely on the operation under low temperature, which allows the processing of thermosensitive compounds. Natural active agents, as the essential oils, are compounds with recognized antimicrobial and antioxidant activities, besides being categorized as compounds of low healthy risk. In this regard, clove essential oil (CEO) (*Eugenia caryophyllus*), a multicomponent active agent naturally rich in eugenol, was incorporated in linear low density polyethylene (LLDPE) films by means of high-pressure CO_2 impregnation. The operational parameters of temperature, pressure, CEO:CO_2 mass ratio, time and depressurization rate were screened in a variable-volume high-pressure cell. The CEO impregnation in LLDPE films was more efficient with increasing CEO:CO_2 mass ratio and temperature while reducing pressure and depressurization rate. The highest amount of CEO was impregnated at 2 hours of processing. Sample processed with pure CO_2 under high-pressure maintained the thermal and mechanical properties of films. The CEO incorporation increased the polymer chain mobility, reducing the tensile strength of films. Films impregnated at the maximum depressurization rate were more susceptible to variations in surface topography and morphology. The CEO migration in aqueous and fatty food simulants was governed by diffusive mass transfer. The effective diffusion coefficient of CEO in LLDPE ranged from 5.4×10^{-13} to 1.0×10^{-12} m^2 s^{-1}. Operational parameters can be adjusted to enhance CEO incorporation, presenting negligible effect over CEO diffusivity in LLDPE and thermomechanical properties of films. The SC-CO_2 impregnation is an alternative and innovative technology to the traditional process of incorporating active compounds in polymer matrices. The CEO-impregnated LLDPE films have a potential application as active food packaging.

Keywords: active packaging, supercritical fluid, eugenol, thermomechanical properties, effective diffusion coefficient.

LIST OF FIGURES

LIST OF TABLES

LIST OF ABBREVIATIONS AND NOMENCLATURE

ANOVA	Analysis of variance
ANVISA	Agência Nacional de Vigilância Sanitária
ASTM	American Society for Testing and Materials
ATR	Attenuated total reflectance
BHA	Butylated hydroxyanisole
BHT	Butylated hydroxytoluene
BV	Ball valve
CEO	Clove essential oil
CO_2	Carbon dioxide
CV	Check valve
DMA	Dynamic mechanical analysis
DPPH	2,2-diphenyl-1-picrylhydracyl
DR	Depressurization rate
DSC	Differential scanning calorimetry
EFSA	European Food Safety Authority
EO	Essential oil
EVA	Ethylene vinyl acetate
FAO	Food and Agriculture Organization
FDA	Food and Drug Administration
FID	Flame ionization detector
FPA	Flexible Packaging Association
FTIR	Fourier transform infrared
G	Gas
GC	Gas chromatography
GRAS	Generally recognized as safe
HDPE	High density polyethylene
HPLC	High performance liquid chromatography
L	Liquid
LDPE	Low density polyethylene
LLDPE	Linear low density polyethylene
MAP	Modified atmosphere packages
MFI	Melt flow index
MS	Mass spectrophotometer
MW	Molecular weight
NIST	National Institute of Standards and Technology
NV	Needle valve
PE	Polyethylene
PET	Polyethylene terephthalate
PL	Pressurized liquid

PLA	Poly(lactic acid)
PP	Polypropylene
PPPO	Poly(2,6-diphenyl-p-phenylene oxide)
PVA	Polyvinyl alcohol
PVC	Polyvinyl chloride
RMSE	Root mean square error
RT	Retention time
S	Solid
SC-CO_2	Supercritical carbon dioxide
SCF	Supercritical fluid
SEM	Scanning electron microscopy
SML	Specific migration limit
UHMWPE	Ultra high molecular weight polyethylene
ULDPE	Ultra low density polyethylene
UV	Ultraviolet
V	Vapor
VL	Vapor-liquid
VLL	Vapor-liquid-liquid
WHO	World Health Organization

LIST OF SYMBOLS

A_{600}	Absorbance at 600 nm	[-]
D	Diffusion coefficient	[m^2 s^{-1}]
D_{AB}	Binary diffusion coefficient	[m^2 s^{-1}]
E	Elastic or Young's modulus	[MPa]
E'	Storage modulus	[MPa]
E''	Loss modulus	[MPa]
j	One-dimensional flux	[kg m^{-2} s^{-1}]
L	Half thickness of film	[m]
l	Film thickness	[mm]
M_t	Cumulative mass of CEO migrated at time t	[g]
M_∞	Mass of CEO migrated at infinite time	[g]
$m_{CEO,i}$	Initial mass of CEO	[g]
$m_{F,i}$	Initial mass of film	[g]
$m_{F,imp}$	Mass of impregnated film	[g]
P	Pressure	[bar]
P_C	Critical pressure	[bar]
$P_{C,i}$	Critical pressure of pure component	[bar]
P_{Cm}	Pseudocritical pressure of the mixture	[bar]
R_a	Average roughness	[µm]
R^2	Coefficient of determination	[-]
T	Temperature	[°C]
T_C	Critical temperature	[°C]
$T_{C,i}$	Critical temperature of pure component	[°C]
T_{Cm}	Pseudocritical temperature of the mixture	[°C]
T_g	Glass transition temperature	[°C]
T_m	Melting temperature	[°C]
t	Time	[s]
$\tan\delta$	Damping factor	[-]
x	Cartesian coordinate	[m]
x_i	Mole fraction of pure component	[-]
ΔH_m	Experimental enthalpy of fusion	[J g^{-1}]
ΔH_m^0	Theoretical enthalpy of fusion	[J g^{-1}]
W	Mass fraction	[-]
ε	Dielectric constant	[-]
ε_b	Elongation at break	[%]
ρ	Mass concentration	[kg m^{-3}]
ρ_i	Initial mass concentration	[kg m^{-3}]

ρ_s	Mass concentration at surface	[kg m^{-3}]
$\bar{\rho}$	Average mass concentration	[kg m^{-3}]
τ_b	Tensile strength at break	[MPa]
χ	Crystallinity degree	[%]

TABLE OF CONTENTS

Chapter 1: Introduction

This introduction chapter presents a conceptual diagram to facilitate the comprehension of the experimental steps and motivation of this study. Also, it brings the background, general and specific objectives, and thesis structure.

1.1 Conceptual diagram

What?

It has been evaluated the use of near-critical and supercritical carbon dioxide as an alternative to produce a polyethylene films impregnated with clove essential oil, naturally rich in antimicrobial and antioxidant compounds, aiming the development of an active food packaging.

Why?

- The increasing demand for safer products boosted the interest in finding innovative solutions to the traditional chemical compounds added to preserve foods as well as new packaging systems;
- Food packages containing active agents in the polymer structure can prevent or reduce food spoilage when in contact with food surface, where deterioration mechanisms generally start;
- Clove essential oil, a naturally-derived active agent, is highly available with strong and recognized biological activities, but it can be degraded at high processing temperatures;
- Linear low density polyethylene is widely used in food industry for packaging applications;
- Main drawbacks of conventional incorporation of active agents in polymer matrices are related to the use of high temperatures that degrade thermosensitive compounds and/or use organic solvents that may remain as residues in polymer films;
- One example of low-temperature and solvent-free technique is the impregnation assisted by carbon dioxide at high-pressures that overcomes most problems related to the use of conventional techniques.

State of the art:

- Food safety remains a public health issue. The successful control of foodborne pathogens requires the use of multiple preservation techniques in manufacture and storage of food products;
- Brazil is one of the largest agricultural producers. The development of new processes and materials will contribute to the

competitiveness of national industry. They aggregate value to food products, also reducing environmental and economic impacts caused by food waste; • Natural active agents are perceived by consumers as compounds with low healthy risk; • Few studies report the incorporation of bioactive agents in polymer films by means of near-critical and supercritical carbon dioxide targeting food packaging applications.
Hypotheses: • It is possible to incorporate clove essential oil in polymer films at relative low temperature using near-critical and supercritical carbon dioxide; • The incorporation of clove essential oil by means of supercritical carbon dioxide does not modify the polymer structure and its properties in a way to make it an unfeasible packaging material; • Once incorporated, clove essential oil can migrate to food.
Which steps? • Production of polymer films; • Impregnation of clove essential oil in films using carbon dioxide at relative high pressure and low temperature; • Quantification of impregnated clove essential oil; • Characterization of polymeric films; • Evaluation of clove essential oil migration from polymer films to food simulant fluids; • Mathematical modeling of migration data.
Expected results: • To understand the influence of processing parameters on clove essential oil incorporation, migration kinetics and final properties of polymer films; • To comprehend the phenomenology involved in mass transfer processes and mechanisms of thermodynamic equilibrium between phases; • To contribute to the development of active packages considering a potential application in food and chemical areas.

1.2 Background

Plastic packages are useful and possess several applications in different segments of industry. In food industry, they facilitate the handling of products, transmit information, and, as a main purpose, they

contain and protect foodstuff. It is well-known that food products are perishable and their quality must be maintained during the entire storage period.

Microbial growth and lipid oxidation are main factors that cause food spoilage. Antimicrobial and antioxidant agents are commonly added to foods to control microbial multiplication, slow oxidative processes and extend shelf life. Food spoilage generally starts on food surface and active agents directly mixed with foods may result in excessive use (WENG; HOTCHKISS, 1993). Thus, the development of packaging films containing active agents is an alternative to overcome problems related with direct application of active agents in foods. These films are incorporated of the active agent and promote a slow and constant release onto food surface, where they are most effective (SUPPAKUL et al., 2011).

The principle of incorporating an active agent into a polymer matrix is related to the concept of active packages. These materials have the potential to interact with the contained product, preventing or reducing their deterioration. Additionally, they confer a selective barrier to moisture and gases, scavenge or emit carbon dioxide (CO_2) and ethylene, besides promoting the release of active compounds with antimicrobial and antioxidant activities (APPENDINI; HOTCHKISS, 2002; GÓMEZ-ESTACA et al., 2014).

Several manufacturing processes have been developed to incorporate active agents in packaging films, such as solvent casting, surface coating, thermocompression, extrusion and by immersion of films into a solution containing the active agent. However, these processes generally require the use of organic solvents, or a large amount of the impregnating solution, or else use high processing temperatures that degrade thermosensitive compounds (DÍEZ-MUNICIO et al., 2011). The impregnation of active agents in polymer films by means of near-critical and supercritical CO_2 (SC-CO_2) has been reported as an alternative to overcome these drawbacks. The relative very low critical temperature of the CO_2 coupled with its versatility as green solvent allows the impregnation of thermosensitive active agents with this technology, producing a final product free of solvent residues just by system depressurization (CHAMPEAU et al., 2015).

In supercritical conditions, the CO_2 shares the favorable properties of both liquid and gases. Supercritical CO_2 has higher diffusivity and lower viscosity than liquids and a solvent capacity stronger than gases. The low viscosity of this fluid combined with its high diffusivity results in high mass transfer rates (DOHRN; BRUNNER, 1995). The

impregnation process is feasible when the active compound is soluble in the supercritical fluid (SCF), the polymer is swollen by the supercritical solution and the partition coefficient is favorable enough to allow the matrix to be charged with enough amount of the active compound (KIKIC; VECCHIONE, 2003).

Active agents from natural sources, as the essential oils, are considered by consumers as compounds of low healthy risk. The clove essential oil (CEO) is one of the most promising naturally-derived active agents due to its strong and extensively reported biological activities (antibacterial, antifungal, antiviral, insecticidal, antioxidant, among others), besides its common use as flavoring agent in foodstuff products (CHAIEB et al., 2007).

Several polymer matrices can be employed in the manufacture of plastic films. Among them, polyethylene and its derivatives are preferable in food packaging applications because of their good mechanical and barrier properties, along with high availability with low cost of production (PEYCHÈS-BACH et al., 2009). Among others polyethylene-based polymers, the linear low density polyethylene (LLDPE) is a semicrystalline polymer broadly used in food industry, representing almost 30% of the total global consumption in food packaging segment (SIMANKE; DE LEMOS; PIRES, 2013).

Based on the above discussed points, the SC-CO_2 impregnation of multicomponent naturally-derived active agents, as the CEO, in polymer matrices, as the LLDPE, is an innovative application of the SCF technology targeting the production of active packaging films. This study seeks to contribute to the development of products and processes for active packaging application in food and chemical areas.

1.3 General objective

This study aims to impregnate CEO in LLDPE films by means of near-critical and supercritical CO_2, evaluating the effect of processing conditions on the impregnation amount, polymer film properties, and migration of CEO to food simulant fluids.

1.4 Specific objectives

a) To evaluate the influence of processing parameters (pressure, temperature, CEO:CO_2 mass ratio, time and depressurization rate) on the impregnated mass of CEO in LLDPE films;

b) To investigate the effect of processing conditions on thermal, mechanical, chemical, optical, morphological and topographic properties of samples;
c) To evaluate the migration kinetics of CEO from LLDPE films in food simulant fluids;
d) To identify the governing mass transfer mechanism in migration assays and to propose a mathematical model to describe the experimental data;
e) To determine the effective diffusion coefficient of CEO in LLDPE.

1.5 Thesis structure

Chapter 2 presents a review of relevant literature, covering current trends and opportunities in the development of active packaging systems with emphasis on the use of SC-CO_2 impregnation. It also describes the physical phenomena and regulations regarding the migration of compounds into food simulant fluids.

In Chapter 3, the CEO incorporation in LLDPE films by means of high-pressure CO_2 impregnation was experimentally studied. The effect of processing parameters (temperature, pressure, CEO:CO_2 mass ratio and time) on impregnation as well as on chemical, thermal and mechanical properties of processed films is discussed.

Chapter 4 discusses the influence of depressurization rate on impregnation and final properties of films, including optical, topographic, morphological and mechanical behavior. The CEO migration from LLDPE into food simulant fluids was also evaluated. A diffusion-based mathematical model was fitted to experimental data, thus giving valuable information on the mass transfer mechanism governing the active compound migration.

Chapter 5 includes conclusions and suggestions to contribute to further understanding and optimization of active packaging systems employing the SC-CO_2 technology.

A general discussion of results from this study, coupled with additional data not presented in Chapters 3 and 4 is included in Appendix A. In appendix B, the description of experimental apparatus and its operation for impregnation runs are presented. Appendix C includes the calibration curves used in the present work. The Annex provides the supplier technical information of CEO and LLDPE pellets.

Chapter 2: Literature review

This chapter addresses a brief literature review related to the polymer matrix used in this study, the employment of essential oils as natural active agents and the use of active food packages. It also describes the process of near-critical and supercritical CO_2 impregnation of active agents in polymer matrices and the reported thermodynamic equilibrium data for the systems LLDPE-CO_2 and CEO-CO_2. The current regulatory aspects concerning the use of food simulant fluids in migration tests and the mathematical approach used to describe experimental data of migration are also discussed.

2.1 Polymer matrices

Numerous polymer matrices are used in the manufacture of plastic packages, including films, trays, lids, pouches, bottles, etc. These materials reinforce metals for lining closures, glass to reduce container breakage and paper for moisture resistance. Multilayer polymer packaging is produced by combining two or more plastic films through co-extrusion, blending, lamination or coating to achieve desired features. Among them, barrier properties to gas, moisture, ultraviolet (UV) and visible light transmission are target features, besides flexibility, heat sealability and other mechanical properties to improve strength or performance characteristics (BHUNIA et al., 2013).

Several types of plastics are currently commercialized, but only few are employed in food packages. Polymers and copolymers obtained from olefins, specifically polyethylene (PE) and polypropylene (PP), are the most extensively used thermoplastic materials in packaging industry due to their good mechanical resistance, inert characteristic and high water vapor barrier properties (MIN; CHUAH; CHANTARA, 2008; PEYCHÈS-BACH et al., 2009). Other examples include ethylene vinyl acetate (EVA), polyethylene terephthalate (PET) and polyvinyl chloride (PVC) (JOERGER, 2007).

Polyethylene is a semicrystalline and flexible polymer which properties are influenced by the relative amount of amorphous and crystalline regions. It is a hydrocarbon derived from ethylene (C_2H_4) with long polymers chains, as schematized in Figure 2.1 (COUTINHO et al., 2003).

Figure 2.1. Representation of polyethylene chemical structure.

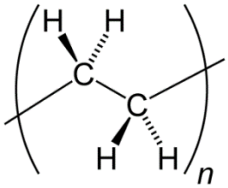

Source: Coutinho et al. (2003).

The manufacturing processes include addition polymerization, condensation polymerization or synthesis of copolymers employing metal catalysts, such as Ziegler-Natta or metallocene catalysts (BHUNIA et al., 2013). Polyethylene-based polymers can be classified according to their branched structure in low density polyethylene (LDPE), high density polyethylene (HDPE), linear low density polyethylene (LLDPE), as demonstrated in Figure 2.2 (COUTINHO et al., 2003).

Figure 2.2. Schematization of typical structures of LDPE, HDPE and LLPDE.

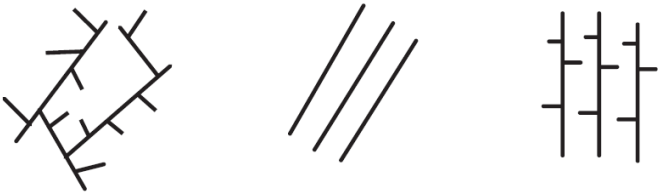

Source: Coutinho et al. (2003).

The advantage of using synthetic polymers in food packaging applications is related to their low cost along with good mechanical and barrier properties, transparency, processability, low energy demand for processing and facility to be printed on (MIN; CHUAH; CHANTARA, 2008; SUNG et al., 2013). Polyethylene and its derivatives are the most common and cheap synthetic polymers widely used as plastic material in food industry (PARK et al., 2012). The manufacturing process differs for each type of PE and influences the resulting physicochemical properties (MIN; CHUAH; CHANTARA, 2008).

Among the PEs, the LLDPE is a copolymer of ethylene with different α-olefins in polymer chain, such as propene, 1-butene, 1-hexene or 1-octene. It presents a molecular structure of linear polymer chains with shorter branches and it is more crystalline than the LDPE. These

branches greatly influence the physical properties, including the density, toughness and tensile strength. For example, the melting temperature (T_m) of LLDPE ranges from 120 to 130 °C while that of LDPE is approximately 110 °C (COUTINHO et al., 2003). The glass transition temperature (T_g) of LLDPE is reported to be around -110 °C (KHONAKDAR, 2015). The LLDPE represents around 30% of total plastic global consumption for food packages due to its good mechanical resistance, barrier properties, flexibility and transparency (SIMANKE; DE LEMOS; PIRES, 2013).

2.2 Natural active agents

The use of synthetic compounds to control food deterioration is becoming restricted due to a possible effect of carcinogenicity, residual toxicity and other secondary effects on foods and humans (ABBASZADEH et al., 2014). Consumers are stimulating the food industry to search for natural additives and special attention has been given to the study of products and processes with green and healthy label, namely the Generally Recognized As Safe (GRAS) status, regulated by the United States Food and Drug Administration (FDA) (IBÁÑEZ et al., 1999).

Essential oils are lipophilic, volatile, natural and complex compounds. They are extracted from aromatic plants by conventional methods with organic solvents, steam or hydro distillation, microwaves and supercritical extraction with carbon dioxide (CO_2). The extraction process uses different parts of plants, as flowers, buds, seeds, leaves, barks, fruits or roots (BURT, 2004; BAKKALI et al., 2008). They are secondary metabolites of plants and often possess biological properties attributed to the presence of several components with different biological activities, including antimicrobial and antioxidant ones (DONSÌ et al., 2014). Essential oil (EO) constituents are prone to oxidative damage, chemical transformations or polymerization reactions that come along with a quality loss after exposure to oxygen, light or high processing temperatures (TUREK; STINTZING, 2013).

The food industry traditionally uses EOs as flavorings, but these compounds are increasing the interest of industry as they represent an interesting natural source of active compounds with potential application for food preservation (HYLDGAARD; MYGIND; MEYER, 2012). Active agents from natural sources are perceived by consumers as compounds with low health risk, since most of them have the GRAS

status or are approved as food additives by several authorities (BURT, 2004; SUPPAKUL et al., 2011).

In many cases, EOs exert the biological effects better than the chemically-synthesized pure component due to a synergistic effect of the complex mixture of components that can interact with multiple active sites of a target organism (SEOW et al., 2014). A synergism occurs when the effect of combined substances is better than the sum of individual effects (BURT, 2004). Essential oils are composed of numerous molecules and their biological activity can be a result of a synergism between all molecules. The presence of several components also influences the fragrance, density, texture and color of EOs. The increased biological activity of EOs compared to the mixture of major individual components suggests that trace components are important to the final antimicrobial and antioxidant activities (BURT, 2004).

2.2.1 Clove essential oil

Clove belongs to the *Myrtaceae* family and is scientifically known as *Syzygium aromaticum* or by the synonyms *Eugenia caryophyllus* or *Eugenia caryophyllata*. It is known for its medicinal properties and uses in dental care as antiseptic and analgesic. Figure 2.3 presents the chemical structure of the main components found in clove essential oil (CEO): eugenol, eugenyl acetate, β-caryophyllene and α-humulene. It can also present other components to a lesser extent or as traces (CHAIEB et al., 2007).

Figure 2.3. Chemical structure of main components in clove essential oil.

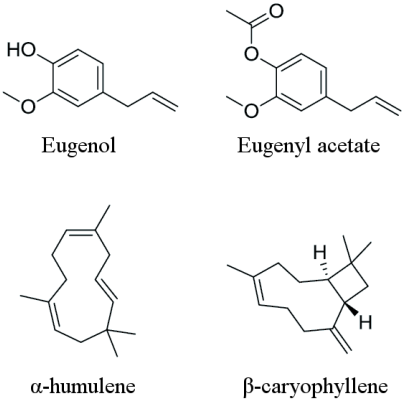

Source: Affonso et al. (2014).

The clove tree is commonly cultivated in coastal areas at maximum altitudes of 200 m above the sea level. The production of flower buds, the most frequent commercialized part of this tree, starts after four years of plantation. Flower buds are manually collected in maturation phase before flowering. Phytohormones can be employed to induce maturation due to ethylene release in the vegetable tissue. The largest producer countries are Indonesia, India, Malaysia, Sri Lanka, Madagascar and Tanzania. In Brazil, clove is cultivated in the northeast region, particularly in the state of Bahia (CORTÉS-ROJAS; DE SOUZA; OLIVEIRA, 2014).

The CEO can be obtained by extraction of clove buds or leaves using different extraction processes, as hydro and steam distillation as well as extractions with organic solvents or supercritical CO_2 (GUAN et al., 2007). The extraction and processing conditions should be conducted at temperatures below 50 °C to avoid thermal degradation of the main components (SEOW et al., 2014).

Eugenol is the major component of CEO and represents around 85-95% of total oil composition. The relative proportion of each component depends on raw material and extraction conditions (BURT, 2004). Clove essential oil possesses antibacterial, antifungal, antiviral, insecticidal and antioxidant properties. It has many therapeutic effects as anti-inflammatory, analgesic, antiseptic and anticarcinogenic. The high content of eugenol in CEO is believed to promote its strong biological activity (GUAN et al., 2007; IVANOVIC et al., 2013).

The mechanism of action of EOs is attributed to the hydrophobicity of the main components, especially terpenes, terpenoids and phenolic compounds (DONSÌ et al., 2014). The most sensitive microorganisms to CEO are yeasts and molds, followed by Gram-positive bacteria (LÓPEZ et al., 2007). Higher concentrations of CEO are required to inhibit Gram-negative bacteria (DEBIAGI et al., 2014), which can be correlated with the presence of an outer membrane in such type of microorganisms that may restrict the diffusion of CEO (HOSSEINI; RAZAVI; MOUSAVI, 2009). Eugenol accumulates in the lipid membrane of target microorganisms causing morphological deformation, protein denaturation and changes in membrane permeability. These mechanisms induce the transport of potassium and ATP out of cells (GUAN et al., 2007; AMIRI et al., 2008).

2.2.2 Eugenol

Eugenol ($C_{10}H_{12}O_2$) is a natural phenolic compound extracted from clove, cinnamon, basil or bay leaf EOs. It can be synthesized in laboratory and industrial scales by allylation of guaiacol with allyl chloride (RAJA et al., 2015). Eugenol is a clear, colorless or pale yellow liquid, depending on the raw material and extraction conditions. It is miscible with alcohol, chloroform, ether and vegetable oils, with a spicy and pungent taste (O'NEIL et al., 2006). The phenolic group in the aromatic ring (Figure 2.3) confers the antioxidant property to scavenge free radicals (RAJA et al., 2015). Some physical properties of eugenol are listed in Table 2.1.

Table 2.1. Physical properties of eugenol.

Physical property	Value	Reference
Molecular weight (g mol^{-1})	164.2	Souza et al. (2004)
Boiling point (°C)	225	O'Neil et al. (2006)
Melting point (°C)	-9.1	O'Neil et al. (2006)
Solubility in water at 21 °C (mg mL^{-1})	1.44	Wang et al. (2011)
Density at 20 °C (g mL^{-1})	1.06	Haynes (2010)
Vapor pressure at 25 °C (mbar)	0.0295	van Roon et al. (2005)
Thermal degradation temperature (°C)	50	Seow et al. (2014)

The Council of Europe and the joint Food and Agriculture Organization/World Health Organization (FAO/WHO) have included eugenol in the list of flavoring substances that can be added to foodstuffs without hazard to public health (OPDYKE, 1975). The acceptable daily intake is 5 mg of eugenol per kg of bodyweight, representing approximately 6 mg of CEO per kg of bodyweight. For a person with 60 kg, the acceptable daily intake is 360 mg of CEO. Eugenol is considered safe, non-carcinogenic and non-mutagenic compound by the FDA (21 CFR-PART 184, 2017). Studies reported that eugenol is eliminated and excreted as expired CO_2 and through urine in rabbit model (RAJA et al., 2015).

The positive list of substances authorized for food contacting materials as well as their specific migration limit (SML), expressed as mg of substance per kg of food, is regulated by several authorities in different countries. These authorities include the Agência Nacional de Vigilância Sanitária (ANVISA) in Brazil, the European Food Safety Authority (EFSA) in Europe and the FDA in the United States. Eugenol, as a food contacting material, does not have any restriction of usage in food packages. Its SML is not specified because it is stated as not detectable by the analytical method of measurement, considering the detection limit of the analytical method as 0.01 mg of substance per kg of food (EC, 2011; BRASIL, 2012; 21 CFR-PART 184, 2017).

2.3 Active food packaging

Food packaging is designed to protect food from external factors as temperature, light, humidity, odors, microorganisms, shocks, dust, vibration and compression forces that can cause degradation or loss of integrity. Active packaging is a kind of package that interacts with the contained product, preventing or reducing its deterioration, also communicating the consumer about the quality of packaged product by color changing (RIBEIRO-SANTOS et al., 2017b). The substances responsible for the active function in these packages may be in a separate container, as a sachet, or can be directly incorporated into the packaging material by techniques as surface coating and immobilization by ion, covalent or non-covalent bonds (APPENDINI; HOTCHKISS, 2002; PIRES et al., 2014). Active packaging aims to extend shelf life, maintain nutritional quality and improve food safety by reducing, inhibiting and/or retarding the microbial growth and lipid oxidation of packaged foods (SEOW et al., 2014).

These packages can be a selective barrier for moisture, also scavenging or emitting gases as oxygen, CO_2 and ethylene (LABUZA; BREENE, 1989; PARK et al., 2012). This concept also involves the incorporation and release of active agents, such as flavorings, antioxidant and antimicrobial compounds to the contained product (MUPPALLA et al., 2014). Several materials can be employed in active food packages, but the most common uses include polymers derived or not from renewable sources. The PE and PP are examples of non-renewable but recyclable materials, and polyesters, chitosan, starch and cellulose exemplifies potential biomaterials to be employed in packaging applications (PEELMAN et al., 2013; RIBEIRO-SANTOS et al., 2017b).

The required EO concentration in foods is usually high to compensate for the interaction with food components. The use of EOs in active food packages is a promising method to overcome the employment of high EO concentration. These packages provide a slow and controlled release of the active agent to the food surface or to the headspace for extended periods of time (HYLDGAARD; MYGIND; MEYER, 2012). The main drawback can be related to the sensory alteration of packaged foods due to the released aroma of EOs (LÓPEZ et al., 2007). However, depending on the application, the volatile characteristic of EOs avoid the necessity of direct contact with foods, which may minimize possible sensory changes. In addition, the released volatiles can be employed as flavors to improve sensory attractiveness of foods (SEOW et al., 2014).

Some examples of antimicrobial and antioxidant active food packages containing CEO or eugenol produced by different methods are shown in Table 2.2. These results reinforce that yeasts and molds followed by Gram-positive and Gram-negative bacteria are the most sensitive microorganisms to the action of CEO. Other published results not included in Table 2.2 also confirm this evidence regardless of the method used to produce the packaging films (HOSSEINI; RAZAVI; MOUSAVI, 2009; TORLAK; NIZAMLIOĞLU, 2011; HERNÁNDEZ-OCHOA et al., 2012; NARAYANAN et al., 2013; ABDALI; AJJI, 2015).

Table 2.2. Antimicrobial and antioxidant active packages with CEO or eugenol produced by different conventional methods.

Polymer matrix	Incorporation method and CEO/eugenol concentration in polymer matrix (w/w %)	Main results	Reference
Blend of cassava bagasse with polyvinyl alcohol (PVA)	Direct incorporation of CEO by thermo-compression (6.5 to 10%) or surface coating with CEO solution (2.5 to 7.5%)	Largest inhibition zones against molds (*Aspergillus niger* and *Penicillium citrinum*), yeast (*Candida albicans*), Gram-positive (*S. aureus*, *Bacillus cereus*, *Streptococcus mutans* and *Enterococcus faecalis*) and Gram-negative bacteria (*E. coli* and *Salmonella* Typhimurium) in trays produced by surface coating with 5 and 7.5%. Trays produced by thermo-compression were only effective against *C. albicans*	Debiagi et al. (2014)
Fish protein	Solvent casting of protein solution with CEO (2.5%)	Incorporation of CEO increased the antioxidant activity of films when compared to control films (without CEO). CEO-incorporated films presented 72% of 2,2-diphenyl-1-picrylhydrazyl (DPPH) radical inhibition	Teixeira et al. (2014)
Blend of LDPE and EVA	LDPE and EVA at concentration of 10% were melt-compounded in an extruder with CEO (0.5 to 4%). The grinded pellets were processed by blowing	CEO-blended films presented antimicrobial activity against *S. aureus* and *E. coli* at concentrations of 2 and 4%. Sliced tomatoes contained in blended films with 4% of CEO did not present visual spoilage during 2 months of storage in comparison with control packaging	Wattananawinrat et al. (2014)

Chitosan	Solvent casting of chitosan solution with CEO (2.5 to 10%)	Antifungal activity of CEO against *Aspergillus oryzae* and *Penicillium digitatum* was higher than its antibacterial activity against Gram-positive *Staphylococcus aureus* and Gram-negative *Escherichia coli*	Wang et al. (2011)
Multilayer film of LLDPE with corn-zein	Surface coating of LLDPE with corn-zein solution containing eugenol (1.5 to 5%). The coated side was laminated with another LLDPE film	Eugenol was released from the multilayered film in gas and liquid phases. Films at concentration of 3% inhibited lipid oxidation of fresh ground beef and maintained the color stability during 14 days of storage	Park et al. (2012)
PP and PE/ethylene vinyl alcohol (EVOH) copolymer	Surface coating with CEO solution (1 and 4%)	The growth of yeasts (*C. albicans*, *Debaryomyces hansenii* and *Zigosaccharomyces rouxii*) was completely inhibited by the released vapors of CEO at concentration of 4%. The growth of molds (*Penicillium islandicum*, *Penicillium roqueforti*, *Penicillium nalgiovense*, *Eurotium repens* and *Aspergillus flavus*) was delayed at the same concentration. Higher concentrations were required to inhibit the growth of Gram-positive (*S. aureus*, *B. cereus*, *Listeria monocytogenes* and *E. faecalis*) and Gram-negative bacteria (*E. coli*, *Yersinia enterocolitica*, *Pseudomonas aeruginosa* and *Salmonella choleraesius*)	López et al. (2007)

Some patents of active packages have claimed positive results of the interaction between EOs and food matrices. The patents described in Table 2.3 evidences that the incorporation of natural active agents in packaging materials is a promising field to be explored in research and development areas. Examples of food products prone to be contained in active packaging systems include fruit or fruit juice, teas, vegetables, noodles, sandwiches, meat, ham, chicken, fish, cheese, bread and cakes (SUPPAKUL et al., 2003).

Table 2.3. Patents of active packaging systems containing EOs.

Patent number	Description	Reference
WO 2013032631 A1	Encapsulation of aromatic compounds of EO's within gelatin capsules to potential application in beverage packaging	Zhang; Given (2013)
WO 2007135273 A3	Materials based on (non)woven fibrous to food preservation, coated with a matrix comprising biodegradable polymers for controlled release of volatile antimicrobials	Ben et al. (2008)
WO 2008149232 A2	Active materials containing essential oils adsorbed in combination with a solvent within a micro-porous solid material for controlled release of essential oil vapors	Sabehat (2008)
WO 2006000032 A1	Antimicrobial packaging material for foodstuffs containing from 0.05% to 1.5% by weight of a natural EO	Miltz et al. (2006)
US 20040034149 A1	Plastic film with at least one incorporated EO to protect and preserve horticulture products and foods against insects	Garcia (2004)

2.4 Impregnation assisted by high-pressure CO_2

There are a variety of techniques for incorporating active compounds in plastic films. In industry, blown film extrusion is one of the most employed. However, this technique among others that employ high processing temperatures, as thermo-compression molding, can volatilize or degrade thermosensitive compounds (QUINTAVALLA; VICINI, 2002; VARTIAINEN et al., 2003; PIRES et al., 2014). Other examples include the mixture of components during the polymer synthesis, surface coating and immersion of the polymer material into a solution containing the active substance to be impregnated (SUPPAKUL et al., 2003; CRAN et al., 2010). Despite being simple methods, they require the use of high volumes of active agents or employ organic solvents that, depending on the application, need to be eliminated at the final step of processing (DÍEZ-MUNICIO et al., 2011). In this context, impregnation methods performed at low temperatures have attracted growing interest. One example of low-temperature and solvent-free technique is the impregnation assisted by carbon dioxide (CO_2) at high pressures. This method overcomes most problems related to the use of conventional techniques. One of its main advantage is that the active compound incorporation occurs into previously formed carrier material, preventing the exposition of thermosensitive compounds to the high temperatures (VARONA et al., 2011). In addition, the final product is recovered dry and free of solvent residues after system depressurization, which avoids purification steps normally performed with organic solvents (CHAMPEAU et al., 2015).

At this point, it is worth reviewing some properties and characteristics of supercritical fluids (SCFs). In the critical region, a substance that is a gas at normal conditions exhibits liquid-like density and an increased solvent capacity that is pressure-dependent (MCHUGH; KRUKONIS, 1994). Table 2.4 lists the critical temperature (T_C) and critical pressure (P_C) of a variety of SCFs. Differences between the critical points of such fluids suggest the use of specific fluids in specific cases. Even though water is a low molecular weight compound, it has a high T_C due to a large amount of thermal energy required to break hydrogen bonds between water molecules. On the other hand, the T_C of CO_2, ethane and ethylene are near the ambient, they are attractive fluids to process thermosensitive compounds (MCHUGH; KRUKONIS, 1994). The physicochemical and transport properties of SCFs layer between those of gases and liquids: a gas-like viscosity, liquid-like density and moderately high diffusivity. The variable solvent capacity of SCFs makes them

excellent solvents, antisolvents or plasticizers for many applications, including polymerization, dissolution, precipitation, swelling, impregnation and extraction processes (NALAWADE; PICCHIONI; JANSSEN, 2006; PEREDA; BOTTINI; BRIGNOLE, 2007; SHINE, 2007).

Table 2.4. Critical points of pure fluids.

Fluids	T_C (°C)	P_C (bar)
Carbon dioxide	31.1	73.8
Ethane	32.2	48.8
Ethylene	9.3	50.4
Propane	96.7	42.5
Propylene	91.9	46.2
Butane	153.2	36.2
Cyclohexane	280.3	40.7
Isopropanol	235.2	47.6
Benzene	289.0	48.9
Toluene	318.6	41.1
p-Xylene	343.1	35.2
Ammonia	132.5	112.8
Water	374.2	220.5

Source: McHugh and Krukonis (1994).

A pure component is considered to be in the supercritical state if its temperature and pressure are higher than the critical values. For pure CO_2 at critical conditions of pressure and temperature, there is no sudden change of component properties, as indicated by the hatched lines in Figure 2.4. Similar effects to that of the supercritical state can be achieved for $P > P_C$ and $T < T_C$, at near-critical temperatures in liquid state, within neighboring conditions of state of a substance (BRUNNER, 1994). At this condition, the liquid is expanded in comparison to its normal state and the liquid density becomes similar to that of a SCF (DARR; POLIAKOFF, 1999).

Compared to other pure compounds, the critical point of CO_2 is low and easily reachable. This reason explains its large use in supercritical processes, besides being chemically inert, nontoxic, nonflammable, highly available and odorless. The CO_2 is considered a sustainable or green solvent as its removal after processing is not energy consuming and its recovery is environmentally friendly (AGHEL et al., 2004; BOYÈRE; JÉRÔME; DEBUIGNE, 2014). Moreover, the CO_2 possesses the GRAS

status stated by the FDA and the EFSA (DÍEZ-MUNICIO et al., 2011; 21 CFR-PART 184, 2017).

Figure 2.4. Pressure-temperature phase diagram of pure CO_2.

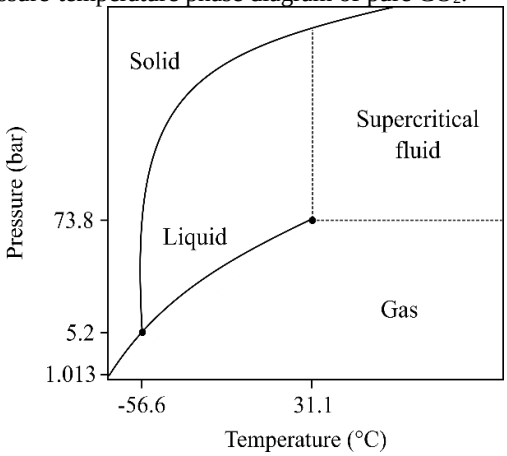

Source: Brunner (1994).

An important application of SCFs has been the impregnation of polymers with supercritical CO_2 (SC-CO_2) or the impregnation of polymers with additives soluble in SC-CO_2. In this process, the sorption of SC-CO_2 lowers the glass transition temperature (T_g) of polymers due to a plasticizing effect. The sorbed gas lubricates the polymer chains which can easily slip over one another, thus facilitating the incorporation of active compounds in the swollen matrix (KIKIC; VECCHIONE, 2003; KIRAN, 2009). The impregnation process of fragrances, pest control agents and pharmaceutical drugs into solid polymer matrices exposed to SCFs has been patented in 1986 (SAND, 1986). In this process, the SCF swells the polymer and allows the thermosensitive material to migrate into the polymer matrix due to an enhancement of its diffusivity by several orders of magnitude. Additionally, the process is conducted at temperatures low enough to avoid thermal degradation of thermosensitive materials. When the system is depressurized, the SCF is removed from the polymer and the thermosensitive compound, which remains trapped in the matrix, slowly diffuses out of the polymer (MCHUGH; KRUKONIS, 1994).

The principle of incorporating an active agent into a polymer matrix by means of SC-CO_2 impregnation is complex and depends on thermodynamic conditions and mass transfer mechanisms. The process

takes the advantage of both density and diffusivity properties of CO_2 at high pressures, as illustrated in Figure 2.5. The SC-CO_2 possesses a good solvent power because of its high density. It solubilizes several nonpolar compounds of low molecular weight, including the EOs. The high diffusivity of SC-CO_2 leads to high diffusion rates of CO_2 into the matrix, which is advantageous to carry the solubilized EO through the polymer network. As the system is depressurized, CO_2 becomes gaseous and its solvent power is reduced, retaining active compounds into the polymer bulk. The non-impregnated active molecules still solubilized in CO_2 are dragged out of the matrix during CO_2 venting. At the final step of processing, the impregnated polymer is recovered free of solvent residue (CHAMPEAU et al., 2015; MIR et al., 2017). Depending on how interactions between the active agent and the polymer occur, an adsorption or a physicochemical attachment of active compound molecules to the polymeric matrix can arise (VARONA et al., 2011). In this context, if the active agent interacts strongly with the polymer, it becomes more susceptible to remain trapped in the matrix during depressurization.

Figure 2.5. Schematic representation of impregnation assisted by SC-CO_2.

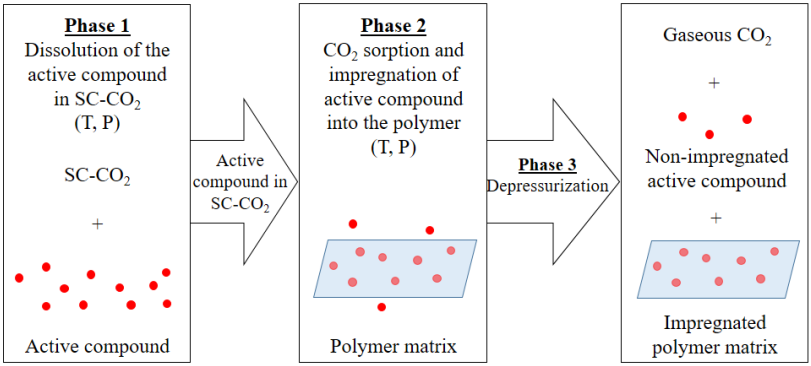

Source: Adapted from Champeau et al. (2015).

One of the major applications of impregnation assisted by SC-CO_2 is the incorporation of drugs in different supporting materials, as transdermal drug delivery systems, intraocular or contact lenses (DUARTE et al., 2007; COSTA et al., 2010; YAÑEZ et al., 2011; BOULEDJOUIDJA et al., 2016). Additionally, the technology of SC-CO_2 impregnation is being commercially used to incorporate fungicide in woods and to dye textile materials (IVERSEN et al., 2003; BANCHERO,

2013). The employment of this technology to incorporate active compounds in packaging films is recent in the scientific literature, as presented in Table 2.5. It is worth mentioning that the use of SCFs is not only restricted to research laboratories but also it has been adopted in commercial scales by several companies. Some examples include the Phasex, Thar Technologies, Micell, Trexel, DuPont, Novasep and Ferro Corporations (TOMASKO et al., 2003; NALAWADE; PICCHIONI; JANSSEN, 2006)

Table 2.5. SC-CO_2 impregnation of active agents in polymer matrices for active packaging applications. P: pressure; T: temperature; DR: depressurization rate.

Matrix	Active compound	Experimental conditions	Main result	Reference
LDPE	*R*-(−)-carvone	P: 76 to 134 bar T: 35, 60 °C Time: 2 h DR: 6 bar min^{-1} Mass fraction: 0.8 mg g^{-1}	Impregnation yield increased with lower CO_2 densities. Maximum: 43.8 mg *R*-(−)-carvone/g LDPE (35 ºC, 76 bar)	Goñi et al. (2018)
LDPE	Two terpenic ketones (Thymoquinone and *R*-(+)-pulegone)	P: 100, 150 bar T: 45 °C Time: 2, 4 h DR: 5, 20 bar min^{-1} Mole fraction: 1.7, 2.5 x 10^{-3}	Contact time and ketone mole fraction significantly influenced the impregnation. Maximum: 55.9 mg ketones/g LDPE (100 bar, 4 h, 20 bar min^{-1}, 2.5 x 10^{-3} mole fraction)	Goñi et al. (2017)
PLA	Thymol	P: 90, 120 bar T: 40 °C Time: 3 h DR: 1, 10, 100 bar min^{-1}	SC-CO_2 impregnation caused strong modifications on thermal and mechanical properties of films. Impregnation increased with low DR. Maximum: 204 mg thymol/g PLA (120 bar, 1 bar min^{-1})	Torres et al. (2017)
LLDPE	Eugenol	P: 100, 120, 150 bar T: 45 °C Time: 4 h DR: 5, 10, 50 bar min^{-1}	Impregnation increased with low DR. Maximum: 56.7 mg eugenol/g LLDPE (150 bar, 5 bar min^{-1}) Minimum: 13.1 mg/g (150 bar, 50 bar min^{-1})	Goñi et al. (2016)

LLDPE	2-nonanone	P: 120, 170, 220 bar T: 40 °C Time: 3 h DR: 10, 100 bar min^{-1}	High impregnation with low P and DR. Maximum: 3.44 mg 2-nonanone/g LLDPE (120 bar and 10 bar min^{-1})	Rojas et al. (2015)
Cassava starch	Cinnamaldehyde	P: 150, 250 bar T: 35 °C Time: 3, 15 h DR: 1, 10 bar min^{-1}	Impregnation increased with P, contact time and DR. Maximum: 2.50 mg cinnamaldehyde/g cassava starch (250 bar, 15 h, 10 bar min^{-1})	Souza et al. (2014)
LLDPE	Thymol	P:70, 90, 120 bar T: 40 °C Time: 4 h DR: no control	Impregnation increased with P. Maximum: 13.20 mg thymol/g LLDPE (120 bar)	Torres et al. (2014)
Alginate	Natamycin	P: 200 bar T: 40 °C Time: 2.5, 4, 14 h DR: 5 bar min^{-1}	Impregnation increased with contact time and ethanol 10% molar. Maximum: 8.89 mg natamycin/g alginate (14 h). Maximum with ethanol: 16.29 mg/g (14 h)	Bierhalz et al. (2013)

2.5 Thermodynamic data of CO_2 at high pressures

The pressure-dependence of CO_2 properties influences the polymer processing. Pressure governs the density, solubility and dielectric constant of CO_2 (SHINE, 2007). Supercritical CO_2 is characterized by a low dielectric constant ($\varepsilon \approx 2$) and it is a good solvent for nonpolar molecules with low molecular weight (KEMMERE, 2005). Moreover, it is a good solvent for few polymers, such as siloxanes and fluorinated polymers, and a poor solvent for high molecular weight polymers. In general, CO_2 solubility depends on temperature, pressure and weak interactions with polymer groups or polymer chains (NALAWADE; PICCHIONI; JANSSEN, 2006).

The design of processes using CO_2 at near or supercritical conditions is highly dependent on the phase equilibrium between all involved components. The knowledge of CO_2 solubility in polymers over the selected temperatures and pressures facilitates the determination of working conditions. The solubility of EOs, specifically the CEO in CO_2, varies according to the operational conditions. For this reason, Table 2.6 lists the values of CO_2 density and its physical state as function of pressures and temperatures covered in this study. The thermodynamic data of the systems polyethylene-based polymers-CO_2 and CEO-CO_2 at high pressures are addressed in the following subsections.

Table 2.6. CO_2 density at temperatures of 25, 32, 35 and 45 °C and pressures of 150 and 250 bar. PL: pressurized liquid; SCF: supercritical fluid.

P (bar)	T (°C)	CO_2 density (g cm^{-3})	Physical state
150	25	0.876	PL
250	25	0.943	PL
150	32	0.835	PL
150	35	0.815	SCF
250	35	0.901	SCF
150	45	0.742	SCF
250	45	0.857	SCF

Source: National Institute of Standards and Technology (NIST) database (LEMMON; MCLINDEN; FRIEND, 2001).

2.5.1 Carbon dioxide and polyethylene-based polymers

The solubilization of CO_2 into a polymer is dependent on the interactions between CO_2 and polymer chains. These interactions are influenced by the polymer chain mobility in the amorphous phase as well as the free volume of polymer (ČUČEK et al., 2013; CHAMPEAU et al., 2014). In general, the solubility of CO_2 increases with the content of polar groups in polymer chains. For semicrystalline polymers, as the LLDPE, the sorption of CO_2 occurs in the amorphous regions, as the crystalline regions (crystallites) are considered impermeable domains (MICHAELS; BIXLER, 1961). For this reason, polyolefins with a semicrystalline structure are good candidates for producing polymer films incorporated of active compounds, as their macrostructure tends to be maintained after CO_2 desorption. On the other hand, polymers with relatively low T_g (below or near the critical temperature of CO_2), as working temperatures are usually above the polymer T_g, and with a predominantly amorphous structure (low crystallinity) are more susceptible to deformation and foaming during SC-CO_2 impregnation. One example is the poly(lactic acid) (PLA) and its copolymers that are useful in the production of scaffolds and porous carrier materials (TOMASKO et al., 2003).

Sato et al. (1999) measured the solubility of CO_2 in HDPE at temperatures of 160, 180 and 200 °C, and pressures from 66 to 181 bar. They reported that the solubility of CO_2 increased almost linearly with pressure and decreased with an increase in temperature, as visualized in Table 2.7. The same influence of pressure (at constant temperature) on the solubility of CO_2 in HPDE and two types of LDPE was also observed in another study (ČUČEK et al., 2013). These authors suggested that polymers with similar molecular weight (MW) present similar values of CO_2 solubility in supercritical medium.

The general trend for semicrystalline polymers within a temperature range of 40 to 200 °C is that the amount of solubilized CO_2 increases with pressure up to around 200 bar. Above this pressure, the additional gas uptake seems to be invariant. For the temperature, this behavior differs when the polymer is in rubbery or molten state. In rubbery state, the solubility of CO_2 decreases with temperature, but it starts to increase when approximating to the polymer T_m due to an increased polymer swelling and CO_2 sorption. After reaching the molten state, the solubility of CO_2 diminishes with temperature due to an increased mobility of polymer chains (LEI et al., 2007; CHEN et al., 2009; SARRASIN et al., 2015). The sorption of CO_2 in semicrystalline polymers causes a reversible swelling of the polymer matrix, also

increasing the apparent volume and chain mobility (HIROSE; MIZOGUCHI; KAMIYA, 1986; KIKIC; VECCHIONE, 2003).

Table 2.7. Values of CO_2 solubility in polyethylene-based polymers.

Polymer	Crystallinity degree (%)	T (°C)	P (bar)	Solubility (g CO_2/ g polymer)	Reference
HDPE	-	160	69.4	0.041	Sato et al. (1999)
			174.5	0.132	
	-	180	70.6	0.035	
			181.2	0.120	
	-	200	66.1	0.032	
			170.2	0.103	
LDPE (high MW)	47.2	100	21.7	0.011	Čuček et al. (2013)
			308.2	0.364	
LDPE (low MW)	44.2	100	2.6	0.001	
			307.1	0.160	
HDPE	74.2	100	21.2	0.006	
			304.6	0.138	

2.5.2 Carbon dioxide and clove essential oil

Phase equilibrium data for the system CEO and CO_2 were evaluated by Souza et al. (2004) at temperatures of 30, 35, 40 and 45 °C from 58.3 to 140.6 bar. In their study, the multicomponent mixture that forms CEO was treated as a pseudo-pure component to facilitate the fit of Peng-Robinson equation of state to the experimental data. The system exhibited two liquid phases in equilibrium with a vapor phase (vapor-liquid-liquid, VLL, equilibrium) at 30 and 35 °C, while at 40 and 45 °C only the vapor-liquid (VL) transition was visualized (Figure 2.6). Above 80 bar, it was observed a region of liquid-liquid ($L_1 + L_2$) and, below it, a region of VL in equilibrium.

Cheng et al. (2000) measured the vapor-liquid equilibrium of pure eugenol and CO_2 at 35, 45 and 55 °C from 14 to 130 bar. These authors reported that the solubility of eugenol in vapor phase is not significant at lower pressures (below the critical point of CO_2).

An interesting observation from both data is that the consideration of pseudo-binary system (CEO-CO_2) made by Souza et al. (2004) is in

well agreement with equilibrium data reported by Cheng et al. (2000) for the binary system (eugenol-CO_2), as demonstrated in Figure 2.6.

Figure 2.6. Vapor-liquid equilibrium of CEO-CO_2 and eugenol-CO_2 at 35 and 45 °C.

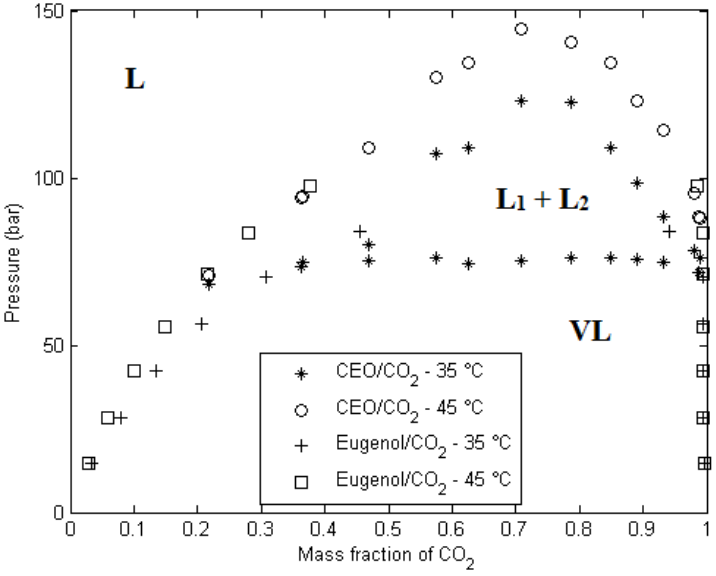

Source: Adapted from Souza et al. (2004) and Cheng et al. (2000).

The solubility of CEO in CO_2 varied from 0.230 to 0.277 g of extract per g of CO_2 (Table 2.8). The CEO was obtained by SC-CO_2 extraction of clove buds (RODRIGUES et al., 2002). Solubility measurements were performed considering a pseudo-ternary system formed by a cellulosic material, the extracted EO and CO_2. The chemical composition of extracts obtained under different experimental conditions (temperature, pressure, CO_2 flow rate and apparatus) showed that eugenol was the major component in all extracts. The solubility of the pseudo-ternary system was only governed by the solubility of eugenol in CO_2.

Table 2.8. Values of CEO solubility in CO_2.

T (°C)	P (bar)	Solubility (g extract/g CO_2)	Reference
15	70	0.230	Rodrigues et al. (2002)
15	80	0.244	
15	100	0.277	
25	100	0.267	
35	100	0.230	

Suárez-Iglesias et al. (2008) determined the binary diffusion coefficient of eugenol at infinite dilution in SC-CO_2 from 40 to 60 °C and between 150 and 350 bar. They observed a decrease in diffusivity with increasing pressure at constant temperature. The variation of binary diffusion coefficient with pressure $(\partial D_{AB}/\partial P)_T$ was lower at high pressures, especially above 250 bar. In addition, the binary diffusion coefficient increased with temperature at constant pressure, but the temperature dependence of $(\partial D_{AB}/\partial T)_P$ was not clear because of the narrow temperature range studied. The values of binary diffusion coefficient of eugenol-CO_2 at 40 °C for pressures covered in the present study were 9.29 x 10^{-9} m^2 s^{-1} (150 bar, 40 °C) and 6.96 x 10^{-9} m^2 s^{-1} (250 bar, 40 °C).

In the region near to the critical point, the binary diffusion coefficient of CO_2 with different substances varies significantly from the near-critical to the supercritical region, thus suggesting a high dependence on solvent density. The effect of pressure and temperature on CO_2 density is well visualized in Figure 2.7. As the density (and pressure) of the solvent increases isothermally, the diffusion coefficient decreases due to an increased number of collisions and a reduced mean free paths for solute molecules. In fact, the high density means that the solvent molecules are very close, thereby impeding the movement of solute particles. In this sense, the binary diffusion coefficient is inversely proportional to the pressure. On the opposite, the diffusion coefficient increases as the temperature increases isobarically. The decrease in CO_2 density with temperature is also associated with an increase of kinetic energy of solute molecules, making them move fast, thus contributing to the increase of diffusion coefficient. However, the dependence of diffusion coefficient on temperature decreases as pressure increases. Therefore, the binary diffusion coefficient is directly related to the temperature (GONZÁLEZ; BUENO; MEDINA, 2001; MEDINA, 2012).

Figure 2.7. Variation of CO_2 density as function of pressure and temperature.

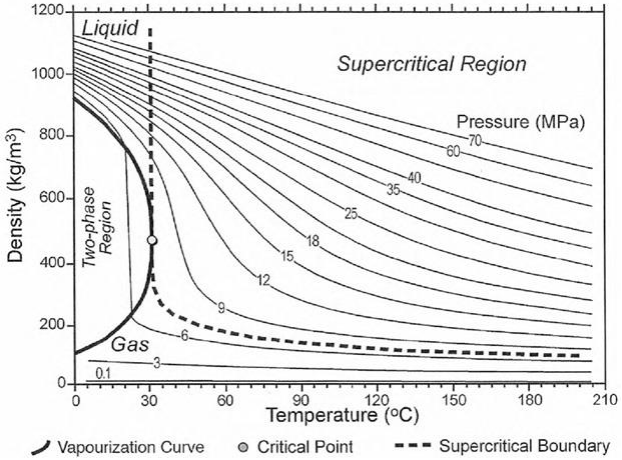

Source: Bachu (2008).

2.6 Migration in food simulant fluids

Food-packaging interactions are a result of mass transfer process between the contained product and the polymer film. These interactions can be classified in three types: migration, permeation and sorption. Specific examples include: 1- migration of plasticizers or contaminants from polymers to food, representing a safety issue, or migration of functional additives to enhance food quality; 2- permeation of gases as oxygen or CO_2 that are benefic in modified atmosphere packages (MAP), but undesirable in carbonated beverages; and 3- sorption of components, such as flavors and odors, which can result in sensory changes (HOTCHKISS, 1997). Migration occurs by two ways: direct contact of package with food surface or indirect contact due to a migration of volatiles into the packaging headspace (CRAN et al., 2010).

Food products are composed by a mixture of substances, as water, carbohydrates, fats, proteins, vitamins, fibers and minerals, which makes difficult the analytical measurement of migration (CRAN et al., 2010). Due to the complexity of foods, migration studies can be performed with food simulant fluids that are less complex than foods and simulate their main physicochemical properties (EC, 2011). Migration tests are performed during a specific period of time and temperature, taking into account the characteristics of usage, storage and the food that will be packaged (RIBEIRO-SANTOS et al., 2017b). The European and

Brazilian guidelines for migration tests of plastic materials to come into contact with foodstuff products are detailed in the following.

The regulation of European Union nº 10/2011 (EC, 2011) of 14 January 2011 listed the following food simulant fluids to be used in migration tests of constituents from plastic materials that will come into contact with foodstuffs:

- Fluid A: aqueous solution of ethanol 10% (v/v);
- Fluid B: aqueous solution of acetic acid 3% (w/v);
- Fluid C: aqueous solution of ethanol 20% (v/v);
- Fluid D1: aqueous solution of ethanol 50% (v/v);
- Fluid D2: aqueous solution of ethanol 95% (v/v) or edible vegetable oils (olive, sunflower or corn oil);
- Fluid E: poly(2,6-diphenyl-p-phenylene oxide) (PPPO), particle size 60-80 mesh, pore size 200 nm.

Food simulants A, B and C are assigned for foods with a hydrophilic character as they are able to extract hydrophilic substances. Food simulant B should be used for foods with a pH below 4.5 (acidic foods) and food simulant C for alcoholic foods with alcohol content up to 20% or foods with relevant amount of organic ingredients that makes the food more lipophilic. Food simulants D1 and D2 are designated for lipophilic foods as they are capable to extract lipophilic substances. Food simulant D1 is intended to be used for alcoholic foods with alcohol content higher than 20% and for oil-in-water emulsions, whereas food simulant D2 should be used for foods with free fats at the surface. Food simulant E is assigned for specific migration in dried foods.

The Brazilian resolution nº 51 of 26 November 2010 (BRASIL, 2010) regulated by ANVISA is based on the above mentioned European regulation for migration tests, with some differences regarding the adopted food simulant fluids, as follows:

- Fluid A: distilled or deionized water;
- Fluid B: aqueous solution of acetic acid 3% (w/v);
- Fluid C: aqueous solution of ethanol 10% (v/v);
- Fluid D: aqueous solution of ethanol 95% (v/v), isooctane, or PPPO;
- Fluid D': edible vegetable oils (olive, sunflower or corn oil) or synthetic mixtures of triglycerides.

Food simulants A and B shall be used for nonacidic (pH > 4.5) and acidic (pH < 4.5) aqueous foods, respectively. Food simulant C is assigned for aqueous and alcoholic foods (alcohol content between 5 and 10%); for foods with an alcohol content higher than 10%, the ethanolic

solution should have the same ethanol concentration as the food. Food simulants D and D' are equivalent and employed for fatty foods.

Testing the migration of chemical compounds from packaging to food simulants involves two basic steps: first, the exposure of the polymer film to the food simulant to allow substances from plastic material to migrate into the fluid; second, the quantification of migrants transferred to the food simulant in terms of SML (BHUNIA et al., 2013). The list of allowed compounds to come into contact with foods along with their maximum SMLs are established by authorities in each country, as previously discussed in Section 2.2. The CEO and its derivatives are labeled as GRAS food contact materials and their SML is stated as not detectable by the legislation of the FDA, EFSA and ANVISA.

2.7 Mathematical modeling of active compound migration

The mechanism of action of active food packages is based on the migration of active compounds from package to food. Therefore, the knowledge of transport properties is important when developing this type of package (CHOI et al., 2005). During migration tests, the active compound release is mainly a diffusion-controlled mechanism, also depending on equilibrium conditions. Convection and chemical reactions can occur depending on the degree of solvent stirring and polymer-solvent interactions. The mass transfer is also influenced by the crystalline state of polymer matrix, as diffusion in glassy polymers is slower than in rubbery ones (MANZANAREZ-LÓPEZ et al., 2011; BHUNIA et al., 2013).

The diffusion mechanism, in this sense, is defined as the mass transfer process resulting from natural and random molecular motion from a region of high concentration (the food-contact layer) to a region of low concentration (usually the food surface). This mass transfer is influenced by food-packaging interactions and the temperature of the system (BHUNIA et al., 2013). The basic theory of interactions package-to-food or -fluid is similar for process of migration, permeation and sorption of active compounds. In general, these interactions are well described by mathematical models based on diffusion mechanism (HOTCHKISS, 1997).

Diffusion of EOs in polymer films can be influenced by several factors, including the polymer properties, the presence of plasticizers in the matrix and the method of film production. In addition, some EOs can interact with the polymer, which prevents or slows the migration process. Considering the case of protein-based films, as example, some

components of EOs can be attached to the film due to amino acid-EO interactions. On the other hand, films with linear molecules and short-branched structure tend to present higher diffusion rates (PREEDY, 2016). During migration, the active compound concentration changes in both contacting phases: the polymer and the food/fluid phases, as illustrated in Figure 2.8. The scheme presents the physical interpretation of mass transfer between the two phases, showing the concentration profile close to the solid-liquid interface and the analogy with a serial association of mass transport resistances, including the resistances of polymer phase, interface and fluid phase (VITRAC; MOUGHARBEL; FEIGENBAUM, 2007).

Figure 2.8. Mass transport between a packaging material and a food simulant fluid showing the (a) concentration profile and (b) comparison with resistances in series. Light gray: residual content in packaging material. Dark gray: diffused amount into the liquid.

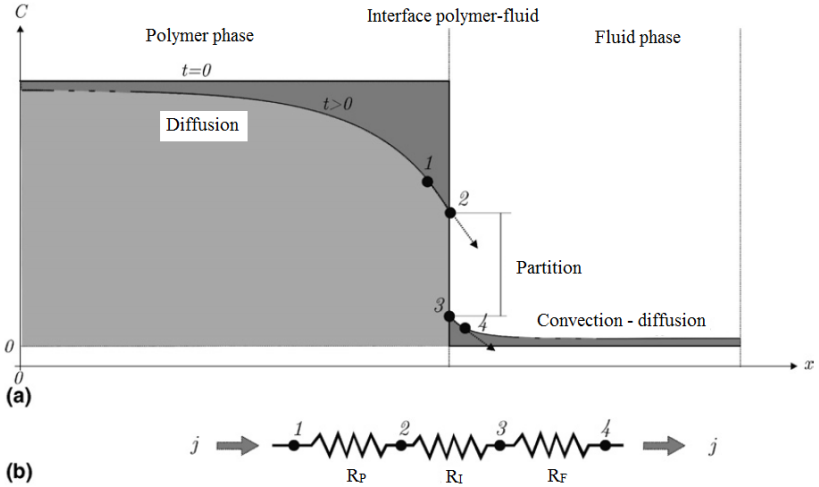

Source: Vitrac, Mougharbel and Feigenbaum (2007).

The use of mathematical modeling to describe or predict migration provides important insights into the main mechanisms governing the mass transfer. It also gives parameters with phenomenological meaning depending on the mathematical approach. The mathematical modeling promotes indications about systems similar to those studied, optimizing the project of new packaging materials and facilitating the scale-up process from laboratory to pilot and industrial scales. These advantages reduce the number of laboratory assays to be undertaken, saving time and

costs of experimental trials (SIEPMANN; SIEPMANN, 2008). Based on the advantages of mathematical modeling in migration processes, the applicability of diffusion models to estimate specific migration parameters has been introduced into the European legislation as technical guidelines to complement the current legislation of food contact materials (SIMONEAU, 2010; EC, 2011).

In this sense, the mathematical modeling of migration can be viewed as a tool to estimate the concentration of a certain type of component initially present in packaging. In the absence of mechanistic mathematical models to predict diffusion coefficients in polymers, it is possible to adopt semi-empirical relationships that may over- or underestimate true diffusion coefficients, but they can be of practical use to check compliance of food contact materials (VITRAC; MOUGHARBEL; FEIGENBAUM, 2007).

The transport of relatively small molecules through a polymer film is mainly due to the random molecular motion of individual molecules. In such processes, the driving force is proportional to the concentration gradient in the polymer matrix. This transport of molecules can be described by analogy to the Fick's law of diffusion in dilute solutions (Equation 2.1), in which the one-dimensional flux (j, [kg m^{-2} s^{-1}]) is proportional to the concentration gradient of the active compound, when the advective flux (diffusion-induced convection) perpendicular to the interface can be neglected (CUSSLER, 2009).

$$j = -D\left(\frac{d\rho}{dx}\right) \tag{2.1}$$

in which ρ is the mass concentration of the active compound (kg m^{-3}), x is the Cartesian coordinate (m), and D represents the diffusion coefficient (m^2 s^{-1}). Equation 2.2 is a result of combining Equation 2.1 with the equation of continuity for the active compound. It considers only unidirectional gradients of concentration, no chemical reaction between the diffusing species, absence of macroscopic flux, and D as a constant parameter, independent of distance, time and concentration. Thus, Equation 2.2 is the basic equation for one-dimensional unsteady state diffusion (CUSSLER, 2009), where t represents time (s).

$$\frac{\partial\rho}{\partial t} = D\left(\frac{\partial^2\rho}{\partial x^2}\right) \tag{2.2}$$

Depending on initial and boundary conditions from migration processes distinct solutions can be obtained to solve Equation 2.2. These conditions and hypotheses that allow the use of this mathematical approach in the present study are further discussed and detailed in Chapter 4.

2.8 State of the art

Foodborne diseases are growing public health problem worldwide despite new improvements in slaughter hygiene, techniques of food production and quality control programs. In fact, food safety still remains a public health issue, as highlighted by the WHO (2007), and the successful control of foodborne pathogens requires the use of multiple preservation techniques, both in the manufacture and storage of food products, to ensure quality, safety and shelf life.

A wide range of food additives are used to extend shelf life by inhibiting microbial growth or oxidative processes in foods. Most of them are chemically synthesized and, in recent years, they are being perceived by consumers as compounds that may offer some health risk. Changes in distribution and commercialization of industrialized products and the demand for safer products have boosted the interest in finding innovative solutions to the traditional chemical compounds added to preserve foods as well as new packaging systems. For this reason, the development of technologies to produce active food packaging with different properties has attracted the interest of food and chemical industries.

The Flexible Packaging Association (FPA) published a study reporting that advances in food packaging technologies will significantly contribute to food waste reduction (MCEWEN ASSOCIATES, 2014). Brazil is one of the largest agricultural producers and exporters worldwide. Thus, it is of fundamental interest that new processes and materials be studied in order to improve the competitiveness of national industry in the field of food packages. These strategies aggregate value to food products, ensure food quality and reduce environmental and economic impacts caused by food waste.

In the context of innovative concepts of food preservation and the trend towards the demand for natural products, the employment of EOs is becoming an attractive choice for developing active food packaging systems. The CEO is a naturally-derived and highly available essential oil with strong and recognized biological activities that justifies its use in SC-CO_2 impregnation processes. Furthermore, as pointed out by Tomasko and coworkers (2003), the use of an innovative and environmentally

friendly technology, as the SC-CO_2 impregnation, to incorporate natural active compounds in polymer matrices is a new and promising research area to be explored.

One of the major applications of impregnation assisted by SC-CO_2 is the incorporation of drugs in support materials for different applications in medical areas. The employment of this technology to incorporate active compounds in packaging films for application in food areas is recent in the scientific literature, as presented in Table 2.5. These studies report the impregnation of chemically synthesized or chemically isolated compounds in different polymer matrices. An advantage of using natural and multicomponent active agents instead of pure and chemically synthesized ones is to keep synergistic effects from the presence of some minor compounds, besides avoiding isolation and purification steps that imply in increased processing costs.

There is a lack of studies reporting the incorporation of multicomponent active agents from natural sources, such as the CEO, in polymer films by means of SC-CO_2 impregnation, which justifies the interest in developing this study. The choice of polymer matrix, the LLDPE, is based on its wide application in food packaging industry. Therefore, this work, unprecedented in scientific literature, has a great relevance for the scientific and technological development in the area of food packaging. It also fulfills the gap of knowledge regarding an innovative application of the SCF technology, also aggregating value to compounds of natural sources in potential industrial applications in food and chemical areas.

Chapter 3: Effect of processing parameters on clove essential oil impregnation in LLDPE films

This chapter has been published as original article in *Innovative Food Science and Emerging Technologies* journal (ISSN 1466-8564), v. 41, p. 206-215, 2017 (DOI: 10.1016/j.ifset.2017.03.008) entitled "High-pressure carbon dioxide for impregnation of clove essential oil in LLDPE films".

Abstract

High-pressure carbon dioxide (CO_2) impregnation is a promising technology in the development of active packaging films. Clove essential oil (CEO), a multicomponent active agent naturally rich in eugenol, was incorporated in linear low-density polyethylene (LLDPE) films by using high-pressure CO_2 impregnation. The parameters of temperature (25, 35 and 45 °C), pressure (150 and 250 bar) and CEO:CO_2 mass ratio (2 and 10%) were screened using a variable-volume view cell for 4 h to determine the best impregnation conditions. Kinetic assays of CEO impregnation were also performed. The highest amount of CEO (40.2 mg g^{-1} of LLDPE) impregnated was obtained at 10% CEO:CO_2 mass ratio, 45 °C and 150 bar. The impregnation at 2 h showed advantage in reducing processing time. A preferential eugenol impregnation was observed due to thermodynamic interactions and mass transfer phenomena. Thermal and mechanical properties of LLDPE films remained stable after high-pressure processing.

Industrial relevance

The development of innovative technologies for active packaging systems has attracted the interest of food, pharmaceutical, and chemical industries. The consumer's demand for products with low healthy risk makes the CEO an advantageous active agent for packaging development purposes, besides possessing strong antimicrobial and antioxidant activities. The employment of high-pressure CO_2 allowed a homogeneous CEO impregnation in LLDPE films without damaging mechanical and thermal properties of the polymer matrix, in the evaluated conditions, which is important for industrial applications. The CEO-impregnated LLDPE films have potential use in antimicrobial and antioxidant packaging systems.

Keywords: active packaging, film properties, supercritical fluid, eugenol.

3.1 Introduction

The principle of incorporating an active agent into a polymer matrix is related to the concept of active packaging, which interacts with food products preventing or slowing their deterioration. Apart from acting as a selective barrier for moisture and gases, these packages include carbon dioxide (CO_2) scavengers or emitters, moisture absorbents, antioxidant and antimicrobial migrating systems (APPENDINI; HOTCHKISS, 2002; GÓMEZ-ESTACA et al., 2014). One of the main causes of food spoilage is the microbial contamination on food surface and, in order to control microbial growth and to extend shelf life, antimicrobial agents can be added to foods. Additionally, antioxidant agents can be incorporated into foodstuff products to delay their auto-oxidation (PARK et al., 2012). However, in some cases, these active agents directly mixed with foods may result an excessive use and/or damage sensory and nutritional characteristics of food products (WENG; HOTCHKISS, 1993). In this context, the development of packaging films containing active agents is an interesting alternative to overcome such problems.

Active agents from natural sources are perceived by consumers as compounds with low health risk. Furthermore, the industrial interest on these compounds has been increased, since most of them have the Generally Recognized As Safe (GRAS) status (BURT, 2004; SUPPAKUL et al., 2011). The clove essential oil (CEO) is among the most prominent naturally derived active agents due to its antimicrobial, antioxidant, antifungal, antiviral, and insecticidal properties, besides being used as fragrance and flavoring agents (CHAIEB et al., 2007). The high content of eugenol in CEO is believed to promote its strong biological activity (GUAN et al., 2007; IVANOVIC et al., 2013). This essential oil is extracted from clove buds or leaves using different processes, including hydro and steam distillation, as well as extraction with organic and supercritical solvents (GUAN et al., 2007). Clove essential oil is naturally rich in eugenol (around 85-95% of total oil composition (ABBASZADEH et al., 2014)), besides presenting β-caryophyllene, α-humulene, and eugenyl acetate in different proportions, depending on raw material and extraction conditions (AFFONSO et al., 2014). The employment of a multicomponent active agent from natural sources, as in the case of CEO, for impregnation purposes, instead of using pure and chemically synthesized components, is a potential synergistic effect of the components in the complex mixture capable to promote antimicrobial and antioxidant activities (SEOW et al., 2014).

Another advantage of using natural active agents is to avoid isolation and purification steps that implies in increased processing costs. Therefore, the use of CEO seems to be more promising in commercial applications than the pure component.

Several manufacturing processes have been developed to incorporate active agents in packaging films, including solvent casting (NARAYANAN et al., 2013), surface coating (ABDALI; AJJI, 2015), hot melt extrusion (WATTANANAWINRAT; THREEPOPNATKUL; KULSETTHANCHALEE, 2014), and immersion of the polymer material with/by/into a fluid phase containing the active substance to be incorporated (DIAS et al., 2011). However, these processes generally require the use of organic solvents that, depending on the application, should not be present in final product, or employ a large amount of impregnating solution, or else, are performed at high temperatures, which may damage thermosensitive active compounds. In this sense, impregnation assisted by high-pressure CO_2 (near-critical or supercritical) overcomes most problems related to conventional techniques. This method is advantageous since the formation of carrier material and incorporation of the active compound occurs in separated steps, avoiding the exposure of such compounds to relative high temperatures commonly applied in polymer processing (VARONA et al., 2011). In addition, many polymers become swollen and plasticized in contact with supercritical CO_2, increasing their free volume and facilitating the active compounds incorporation at low temperatures (NALAWADE; PICCHIONI; JANSSEN, 2006).

The development of sustained processes is becoming a priority for industries due to environmental concerns and stricter legislation. In this context, the use of supercritical CO_2 in place of conventional organic solvents has attracted increased interest, since it is chemically inert, nontoxic, non-flammable, non-polluting and highly available (CHAMPEAU et al., 2015). Additionally, its critical point is relatively low and easily reachable (critical temperature, $T_C = 31.1$ ºC; and critical pressure, $P_C = 73.8$ bar) when compared to other pure compounds, making it the most employed supercritical fluid (WRIGHT et al., 1988). The combination of gas-like viscosity and liquid-like density of supercritical CO_2 makes it an excellent solubilizing agent for many applications in polymer processing with improved product quality, as compared to conventional methods that employ organic solvents. The use of supercritical CO_2 does not create a problem concerning the greenhouse effect, as it can be recovered during processing (NALAWADE; PICCHIONI; JANSSEN, 2006). The advantage of CO_2 in impregnation

process is attributed to its ability in solubilizing many active compounds, especially nonpolar low molecular weight ones, along with its near zero surface tension that allows its rapid diffusion into a wide range of polymers (DÍEZ-MUNICIO et al., 2011). At the final processing stage, CO_2 is completely removed through depressurization with no degradation of active compounds as well as polymer matrix, also avoiding purification steps that are usually performed with organic solvents (CHAMPEAU et al., 2015).

Depending on how interactions between active agent, polymer and CO_2 occur during impregnation process, a physicochemical attachment of targeted compounds to the active sites of polymer matrix can arise, or a physical entrapment of the active agent in polymer network takes place when CO_2 is removed (MANNA et al., 2007; VARONA et al., 2011).

Numerous plastic materials are commercialized for active packaging applications, including polyethylene and its derivatives, such as the linear low-density polyethylene (LLDPE). These polymers are one of the most employed due to their good mechanical resistance, thermal stability, high water vapor barrier property and availability (PEYCHÈS-BACH et al., 2009).

In this sense, the main goal of this work was to incorporate CEO into a polymeric film of LLDPE by using supercritical CO_2 as impregnation fluid, evaluating the influence of operational conditions (pressure, temperature, CEO:CO_2 mass ratio, and impregnation time) on CEO incorporation in LLDPE films by means of near-critical and supercritical CO_2 impregnation, quantifying the amount of CEO impregnated, the eugenol content into the film, as well as thermal and mechanical properties of polymer films after impregnation process.

3.2 Materials and methods

3.2.1 Materials

Pellets of LLDPE (MFI: 0.95 g/10 min at 190 °C/2.16 kg, density: 919 kg m^{-3}, Dowlex TG 2085B) were kindly supplied by Videplast (Videira, SC, Brazil). Clove essential oil (*Eugenia caryophyllus* leaves, 99%, CAS Number 8015-97-2) obtained by steam distillation was purchased from Ferquima (Brazil). Carbon dioxide (99.9%, White Martins, Brazil) was used as impregnation medium. Other chemicals of analytical grade for GC analyses included eugenol standard (> 99%, Sigma-Aldrich, Brazil), helium (99.9%, White Martins, Brazil),

chloroform (99.5%, Sigma-Aldrich, Brazil) and methanol (99.97% HPLC grade, J. T. Baker, Mexico).

3.2.2 Film preparation

The LLDPE films were produced by thermo-compression of pellets in a hydraulic press (PHS 15t, Ico Comercial, Brazil) at 130 °C, using a 250 μm polyester film as frame, as detailed in Appendix A.1. First, 4 g of LLDPE pellets were placed at the center of frame without applying pressure to ensure a uniform heat flow during 5 min throughout the material until melting. Then, pellets were gradually pressed under 0.3 MPa (30 s), 1.3 MPa (1.5 min), 2 MPa (3 min), and 2.6 MPa (5 min) to liberate trapped air bubbles (RAMOS et al., 2012). The obtained film was removed from the press, cooled at room temperature (25 °C) and stored in desiccator until impregnation experiments. They were transparent, flexible and homogeneous without trapped air bubbles, with average thickness of 300 μm measured with a digital micrometer (Mitutoyo, Japan, ±0.001 mm accuracy) at three random positions.

3.2.3 CEO impregnation in LLDPE films

The CEO impregnation in LLDPE films was conducted in a variable-volume high-pressure cell schematically represented in Figure 3.1. The experimental apparatus and procedure is the same employed in a variety of previous studies (ROSSO et al., 2013; BENELLI et al., 2014; REBELATTO et al., 2015). Briefly, the apparatus consists of a variable-volume view cell with two sapphire windows (Swiss Jewel, USA) for internal visualization and a movable piston that allows the control of pressure inside the cell. The pressure is controlled by a syringe pump (260HP, Teledyne Isco, USA), wherein the solvent (CO_2) acts as pneumatic fluid of pressurization. The system pressure is measured by a pressure transducer (LD301, Smar, Brazil) and viewed by a universal indicator (N1500, Novus, Brazil). The cell is connected to a thermostatic water bath (MQBTC99-20, Microquímica, Brazil) and a thermocouple J type (Salcas, Brazil). A magnetic stirrer (753A, Fisatom, Brazil) and a Teflon-coated stirring bar maintained the continuous agitation of the cell content.

Before impregnation process, one sample of LLDPE film with 7.2 x 1.2 cm and 300 mg was placed inside the variable-volume view cell. The film sample was cut at the maximum length and width considering the inner dimensions of the cell. A precise amount of CEO was weighed

in analytical balance (AUY 220, Shimadzu, Philippines, ±0.0001 g accuracy) and loaded into the cell. A known amount of CO_2 in liquid state at 7 °C and 100 bar (density of 0.9374 g cm^{-3} (LEMMON; MCLINDEN; FRIEND, 2001)) was loaded using the syringe pump until a desired mass ratio of CEO to CO_2 was achieved.

Figure 3.1. Schematic diagram of experimental apparatus for impregnation. CV: check valve; BV: ball valve; NV: needle valve; PT: pressure transducer; TC: thermocouple J type; MS: magnetic stirrer. Adapted from Franceschi et al. (2006).

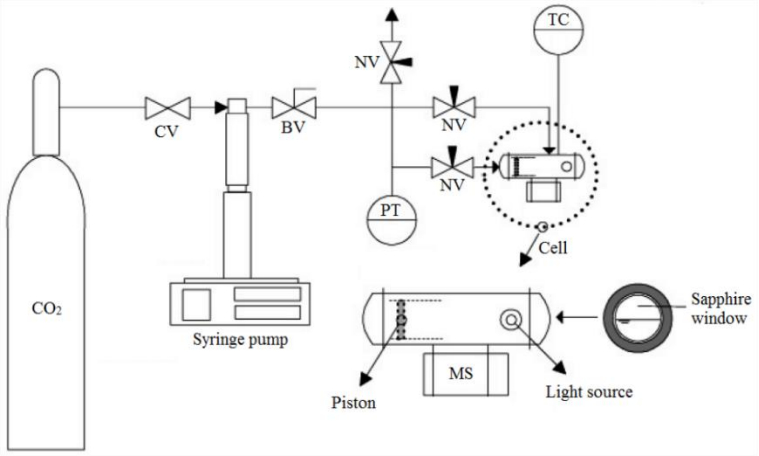

Impregnation assays were performed under the subsequent conditions: CEO:CO_2 mass ratios (2 and 10%), pressures (150 and 250 bar), and temperatures (25, 35 and 45 °C). The level of process variables was based on phase equilibria of CEO and CO_2 (SOUZA et al., 2004) and of eugenol and CO_2 (CHENG et al., 2000), to define operation in a single phase system at the lowest possible pressure, covering liquid and supercritical regions, also considering the maximum internal volume of the cell. Thermophysical properties of pure components (eugenol, major component of CEO, and CO_2) and their mixtures at different mass fractions are presented in Appendix A.2. The 4 h of processing time was defined by assuming that CEO was impregnated only by diffusion. This estimation took into account: the thickness of LLDPE films (300 µm); the effective diffusion coefficient of eugenol in LLDPE (3.5 x 10^{-13} m^2 s^{-1} at 40 °C) (DHOOT et al., 2009); the CEO solubility in CO_2 (0.230 g of oil/g of CO_2 at 35 °C and 100 bar) (RODRIGUES et al., 2002); and the maximum CEO:CO_2 mass ratio used in this study (0.1 g of CEO/g of

CO_2). All the operational conditions were analyzed in duplicate, totalizing 24 experiments at batch mode. The experimental procedures for pressurization and depressurization of the high-pressure system are described in Appendices B.1 and B.2.

Once finished the impregnation time, the system was depressurized, the LLDPE films were recovered from the cell and the non-impregnated CEO remaining on film surface was removed by using a paper towel. Afterwards, LLDPE films were quickly washed by dipping in methanol at room temperature (25 °C) to ensure no residual CEO on surface and weighed in analytical balance (AUY 220, Shimadzu, Philippines, ±0.0001 g accuracy) to determine the mass of CEO impregnated in LLDPE films (expressed as mg of CEO per g of film) by the gravimetric method. The impregnated films, protected by aluminum foil, were stored at -18 °C in a domestic freezer until characterization analyses. After one year of storage at this temperature, the mass of impregnated films were measured in order to measure the CEO retention in LLDPE films. Results are presented in Appendix A.3.

The conditions for kinetic assays were based on previous results of CEO impregnation as function of pressure, employing the specified conditions: constant pressure (150 bar), CEO:CO_2 mass ratios (2 and 10%) and temperatures (25, 35 and 45 °C), varying the impregnation time in intervals up to 4 h. Each kinetic point represented a different assay (destructive experiments). Kinetics of conventional CEO incorporation by immersing LLDPE films in CEO without applying pressure was also performed. For this assay, the LLDPE film was placed in a Petri dish with 5 mL of CEO at 25 °C for 4 hours. At each pre-established time, the film was removed from the dish, carefully cleaned with paper towel, washed in methanol, weighed in analytical balance (AUY 220, Shimadzu, Philippines, ± 0.0001 g accuracy) and placed back in contact with CEO until next measurements.

3.2.4 Chemical composition of CEO and quantification of eugenol

The chemical composition of CEO used in impregnation assays was determined in a gas chromatograph equipped with a mass spectrophotometer (GC-MS, model 7890 A, mass detector 5975C, Agilent Technologies, USA), attached to a HP-5MS column (30 m x 0.25 mm internal diameter, 0.25 µm film thickness, Agilent Technologies, USA). Helium was the carrier gas with 1 mL min^{-1} flow rate, split ratio 1:50, injector and detector temperatures of 240 and 250 °C, respectively, while column temperature was linearly programmed at rate

of 3 °C min^{-1} from 70 to 180 °C (GUAN et al., 2007). Then, 1 µL of CEO solution (1% v/v in chloroform) was injected into the equipment and the main components were identified by comparing their mass spectra and retention times with NIST 11 mass spectral library available on the GC-MS equipment.

The amount of eugenol, the major component of CEO, impregnated in LLDPE films was determined in a gas chromatograph coupled to a flame ionization detector (GC-FID, model 7890 A, Agilent Technologies, USA), attached to a HP-5MS column (30 m x 0.25 mm internal diameter, 0.25 µm film thickness, Agilent Technologies, USA). The helium (carrier gas) flow rate was 1 mL min^{-1}, split ratio of 1:20, injector and detector temperatures of 250 °C, and column temperature was linearly programmed at rate of 6 °C min^{-1} from 60 to 250 °C. Impregnated film samples (120 mg) were contained into glass vials with 10 mL of methanol. These vials were sealed and left to extract for 24 h at room temperature (25 °C). Then, a second extraction was performed in which the same film samples were placed in fresh methanol (10 mL) and left to extract for further 24 h to ensure a complete release of eugenol in methanol (AVISON et al., 2001). Aliquots from the two extractions (1 µL) were injected into the equipment. The quantification was based on an analytical curve of eugenol standard in methanol, which was linear over the concentration range of 5 to 200 µg mL^{-1} with a coefficient of determination of 0.999.

3.2.5 Mechanical properties

The tensile strength, elongation at break and Young's modulus of film samples before and after CEO impregnation were determined in a texture analyzer (TA-HD Plus, Stable Micro Systems, UK) to evaluate the effect of high-pressure processing and CEO incorporation on mechanical properties of LLDPE films according to ASTM D882-12 method (ASTM D882-12, 2012). Tensile tests were conducted with samples of 72 x 6 mm using a 750 kg load cell, initial grip separation of 30 mm and crosshead speed of 10 mm s^{-1}.

3.2.6 Differential scanning calorimetry (DSC)

Thermal properties of untreated and CEO-impregnated LLDPE films were determined using a Perkin-Elmer differential scanning calorimeter (Jade DSC, USA) previously calibrated with indium and zinc. Samples of approximately 7 mg were sealed in aluminum pans and heated

at 10 °C min^{-1} from -10 to 150 °C with nitrogen flow of 20 mL min^{-1}. The melting temperature (T_m) and enthalpy of fusion (ΔH_m) were taken from the first and second heating curves, in agreement with ASTM D3418-12 method (ASTM D3418-12, 2012). The crystallinity (χ) percentage of each sample was calculated according to Equation 3.1 (RAMOS et al., 2012).

$$\chi(\%) = \frac{\Delta H_m}{W \Delta H_m^0} \times 100 \qquad (3.1)$$

in which ΔH_m (J g^{-1}) is the experimental LLDPE enthalpy of fusion, W is the LLDPE mass fraction in samples (excluding the impregnated CEO mass fraction), and ΔH_m^0 is the theoretical enthalpy of fusion of 100% crystalline LLDPE, assumed as 288.7 J g^{-1} (SEGUELA; RIETSCH, 1986).

3.2.7 Attenuated total reflectance Fourier transform infrared (ATR-FTIR) spectroscopy

The evidence of CEO impregnation in LLDPE films was evaluated in a FTIR spectrometer (Cary 600 series, Agilent Technologies, Brazil) equipped with an ATR crystal of zinc selenide. The FTIR spectra of CEO as well as the LLDPE films before and after impregnation were obtained with resolution of 4 cm^{-1} in a wavenumber range from 4000 to 400 cm^{-1} and 30 scans (TORRES et al., 2014).

3.2.8 Confocal fluorescence microscopy

The presence and distribution of impregnated CEO in LLDPE films were determined by confocal fluorescence microscopy, employing Nile red as lipophilic fluorescent stain. The CEO was dyed in a concentration of 0.1 mg of Nile red per mg of oil (ZIANI et al., 2011). The mixture was covered with aluminum foil to avoid photobleaching and stirred until complete dissolution. The dyed CEO was loaded into the cell and impregnation was performed for a selected condition of constant pressure (150 bar) and temperature (45 °C) using two CEO:CO_2 mass ratios (2 and 10%). The fluorescence visualization was achieved in a confocal microscope (CTR 6500, Leica Microsystems, Germany) using 20x objective lens. The emission spectra for Nile red was detected in the wavelength range from 590 to 700 nm.

3.2.9 Statistical analysis

The results of CEO impregnation and thickness of LLDPE films were statistically evaluated by ANOVA procedures of Statistica software version 13 (Dell Inc., USA) with Tukey's test when significant differences at level of 5% were observed.

3.3 Results and discussion

3.3.1 CEO impregnation with near-critical and supercritical CO_2

The CEO was completely soluble in CO_2 in all conditions of CEO:CO_2 mass ratios (2 and 10%), pressures (150 and 250 bar) and temperatures (25, 35 and 45 °C) covered in this study, as visualized though the sapphire windows, evidencing that the system was in single phase region. The results of impregnated mass of CEO and eugenol per mass of LLDPE film, expressed as mg g^{-1}, gravimetrically and chromatographically determined as function of processing conditions after 4 h of impregnation are presented in Table 3.1. Values of impregnation efficiency (*I*%) are presented in Appendix A.6.

The impregnation values in gravimetric method ranged from 10.5 to 40.2 mg of CEO per g of LLDPE, with the highest amount incorporated at 45 °C and 10% CEO:CO_2 mass ratio and the lowest at 25 °C with 2% mass ratio. In both cases, the pressure enhancement was not statistically significant. Analogously, Goñi et al. (2016) obtained the highest incorporation of eugenol in LLDPE films at 150 bar and 45 °C. Lower CO_2 pressures also increased the amount of 2-nonanone impregnated in LLDPE films (ROJAS et al., 2015). On the contrary, Torres et al. (2014) varied the pressure from 70 to 120 bar at constant temperature of 35 °C and observed an increase on thymol retention in LLDPE films, with a maximum value of 15.2 mg of active agent per g of polymer. Thus, the best impregnation conditions in this study were achieved with increasing temperature and CEO:CO_2 mass ratio whereas the pressure augmentation did not exert significant effect, which means that the active compound incorporation can be performed at lower pressures. In addition, the highest amount of impregnated CEO in LLDPE films (40 mg of CEO per g of film) has the potential to inhibit yeasts and molds growth at concentrations ranging from 25 to 40 mg of CEO per g of film. This observation is based on studies reported by López et al. (2007) and Wang et al. (2011) that determined antimicrobial activity of CEO-loaded films.

Table 3.1. Impregnated mass of CEO and eugenol in LLDPE films under different operational conditions of P, T and CEO:CO_2 mass ratios.

P (bar)	T (°C)	Mass ratio (%)	Mass of CEO (mg g^{-1})[1]	Mass of eugenol (mg g^{-1})[2]	Eugenol/CEO mass ratio (%)
150	25	2	14.4 ± 2.1^{d}	14.3	99
250			10.5 ± 0.9^{d}	11.5	109
150	35		21.3 ± 1.9^{c}	23.8	112
250			12.7 ± 0.2^{d}	15.1	119
150	45		33.3 ± 0.7^{a}	35.9	108
250			26.9 ± 1.2^{b}	32.3	120
150	25	10	20.4 ± 2.0^{C}	21.1	103
250			18.1 ± 1.8^{C}	18.5	102
150	35		27.7 ± 2.6^{B}	31.8	115
250			23.7 ± 1.1^{BC}	25.2	106
150	45		40.2 ± 1.8^{A}	43.9	109
250			38.1 ± 0.2^{A}	41.3	108

[1] Same letter in the same column indicate no statistical difference between values ($p < 0.05$): Uppercase letters compare impregnations with 10% mass ratio; Lowercase letters compare impregnations with 2% mass ratio. Results determined by gravimetric method.
[2] Results determined by chromatographic method.

The high-pressure impregnation takes the advantage of both solubility and diffusivity properties of CO_2, which are boosted by temperature and pressure control. This fluid solubilizes many active compounds, especially lipophilic and low molecular weight ones, due to a good solvation power closely related with its relative high density. Moreover, the high diffusivity and low viscosity facilitates CO_2 diffusion through several polymer matrices, by reversible swelling and plasticization effect. A swollen polymer has an increased free volume that enables further entrance of CO_2 and allows a free motion of the active molecules between the polymer chains. In this context, the mechanism by which an active compound is incorporated in a polymer matrix can be explained by two main steps. The first involves the active compound solubilization in supercritical CO_2 followed by the diffusion of active compound-loaded CO_2 into the polymer matrix. After the impregnation time, as the system is rapidly depressurized, the supercritical CO_2 leaves the matrix almost instantaneously, returning to its gaseous state (at atmospheric pressure) and the solubility of the active compound is reduced, while the polymer macrostructure is restored to its original

structure. As consequence of depressurization, the active compound molecules, which are not soluble in gaseous CO_2, remain entrapped in the polymer matrix (AVISON et al., 2001; DÍEZ-MUNICIO et al., 2011; CHAMPEAU et al., 2015). In this situation, the CO_2 can be viewed as a carrier that favors compound impregnation, resulting in a polymer matrix free of solubilizing agent after system depressurization.

An increased active compound incorporation was observed when increasing the CEO:CO_2 mass ratio. In this case, this result can be attributed to the higher concentration gradient, which is the driving force for impregnation, besides an increased affinity of CEO to the matrix. When elevating the temperature from 25 to 45 °C, the diffusion rates of CEO and CO_2 are increased into the polymer matrix due to the reduction of CO_2 density coupled with the increase of polymer chain mobility (AVISON et al., 2001). Thus, the concentration gradient enhancement associated with an increased diffusion rate of the active agent in high-pressure medium was able to promote the highest impregnation. On the other hand, pressure exerted almost no influence on CEO incorporation when it was augmented from 150 to 250 bar. This observation is closely related to CEO solubility in high-pressure CO_2: with increasing pressure and CO_2 density, as consequence, the active agent solubility is enhanced due to the high solubilization power of CO_2, which strengthen interactions between CEO and CO_2 (SOUZA et al., 2004; SOVOVÁ, 2012). For this reason, it would be expected an increase of active compound impregnation, as the more the CO_2 is loaded and the easier it diffuses through the polymer matrix, the larger should be the uptake. However, the opposite effect was experimentally observed. Once the system is rapidly depressurized, the essential oil tends to diffuse out from the LLDPE film because of its high affinity with CO_2, especially at higher pressures as 250 bar, thus reducing the amount of CEO remained in the polymer matrix after processing.

In addition to the aforementioned, an inverse linear correlation was established for the CEO impregnation as function of CO_2 density, as best viewed in Figure 3.2, in which the highest impregnated amount of active agent was achieved at the lowest CO_2 density. This effect can be attributed to the high CEO affinity to the CO_2 phase as function of increasing pressure. This observation corroborates with previous discussion about the effect of pressure on impregnation, once higher density values favor the CEO-CO_2 interaction in detriment of CEO-LLDPE interaction during system depressurization, thus influencing the mass of essential oil retained in the film.

Figure 3.2. Impregnated mass of CEO in LLDPE films as function of CO_2 density. The points represent the experimental conditions: [150 bar, 45 °C], [150 bar, 35 °C], [250 bar, 45 °C], [150 bar, 25 °C], [250 bar, 35 °C] and [250 bar, 25 °C] for 2 and 10% CEO:CO_2 mass ratio. Data points contained in dashed squares correspond to the same CO_2 density. Values of CO_2 density obtained from NIST database (LEMMON; MCLINDEN; FRIEND, 2001).

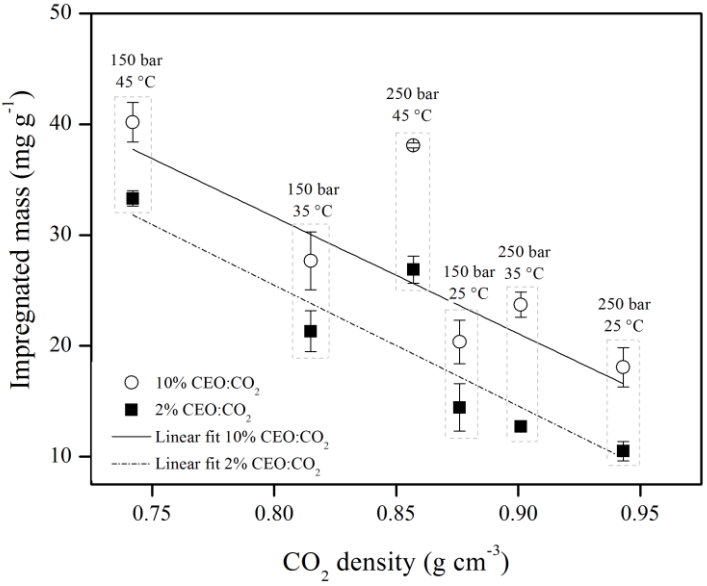

3.3.2 Chemical composition of CEO and quantification of eugenol

The sample chromatogram obtained by GC-MS allowed the identification of three components in CEO. Eugenol was the major component, followed by β-caryophyllene and α-humulene. Results are presented in Table 3.2 and in Figure 3.3. These results are in accordance with the Technical information of CEO provided by Ferquima (Brazil), as presented in the Annex.

Table 3.2. Components identified in CEO by GC-MS.

Compound	RT[1] (min)	Peak area (%)
Eugenol	15.56	89.86
β-caryophyllene	17.82	9.00
α-humulene	19.11	1.14

[1] RT: retention time.

Figure 3.3. Chromatogram of pure CEO.

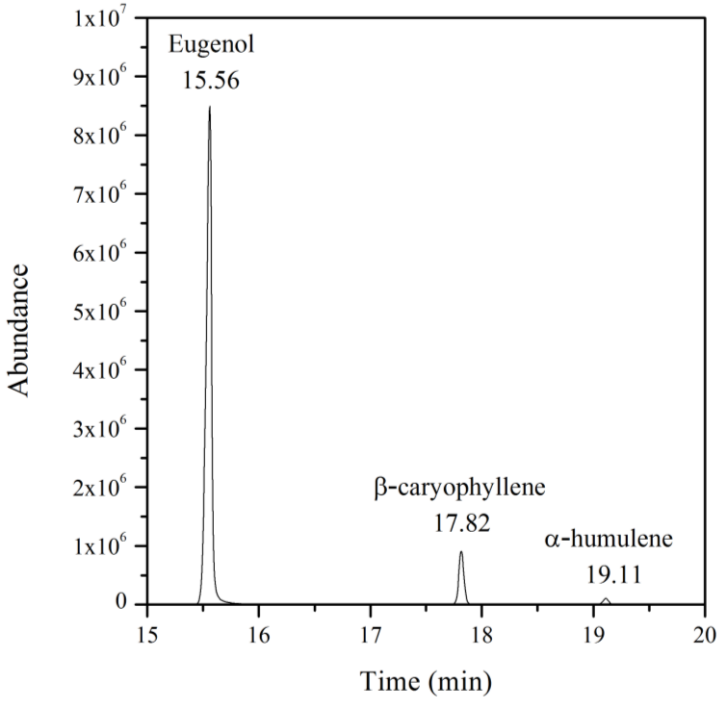

The quantification of eugenol incorporated in LLDPE films was determined by GC-FID. Impregnated films were subjected to two extraction procedures by using methanol. The CEO and eugenol quantification by gravimetric and chromatographic methods showed similar and coherent results, as expected, since the CEO is naturally rich in eugenol (Tables 3.1 and 3.2). Although the chromatographic method is more accurate than the gravimetric, as observed by the small differences in individual values, the gravimetric procedure can be employed in situations where fast insights on impregnation processing are required, as it is simple to perform for a large number of samples with relatively good approximation of results. In addition, the impregnated eugenol/CEO mass ratio suggested a preferential eugenol impregnation in samples processed with 10% CEO:CO_2 mass ratio at 150 bar as well as in those impregnated with 2% mass ratio at 250 bar. The combined effect of pressure and concentration gradient in such cases probably favored the solubilization of eugenol-rich fraction of CEO under high-pressure CO_2, which is driven by thermodynamic interactions and mass transfer phenomena.

It is important to emphasize that the high amount of eugenol in CEO directly impacts on the potential antimicrobial and antioxidant activities of CEO-loaded LLDPE films. However, it is also important to consider a synergistic effect of its three main components in biological activities, especially due to the presence of sesquiterpenes β-caryophyllene and α-humulene, which are reported to act as strong microbial inhibitors (MICHIELIN et al., 2009). In fact, essential oils from natural sources are composed by a variety of compounds and there is an evidence that even minor components play a significant role on antimicrobial and antioxidant activities that is attributed to the synergism between them (BURT, 2004; CABRAL; PINTO; PATRIARCA, 2013; RIBEIRO-SANTOS et al., 2017a). Jirovetz et al. (2006) reported that CEO exhibited higher antioxidant activity than its major component, eugenol, and the synthetic antioxidants butylated hydroxytoluene (BHT) and butylated hydroxyanisole (BHA). These results were expressed in scavenging ability against the 2,2-diphenyl-1-picrylhydracyl (DPPH) radical and reinforce the evidence of synergistic effect between the components in the essential oil when compared with pure and chemically synthesized ones.

3.3.3 Mechanical properties

Representative stress-strain curves of pure and CEO-impregnated LLDPE films processed during 4 h at 150 bar and 45 °C with 2 and 10% CEO:CO_2 mass ratios are presented in Figure 3.4. The same behavior of stress-strain curves was observed for all analyzed samples, indicating a curve profile typical of semicrystalline and flexible polymer materials with neck formation that represents the plastic deformation determined by the yield point after the initial reversible linear part of the curve (NADDEO et al., 2001).

The mechanical properties determined from these curves included the tensile strength at break, elongation at break and Young's modulus. The values of these parameters and the correspondent film thickness are described in Table 3.3. Samples processed with high-pressure CO_2 in absence of essential oil did not present significant modifications on their mechanical properties compared with non-processed LLDPE films. In addition, it could be observed a decreasing trend in the values of mechanical parameters when increasing the CEO content in LLDPE films. In the specific case of films processed at 150 bar, 45 °C with 10% mass ratio, which was the condition of highest CEO incorporation, the reduction of mechanical properties was equal to 31%, 11% and 14% for

tensile strength at break, elongation at break and Young's modulus. The reduction in tensile properties can be attributed to the mobility of polymer chains caused by essential oil incorporation in LLDPE films, thus modifying their mechanical properties. These results suggest a plasticization of polymer matrix caused by CEO impregnation, as also reported for LLDPE films incorporated with different essential oils (TORRES et al., 2014; GOÑI et al., 2016).

Figure 3.4. Stress-strain curves of LLDPE films before and after CEO impregnation (P = 150 bar; T = 45 °C; CEO:CO_2 mass ratio = 2 and 10%).

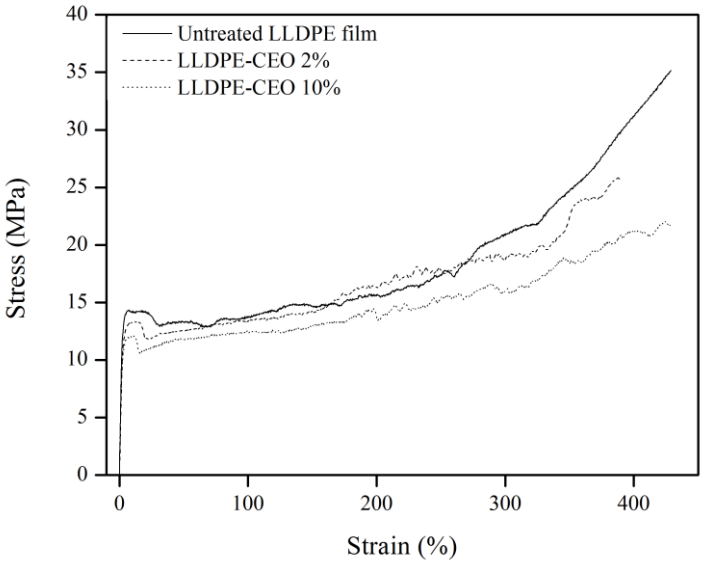

Table 3.3. Mechanical properties of original, treated with CO_2 and CEO-impregnated LLDPE films.

Sample	P (bar)/T (°C)/CEO:CO_2 mass ratio (%)	Film thickness (μm)[1]	Tensile strength at break (MPa)	Elongation at break (%)	Young's modulus (MPa)
Pure LLDPE	-	291 ± 21	34.7 ± 2.1	399 ± 53	410 ± 46
LLDPE-CO_2	150/25/-	310 ± 22	32.7 ± 5.2	414 ± 74	370 ± 178
	250/25/-	314 ± 5	36.4 ± 0.3	353 ± 18	364 ± 30
	150/35/-	300 ± 9	35.6 ± 0.7	393 ± 34	573 ± 26
	250/35/-	305 ± 6	31.3 ± 1.0	361 ± 60	358 ± 116
	150/45/-	295 ± 22	40.0 ± 1.7	423 ± 17	261 ± 104
	250/45/-	337 ± 7	42.2 ± 1.4	455 ± 35	328 ± 76
LLDPE-CEO	150/25/2	325 ± 37	29.6 ± 6.8	373 ± 66	308 ± 23
	250/25/2	330 ± 36	32.8 ± 0.6	362 ± 56	289 ± 40
	150/35/2	310 ± 43	30.8 ± 0.9	409 ± 3	254 ± 14
	250/35/2	314 ± 49	38.1 ± 0.9	481 ± 16	366 ± 124
	150/45/2	295 ± 54	28.0 ± 3.0	418 ± 43	293 ± 69
	250/45/2	290 ± 39	35.2 ± 0.5	484 ± 11	284 ± 41
	150/25/10	288 ± 63	27.5 ± 7.4	350 ± 146	397 ± 67
	250/25/10	297 ± 36	30.3 ± 2.3	491 ± 9	427 ± 33
	150/35/10	293 ± 59	30.8 ± 1.5	460 ± 42	434 ± 86
	250/35/10	324 ± 51	26.4 ± 2.5	304 ± 2	358 ± 3
	150/45/10	302 ± 56	24.0 ± 0.8	355 ± 200	353 ± 41
	250/45/10	304 ± 39	31.9 ± 6.4	422 ± 34	368 ± 89

[1] No statistical difference between values ($p < 0.05$).

3.3.4 Thermal properties

The effect of high-pressure processing and CEO impregnation on thermal properties of LLDPE films was analyzed by DSC. Data from the first and second heating curves are shown in Table 3.4. The LLDPE films presented melting temperature at around 120 °C, with no major influence of high-pressure processing with pure CO_2 or CEO impregnation. The glass transition temperature (T_g) of LLDPE is around -110 °C (KHONAKDAR, 2015), which was not observed in the measured range of temperature.

The calculation of crystallinity degree was performed excluding the amount of CEO contained in samples. In the first heating curve, the crystallinity degree of pure LLDPE was equal to 64.5% and shifted to lower values after CEO impregnation. In the second heating curve, the crystallinity degree varied from 42-48%. These values of crystallinity degree are typical of semicrystalline polymers formed by linear chains with shorter branches, as the LLDPE (COUTINHO et al., 2003).

From these data, the melting temperature and crystallinity degree of samples processed with pure CO_2 were not affected by high-pressure processing. Caskey, Lesser and McCarthy (2001) reported that the CO_2 in supercritical conditions acted as a reversible swelling agent and the crystallinity degree and melting temperature of LLDPE films remained unchanged after processing, which agrees with our results. However, a reduction in the crystallinity degree of CEO-impregnated samples, which is best viewed in data from the first heating curve, may indicate a reorganization of polymer chains after CEO impregnation. Additionally, the lowest T_m value in the first and second heating curves was observed for samples processed at 45 °C with 10% CEO:CO_2 mass ratio, the condition of highest active compound incorporation. The T_m reduction, in this case, may be attributed to molecular interactions between CEO and ethylene molecules. The presence of active agents favors the mobility and reorganization of low molecular weight polymer chains, reducing the melting temperature and crystallinity degree of films (ČUČEK et al., 2013). Similar results were reported after eugenol impregnation in commercial LLDPE films (GOÑI et al., 2016) and thymol impregnation in extruded LLDPE films (TORRES et al., 2014).

Table 3.4. Melting temperature (T_m), enthalpy of fusion (ΔH_m) and crystallinity degree (χ) of pure, treated with CO_2 and CEO-impregnated LLDPE films.

Sample	P (bar)/T (°C)/CEO:CO_2 mass ratio (%)	First heating curve			Second heating curve		
		T_m (°C)	ΔH_m (J g^{-1})	χ (%)	T_m (°C)	ΔH_m (J g^{-1})	χ (%)
Pure LLDPE	-	121.4	186.3	64.5	120.0	147.1	47.0
LLDPE-CO_2	150/25/-	-	-	-	121.2	120.1	41.6
	250/25/-	-	-	-	121.0	135.1	46.8
	150/35/-	-	-	-	121.0	128.5	44.5
	250/35/-	-	-	-	121.0	135.9	47.1
	150/45/-	-	-	-	121.2	130.5	45.2
	250/45/-	-	-	-	121.6	127.2	44.1
LLDPE-CEO	150/25/2	122.7	181.8	62.3	121.5	126.0	43.2
	150/35/2	121.1	129.0	43.8	120.4	125.1	42.5
	150/45/2	120.9	179.1	60.1	119.5	140.3	47.1
	150/25/10	120.8	187.7	63.8	119.5	141.4	48.1
	150/35/10	121.0	134.5	45.3	119.8	128.1	43.2
	150/45/10	120.8	163.5	54.6	119.4	134.3	44.8

Representative DSC curves of pure LLDPE, CO_2-treated and CEO-impregnated films at 150 bar and 45 °C with 10% CEO:CO_2 mass ratio are exhibited in Figure 3.5, with data from the second heating curve. The same behavior was observed for all analyzed samples, from the first and second heating curves.

Figure 3.5. DSC curves of pure, CO_2-treated (150 bar, 45 °C) and CEO-impregnated LLDPE films (150 bar, 45 °C, 10% CEO:CO_2 mass fraction).

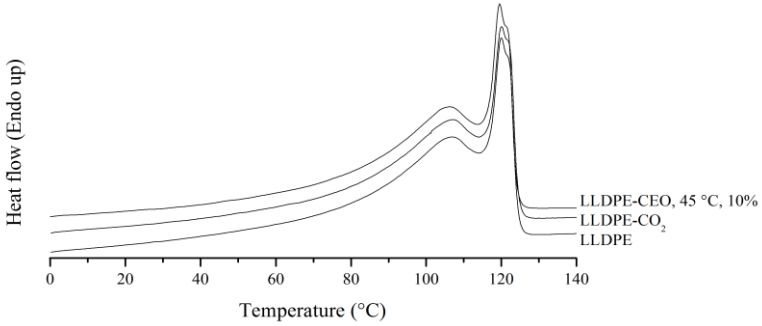

It is also important to highlight that CEO impregnation by means of high-pressure CO_2 was performed below the active compound degradation temperature, reported to be above 50 °C (SCOPEL et al., 2014), indicating that CEO components were not thermally degraded. In general, no significant differences of thermal and mechanical properties were observed between CEO-impregnated, supercritical CO_2-treated and pure LLDPE samples, so the film properties remained stable after processing, which is advantageous for impregnation purposes. In fact, taken into account published results of supercritical CO_2 impregnation of thymol in LLDPE films produced by extrusion in pilot extruder (TORRES et al., 2014) and of eugenol incorporation in commercial LLDPE films (GOÑI et al., 2016), no remarkable differences on mechanical and thermal properties were observed between those films and the LLDPE films produced by thermo-compression, as in this study, demonstrating that different techniques can be employed to produce polymer films for active packaging applications.

3.3.5 Kinetic assays of CEO impregnation

The CEO impregnation in LLDPE films as function of different operational conditions (Table 3.1) evidenced that the pressure of 150 bar

has the potential to incorporate higher amounts of active agent when compared to 250 bar. Therefore, considering that 150 bar was the lowest pressure employed in impregnation runs for a system in single phase (Section 3.2.3) and that it implies in low energy consumption, it was defined to perform the kinetic assays of CEO impregnation while varying the parameters: CEO:CO_2 mass ratio, temperature and impregnation time.

As shown in Figure 3.6, the highest amount of active agent was incorporated at 45 °C with 10% CEO:CO_2 mass ratio under all impregnation times. For all temperatures and mass ratios covered in impregnation kinetic assays, the amount of CEO incorporated at 2 and at 4 h was very similar, indicating that the active compound impregnation in LLDPE films can be performed in 2 h or less, which is favorable for reducing operational costs and processing time. In addition, the maximum incorporated amount of CEO by high-pressure impregnation at 150 bar, 45 °C and 10% CEO:CO_2 mass ratio was 8 times higher than the impregnated amount by the conventional method (immersion without pressure). This result reinforces the potential of using CO_2 as impregnation medium due to an increased CEO incorporation in polymer films, employing lower amounts of active agent and reducing processing time.

Figure 3.6. Kinetic assays of CEO impregnation in LLDPE films by high-pressure (150 bar) and conventional methods.

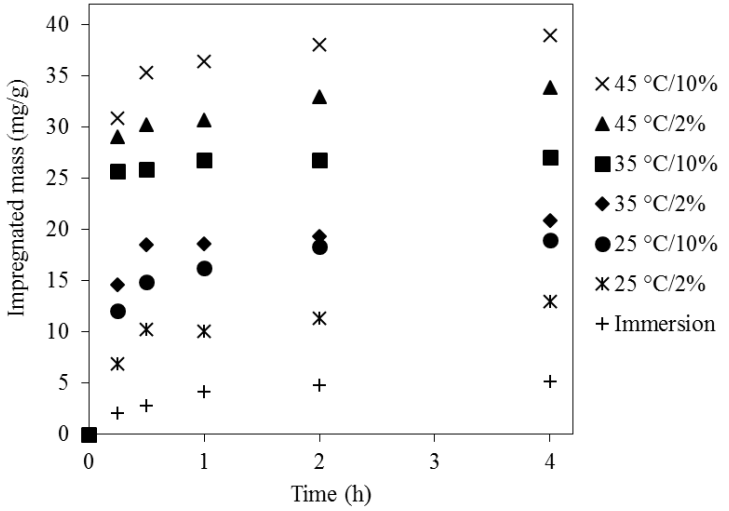

These results also suggest that the effective diffusion coefficient of the mixture CEO-CO_2 in LLDPE is higher than that of pure eugenol diffusing without pressure in LLDPE, as reported by Dhoot et al. (2009). The differential of this work is directly related to the employment of high-pressure CO_2 to impregnate active agents in polymer films, which is advantageous due to the presence of CO_2 that solubilizes and carries the active components through the polymer network, making the process faster than those employing only the pure component in absence of pressure.

3.3.6 ATR-FTIR analysis

The evidence of CEO impregnation in LLDPE films as well as possible interactions between the active agent and the polymer matrix on the solid state were evaluated by ATR-FTIR spectroscopy. The spectra of pure essential oil, untreated and CEO-impregnated LLDPE films processed at 150 bar and 45 °C employing the CEO:CO_2 mass ratios of 2 and 10% are shown in Figure 3.7, which are representative of samples processed under all other operational conditions. The dashed square highlights the region from 1550 to 1250 cm^{-1} in which the characteristic peaks of eugenol, the major component of CEO, were detected.

Figure 3.7. FTIR spectra of pure CEO, untreated and CEO-impregnated LLDPE films. (P = 150 bar; T = 45 °C; CEO:CO_2 mass ratio = 2 and 10%).

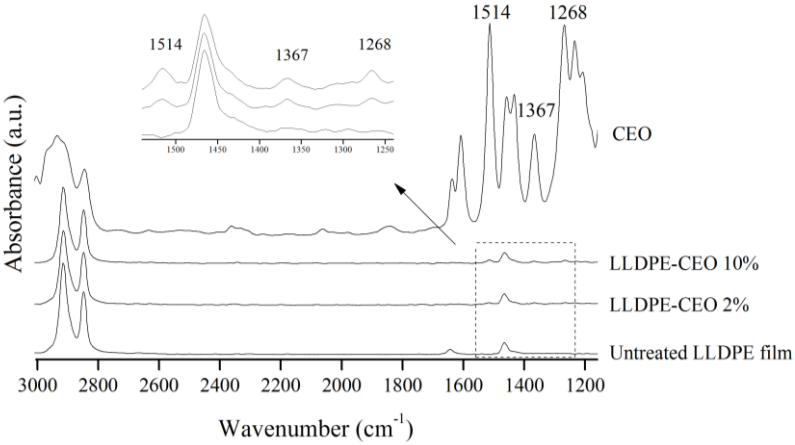

It was observed an augmentation of absorbance peaks at 1514 and 1268 cm^{-1} bands when the concentration of CEO was increased from 2 to 10%, thus confirming the presence of the active agent in impregnated samples and its enhancement with the concentration gradient. These peaks are attributed to the stretching vibration of R−C=C chemical bound of aromatic ring of eugenol and its phenolic hydroxyl, respectively (WANG et al., 2011). Moreover, the characteristic peaks of CEO and LLDPE did not disappear or shift, implying that neither chemical bonding nor structural modifications have occurred between the active agent and the polymer matrix during impregnation. These results also indicate a physical entrapment of the active agent in the polymer matrix that may occur due to molecular interactions with no major influence on thermal and mechanical properties of impregnated films, as previously discussed.

3.3.7 Confocal fluorescence microscopy

The presence and distribution of CEO in LLDPE films were evaluated by confocal fluorescence microscopy employing Nile red as lipophilic fluorescent dye. The stained CEO was impregnated in polymer films under conditions of the highest active compound incorporation (150 bar, 45 °C, 2 and 10% CEO:CO_2 mass ratio). The micrographs of Nile red fluorescence distribution, as well as the bright field and merged images of samples are presented in Figure 3.8.

Confocal fluorescence images not only allowed to confirm the presence of CEO in samples, but also to qualitatively analyze the impregnation homogeneity based on the differences of red fluorescence intensity patterns in micrographs. Moreover, neither residual CEO droplets on film surface nor color modifications were observed in impregnated films, since all samples were washed in methanol before characterization analyses. For this reason, the large spots noticed in images with 10% mass ratio were located inside polymer films, once the essential oil possibly interacted only with amorphous regions of the polymer matrix and these spots may be concentrated in amorphous domains.

Figure 3.8. Confocal fluorescence microscopy images of CEO-impregnated LLDPE films. Left: CEO stained with Nile red, middle: bright field, right: merged

images, scale bars: 50 µm. (P = 150 bar; T = 45 °C; CEO:CO_2 mass ratio = 2 and 10%).

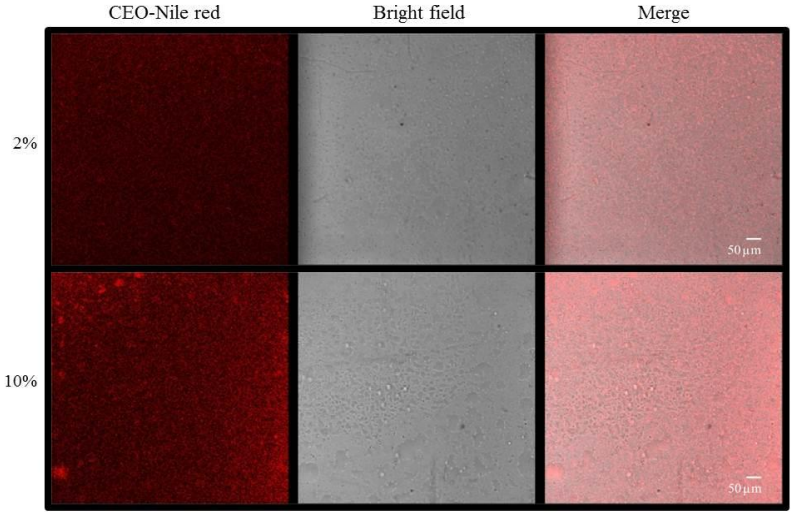

3.4 Conclusions

Studies related to the CEO incorporation in polymer films intended for active packaging development by means of high-pressure CO_2 impregnation are innovative in literature. The differential of this study is related to the employment of CO_2 under high-pressure conditions to incorporate CEO in LLDPE films: a clean process that uses CO_2 as solubilizing agent capable to carry the active components through the polymer chains, making the process faster than those employing only the pure component. The incorporation of CEO in LLDPE films was successfully performed in high-pressure medium in which the highest amount of impregnated active agent is achieved at the highest CEO:CO_2 mass ratio (10%) due to the increased concentration gradient for impregnation; the highest temperature (45 °C) that enhances CO_2 and CEO diffusion rates through the polymer matrix; and the lowest pressure (150 bar), which weaken interactions between CEO and CO_2, enhancing the amount of active compound retained in the polymer film. Therefore, higher CEO impregnation amounts are obtained in conditions of lower CO_2 density. This optimized operational procedure is also advantageous due to the reduction of processing time, besides promoting a homogeneous distribution of the active agent throughout the polymer.

The mechanical resistance and thermal properties of LLDPE films remained stable after high-pressure processing, which is of great relevance for industrial active packaging applications. The present results confirm that the impregnation of multicomponent active agents, especially thermosensitive ones, in polymer matrices assisted by high-pressure CO_2 technology is a promising field and can be a useful tool in the development of antimicrobial and antioxidant packaging films.

Acknowledgements

The authors acknowledge Videplast (Brazil) for supplying the LLDPE pellets, and Brazilian governmental agencies: National Council for Scientific and Technological Development (CNPq), project number 473153/2012-2, Foundation to Support the Research and Innovation in Santa Catarina State (FAPESC), project number 6342/2011-8, and Coordination for the Improvement of Higher Education Personnel (CAPES) for the financial support and G. R. Medeiros scholarship. The authors also thank the laboratories Central de Análises and Laboratório Central de Microscopia Eletrônica (LCME) from the Federal University of Santa Catarina for the technical support with characterization analyses.

Chapter 4: Impregnation temperature and depressurization rate effects on clove essential oil-LLDPE films obtained by high-pressure CO_2: thermomechanical and transport properties

Abstract
Clove essential oil (CEO) was impregnated in linear low-density polyethylene (LLDPE) films by high-pressure CO_2 technique. Impregnations were performed at 150 bar, 25 and 32 °C for 2 h followed by depressurization at 10, 50 and 100 bar min^{-1}. The influence of operational parameters was observed on impregnation, optical, topographic, morphological, and thermomechanical properties of films. Higher amounts of CEO were impregnated when reducing depressurization rate and increasing temperature, with a maximum of 26.83 mg CEO/g LLDPE. Diffusion mechanism governed CEO migration from LLDPE in aqueous and fatty food simulant fluids. The effective diffusion coefficient of CEO in LLDPE ranged from 5.4×10^{-13} to 1.0×10^{-12} m^2 s^{-1}. Operational parameters can be adjusted to enhance CEO incorporation, presenting negligible effect over diffusivity in LLDPE and thermomechanical properties. The results suggest the potential for developing active packaging materials by green processes that aggregate value to compounds from natural sources.

Industrial relevance
Innovative technologies for active food packaging attract the interest of food, pharmaceutical, and chemical industries. The CEO is a multicomponent active agent obtained from natural sources. An advantage of using such components in industrial applications is to keep synergistic effects in biological activities from the presence of some minor compounds, besides avoiding isolation and purification steps that increase processing costs. The high-pressure CO_2-assisted impregnation, an innovative and eco-friendly technology, allowed the incorporation of CEO in LLDPE films, producing polymer materials free of any solvent residues with potential application as active food packaging.

Keywords: active packaging; eugenol; *Eugenia caryophyllus*; controlled release; diffusion coefficient.

4.1 Introduction

Innovation and recent trends in food packaging technology result from consumer's preference towards products with enhanced shelf life and convenience. These factors in conjunction with changes in current lifestyle boost research and development of packaging systems without compromising food safety and quality (MAJID et al., 2016). Most foodstuffs are commercialized in packaged form. In this context, food packaging aims to prevent physical, chemical and microbiological contamination of foods during transport, distribution, handling, and storage until reaching final consumer. Furthermore, active agents can be incorporated in packaging materials to promote antioxidant and antimicrobial activities mainly on food surface where lipid oxidative process and microbial growth commonly starts (APPENDINI; HOTCHKISS, 2002). These food contact materials consist mostly of plastics, paper, and metals with or without coatings (SEILER et al., 2014).

The principle of incorporating active agents in packaging materials is related to the concept of active food packaging: a technological material incorporated of active substances capable to interact with foods. It may release or absorb substances, preventing or reducing food deterioration, prolonging shelf life and increasing the attractiveness of the packaged product to retailers and consumers (MUPPALLA et al., 2014; SEOW et al., 2014; FANG et al., 2017). In this type of packaging, substances initially present on packaging migrate from film to the contained product in a mass transfer process known as chemical migration (FRANZ, 2005; SEILER et al., 2014). For this reason, active food packaging can be seen as an alternative to reduce the number of chemical compounds commonly added to foods, also providing a sustained release of active components during storage. Furthermore, food spoilage often occurs on food surfaces and chemicals that are mixed directly with food may result in overuse (WENG; HOTCHKISS, 1993; GÓMEZ-ESTACA et al., 2014).

Active agents from natural sources are perceived by consumers as compounds of low health risk as most of them have the Generally Recognized As Safe (GRAS) status (SUPPAKUL et al., 2011). Among them, clove essential oil (CEO) is one of the most prominent multicomponent active agent obtained from natural sources due to its antimicrobial, antioxidant, antifungal, antiviral, and insecticidal properties. The strong biological activity of CEO is attributed to its high content of eugenol along with other components, such as β-caryophyllene and α-humulene (CHAIEB et al., 2007; GUAN et al., 2007; IVANOVIC et al., 2013). CEO can be obtained by extraction of clove buds or leaves

using different extraction processes, as hydro or steam distillation as well as extractions with organic solvents or supercritical CO_2 (REVERCHON; MARRONE, 1997; GUAN et al., 2007). An advantage of using natural and multicomponent active agents instead of pure and chemically synthesized ones is to keep synergistic effects from the presence of some minor compounds, besides avoiding isolation and purification steps that imply in increased processing costs (BURT, 2004; CABRAL; PINTO; PATRIARCA, 2013; SEOW et al., 2014).

Impregnation assisted by high-pressure carbon dioxide (CO_2) is an innovative manufacturing process to incorporate thermosensitive active agents in polymer matrices. In this technique, the film production and active compound incorporation occur in separated processes, avoiding exposure of active substances to high temperatures required in plastic film production (VARONA et al., 2011). It also takes the advantage of solubility and diffusivity properties of CO_2, which depends on pressure and temperature conditions of the system. CO_2 near or above its supercritical state is a reversible swelling and plasticizing agent of polymers due to its high diffusivity and low viscosity. The reversible swelling coupled with a near zero surface tension allows a rapid diffusion of CO_2 through the polymer network, resulting in an effective active compound incorporation at low temperatures (NALAWADE; PICCHIONI; JANSSEN, 2006; DÍEZ-MUNICIO et al., 2011). The active compound impregnation in polymer matrices by supercritical CO_2 is based on the following mechanisms: (i) the active compound solubilization in CO_2 under specific conditions of pressure and temperature, defined by phase equilibrium measurements; (ii) diffusion of solubilized active compound in the polymer network; and (iii) system depressurization and reduction of active compound solubility in CO_2. When CO_2 returns to atmospheric pressure, the active molecules remain entrapped in the polymer matrix, since they are not soluble in gaseous CO_2, and the packaging material is recovered free of any solvent residues as the CO_2 is gas at environmental conditions (AVISON et al., 2001; CHAMPEAU et al., 2015).

There is a lack of studies reporting the incorporation of multicomponent active agents from natural sources, such as essential oils, in polymer films by means of this technology. Therefore, the present work aimed to produce LLDPE films impregnated with CEO by high-pressure CO_2 technique, evaluating the chemical profile of the impregnated oil; the topographic, morphological, and thermomechanical properties of films; and the release kinetics and transport properties of CEO from LLDPE films to food simulant fluids.

4.2 Materials and methods

4.2.1 Materials

Pellets of LLDPE (Melt Flow Index: 0.95 g/10 min at 190 °C/2.16 kg, density of 919 kg m^{-3}, Dowlex TG 2085B) kindly supplied by Videplast (Videira, Brazil) were thermo-compressed at 130 °C in a hydraulic press (PHS 15t, Ico Comercial, Brazil), as detailed in Appendix A.1, resulting in transparent and homogeneous films of approximately 300 µm thick, used for impregnation experiments. Essential oil of clove leaves (*Eugenia caryophyllus*, 99%, CAS Number 8015-97-2, Ferquima, Brazil) and carbon dioxide (99.9%, White Martins, Brazil) were used as natural multicomponent active agent and impregnation medium, respectively. Other chemicals of analytical grade were eugenol standard (>99%, Sigma-Aldrich, Brazil), helium (99.9%, White Martins, Brazil), methanol (99.97% HPLC grade, J. T. Baker, Mexico) and ethanol (99.8%, Neon, Brazil).

4.2.2 CEO impregnation in LLDPE films

CEO impregnation in LLDPE films by means of near-critical and supercritical CO_2 was performed in an experimental apparatus built up to work under high-pressure conditions, as schematically presented in Figure 4.1. It consists of a variable-volume cell with a maximum internal volume of approximately 25 cm^3, a movable piston for inner pressure control, and two sapphire windows (Swiss Jewel, USA) for visualization. The pressure was controlled by a syringe pump (260HP, Teledyne Isco, USA) using CO_2 as pressurizing fluid and measured by a pressure transducer (LD301, Smar, Brazil). The cell temperature was maintained by a thermostatic water bath (MQBTC99-20, Microquímica, Brazil) and measured by a J-type thermocouple (Salcas, Brazil) connected to a universal indicator (N1500, Novus, Brazil). A magnetic stirrer (753A, Fisatom, Brazil) kept the cell content under continuous agitation. This apparatus was described in detail in previous studies (ROSSO et al., 2013; BENELLI et al., 2014; MEZZOMO et al., 2015).

Figure 4.1. Schematic diagram of experimental apparatus for impregnation. CV: check valve; BV: ball valve; NV: needle valve; P: pressure transducer; T: thermocouple.

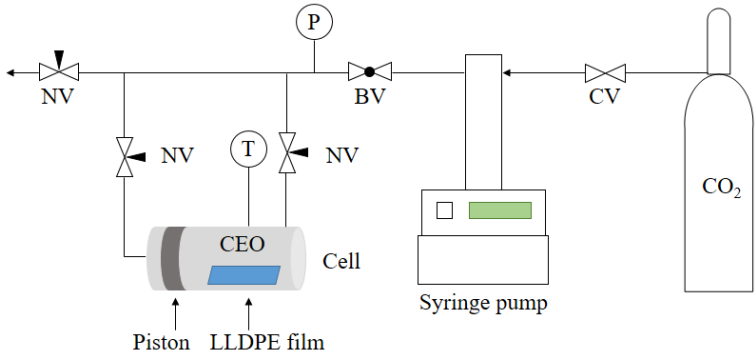

Experimental set-up for temperature (25 and 32 °C), pressure (150 bar) and impregnation procedure followed previous studies reported by Medeiros, Ferreira and Carciofi (2017). Before impregnation, sample films were selected from the thermo-compressed LLDPE film, excluding non-uniform film thickness. The LLDPE film sample (7.2 x 1.2 cm surface, 300 mg) was individually placed inside the cell and a precise amount of CEO was weighed in an analytical balance (AUY 220, Shimadzu, Philippines, ± 0.0001 g accuracy) and then loaded in the cell. CO_2 in the liquid state at 7 °C and 100 bar, resulting in a density of 0.9374 g cm^{-3} (LEMMON; MCLINDEN; FRIEND, 2001), was loaded using the syringe pump until reaching 0.10 of CEO:CO_2 mass ratio. The CEO concentration was defined to ensure a complete miscibility in CO_2 under all operational conditions, according to literature reports (CHENG et al., 2000; SOUZA et al., 2004). Thermophysical properties of pure components (eugenol, major component of CEO, and CO_2) and their mixtures at different mass fractions are presented in Appendix A.2. Impregnation runs were performed at constant pressure and temperature for 2 hours. After impregnation, the internal cell pressure was reduced at controlled depressurization rate (DR): 10, 50 or 100 bar min^{-1}. All experimental conditions were performed in duplicate at batch mode. Isochoric data (specific mass at constant volume) of the system is presented in Appendix A.4. The detailed procedure of pressurization and depressurization at controlled rate are presented in Appendices B.1 and B.3. The calculation of depressurization time based on the selected depressurization rates is detailed in Appendix A.5.

Impregnated samples were carefully cleaned with paper towel followed by quick methanol washing at 25 °C to remove residual non-impregnated CEO adhered over film surface. The amount of impregnated CEO (I), expressed as mg of CEO per g of film, was estimated by gravimetric method in analytical balance (AUY 220, Shimadzu, Philippines, ± 0.0001 g accuracy), as shown in Equation 4.1.

$$I = \frac{\left(m_{F,imp} - m_{F,i}\right) \text{ x } 1000}{m_{F,i}} \qquad (4.1)$$

in which $m_{F,imp}$ is the mass of impregnated film (g) and $m_{F,i}$ is the initial mass of film (g). Impregnated samples were protected by aluminum foil and stored at -18 °C until further characterization analyses.

4.2.3 Chemical profile of CEO impregnated in samples

The identification and relative quantification of CEO components impregnated in LLDPE films was determined in a gas chromatograph equipped with mass spectrophotometer (GC-MS, model 7890 A, mass detector 5975C, Agilent Technologies, USA) attached to HP-5MS column (30 m x 0.25 mm, 0.25 μm, Agilent Technologies, USA). The carrier gas was helium with 1 mL min^{-1} flow rate, split ratio 1:50, injector and detector temperatures of 240 and 250 °C, respectively, and column temperature was linearly programmed at a rate of 3 °C min^{-1} from 70 to 180 °C (GUAN et al., 2007). Impregnated film samples (120 mg) were contained into amber glass vials with 10 mL of methanol that were sealed and left to extract for 24 h at 25 °C. Then, a second extraction was performed with the same film samples placed in fresh methanol (10 mL) and left to extract for further 24 h to ensure a complete release of the multicomponent active agent (AVISON et al., 2001). Aliquots from the two extractions (1 μL) were injected into the equipment and the CEO components impregnated in LLDPE films were identified by comparing the mass spectra and retention time with NIST 11 mass spectral library available on the GC-MS equipment.

4.2.4 Optical properties and surface characterization of films

4.2.4.1 Opacity

Film absorbance at visible wavelength was measured by a UV-visible spectrophotometer (800 XI, Femto, Brazil) before and after CEO impregnation in the same LLDPE sample. Equation 4.2 was employed to estimate opacity of films (TEIXEIRA et al., 2014):

$$Opacity = \frac{A_{600}}{l} \quad (4.2)$$

in which A_{600} is the absorbance at 600 nm and l the film thickness (mm). For measurements, film samples were cut at the same dimension of the glass cuvette. Results were expressed as the average of four readings at different positions for each film.

4.2.4.2 Contact angle

The static contact angle of distilled water over impregnated and non-impregnated LLDPE films was measured at room temperature (25 °C) by the sessile drop method in a goniometer (250-F1, Ramé-Hart Instrument, USA). Duplicates with 10 readings were taken for each film.

4.2.4.3 Surface roughness

The surface roughness (*R*a) of LLDPE films before and after CEO impregnation was analyzed by surface topography without contact in a white light optical interferometer (NV 7300, Zygo NewView 7300, USA) using 5x objective lens. The sampling area was 64 mm^2 and the resulting *R*a represents the arithmetic average of measurements at four different sub-regions in this area.

4.2.4.4 Scanning electron microscopy

The effect of high-pressure processing and CEO impregnation on surface morphology of films was evaluated by scanning electron microscopy (SEM) in a JSM-6390LV scanning electron microscope (Jeol, Tokyo, Japan) at 15 kV. For image analyses, samples were mounted

on metal stubs using a double-sided adhesive carbon tape and coated with a thin layer of gold under vacuum.

4.2.5 Thermomechanical properties

4.2.5.1 Tensile analysis

The tensile strength at break (τ_b), percent elongation at break (ε_b) and elastic or Young's modulus (E) of LLDPE samples were determined in a texture analyzer (TA-HD Plus, Stable Micro Systems, UK) according to ASTM D882-12 method (ASTM D882-12, 2012). Samples before and after CEO impregnation as well as after migration in food simulant fluids were analyzed. Tensile tests were conducted with samples of 36 x 6 mm using a 750 kg load cell, crosshead speed of 10 mm s^{-1} and initial grip separation of 30 mm.

4.2.5.2 Dynamic mechanical analysis

Dynamic mechanical analysis (DMA) of pure and CEO-impregnated samples (10 mm x 6 mm x 0.3 mm) were conducted in a dynamic mechanical analyzer (242E Artemis, Netzsch, Germany) operating in tensile mode. Measurements were carried out from -150 to 100 °C at a frequency of 1 Hz with a heating rate of 5 °C min^{-1} (KHONAKDAR, 2015). Curves of storage modulus (E'), loss modulus (E'') and damping factor ($\tan\delta = E''/E'$) versus temperature were used to evaluate the dynamic mechanical behavior of samples.

4.2.6 CEO migration in food simulant fluids

4.2.6.1 Experimental procedure

The evaluation of equilibrium conditions and mass transfer properties of CEO from LLDPE films into food simulant fluids were performed through migration assays. Aqueous solutions of ethanol at 10 and 95% (v/v) were employed as aqueous and fatty food simulant fluids, respectively (BRASIL, 2010; EC, 2011). Pure film (control sample) and CEO-impregnated films (1.2 x 3.6 cm) processed at different experimental conditions were totally immersed in 40 mL of each fluid, according to the ASTM D4754-11 method (ASTM D4754-11, 2011). Samples were contained in capped Erlenmeyer flasks (50 mL) with metal supports to avoid film buoyancy and contact with the glass wall. Flasks

were kept under continuous agitation in an orbital shaker (MA 410, Marconi, Brazil) at 100 rpm and 25 °C (Labortherm-N, Germany, ± 0.1 °C accuracy).

Migration kinetics were determined by sampling 1 mL aliquots from the flasks containing the film immersed in the simulant fluid. In all assays, CEO concentration in both simulant fluids was maintained below 10% of the saturated value, estimated by eugenol solubility in ethanol:water solution with 5:95 (v:v) (1.63 mg mL^{-1} at 21 °C) (CHEN; DAVIDSON; ZHONG, 2014) and eugenol solubility in ethanol:water solution with 95:5 (v:v) (> 100 mg mL^{-1} at 21 °C) (KEITH; WALTERS, 1992).

The CEO concentration in each aliquot was quantified in a UV-visible spectrophotometer (Q898U2M5, Quimis, Brazil) at 281 and 283 nm for aqueous solutions of ethanol at 10 and 95%, respectively, using previously determined calibration curves of CEO in both fluids. The linear relationship between absorbance and CEO concentration was verified in the range of 10 to 100 µg mL^{-1} and 5 to 50 µg mL^{-1} for the aqueous solution of ethanol at 10 and 95%, respectively, with a coefficient of determination (R^2) of 0.999 for both fluids. The wavelength scans and calibration curves of CEO and eugenol (major component) in both food simulant fluids are presented in Appendices C.4 to C.7. All experiments were performed in duplicate. Mass and thickness of films before and after migration assays were also determined.

4.2.6.2 Mass transfer model and numerical solution

The migration process was described by analogy to the Fick's law of diffusion in dilute solutions in combination with the equation of continuity for the active component, considering unidirectional gradients of concentration, absence of chemical reaction, and macroscopic flux only by diffusion at unsteady state (Equation 4.3).

$$\frac{\partial \rho}{\partial t} = D\left(\frac{\partial^2 \rho}{\partial x^2}\right) \tag{4.3}$$

in which ρ is the active compound mass concentration (kg m^{-3}), x is the Cartesian coordinate (m) from center to the film surface, t is the time (s) starting at soaking the film into the solution, and D represents the diffusion coefficient (m^2 s^{-1}) of the active compound in LLDPE, a constant parameter assumed as independent of distance, time and

concentration. In this model, Equation 4.4 represents the initial condition of uniform active compound distribution throughout the film, evidenced by confocal microscopy images (MEDEIROS; FERREIRA; CARCIOFI, 2017), which value is the initial amount of CEO in LLDPE. Equations 4.5 and 4.6 represent the boundary conditions of axial symmetry at the center of film and the CEO concentration at film surface in equilibrium with the simulant fluid, in which was assumed negligible mass transfer resistance, respectively.

$$t = 0;\ \ 0 \leq x \leq L; \rho = \rho_i \tag{4.4}$$

$$t > 0;\ x = 0;\ \frac{\partial \rho}{\partial x} = 0 \tag{4.5}$$

$$t > 0;\ x = L;\ \rho = \rho_s \tag{4.6}$$

in which ρ_i is the initial CEO mass concentration in the film (kg m^{-3}), ρ_s is the CEO mass concentration at surface in equilibrium with food simulant fluid (kg m^{-3}), and L is the film half-thickness (m). This mathematical model also considers that: there is no CEO in simulant fluid at t = 0, i.e., ρ_s = 0; there is no polymer swelling, evidenced by measurements of film thickness before and after migration, and L remains constant and equal to 150 μm (average half-thickness); CEO is instantaneously dispersed in the bulk fluid during the continuous agitation; CEO concentration in bulk fluid remains well below its saturation value throughout the migration experiment, as previously described. The analytical solution of Equations 4.3 to 4.6 is given by Equation 4.7 (CRANK, 1975).

$$\frac{M_t}{M_\infty} = \frac{\bar{\rho} - \rho_s}{\rho_i - \rho_s} = 1 - \frac{8}{\pi^2} \sum_{n=0}^{\infty} \frac{1}{(2n+1)^2} \exp\left[-(2n+1)^2 \pi^2 \frac{Dt}{4L^2}\right] \tag{4.7}$$

in which M_t and M_∞ represent the cumulative CEO mass migrated from LLDPE to the simulant fluid at any instant t and at a sufficiently long time to reach equilibrium, respectively; and $\bar{\rho}$ is the average CEO mass concentration in the film (kg m^{-3}). Equation 4.7 was fitted to experimental migration kinetic data using a computational routine (Matlab® software R2013a, MathWorks, USA). This procedure resulted in an optimal D value, the adjustable parameter of the mathematical model, by

minimizing the sum of squared errors (residuals) between measured and estimated values (CARCIOFI et al., 2002; PORCIUNCULA et al., 2013).

4.2.7 Statistical analysis

The results were analyzed by one-way analysis of variance (ANOVA) followed by Tukey's multiple comparison tests for significant differences ($p < 0.05$) using Statistica software (version 13, Dell Inc., USA). Data are presented as mean ± standard deviation.

4.3 Results and discussion

4.3.1 CEO impregnation in LLDPE films

Based on the experimental parameters evaluated in this study, at 25 °C and 150 bar CO_2 is in the liquid state as a pressurized fluid, while at 32 °C and 150 bar it is a supercritical fluid, as its temperature and pressure are above the critical values: critical temperature, T_C = 31.1 °C and critical pressure, P_C = 73.8 bar (BRUNNER, 1994). In both conditions, CEO was completely soluble in CO_2 phase. The effect of parameters temperature and depressurization rate, DR, on the impregnated amount of CEO in LLDPE is presented in Table 4.1. Values of impregnation efficiency (*I*%) are presented in Appendix A.6. Moreover, in this study, the pressure was maintained constant at 150 bar, since the pressure enhancement did not exert a significant effect on CEO impregnation in LLDPE films (MEDEIROS; FERREIRA; CARCIOFI, 2017). Other studies reported the same behavior during the incorporation of nonpolar active compounds in different types of polymer matrices (VARONA et al., 2011; HUSSAIN; GRANT, 2012; IVANOVIC et al., 2016).

In general, the amount of impregnated CEO increased when reducing DR and increasing temperature. The values of CEO impregnation ranged from 19.75 to 26.83 mg CEO/g LLDPE, with the lowest amount incorporated at 25 °C/100 bar min^{-1} and the highest at 32 °C/10 bar min^{-1}. Considering the effect of DR on the impregnation of active agents, Rojas et al. (2015) concluded that slower depressurization rates, at constant temperature and pressure, favors the retention of nonpolar active compounds in LLDPE films. An opposite effect is observed when a fast DR is applied to the system, as it rapidly reduces the affinity between molecules of active compounds and CO_2 (YOKOZAKI et al., 2015). Indeed, when increasing temperature both

CEO and CO_2 diffusion rates are increased in the polymer matrix due to a reduction in CO_2 density and enhancement of polymer chain mobility (AVISON et al., 2001). Increased diffusion rates of the mixture in supercritical CO_2 coupled with a slower DR of the system augmented the amount of CEO retained in the polymer film.

Table 4.1. Impregnated mass of CEO in LLDPE films under different temperature and depressurization rate (Pressure = 150 bar and total impregnation time = 2 h).

T (°C)	DR (bar min^{-1})	Impregnated mass (mg CEO/g LLDPE)[1]
25	10	21.09 ± 0.21^{c}
	50	$20.17 \pm 0.02^{c,d}$
	100	19.75 ± 0.34^{d}
32	10	26.83 ± 0.39^{a}
	50	$26.35 \pm 0.28^{a,b}$
	100	25.51 ± 0.04^{b}

[1] Same letter indicates no statistical difference between values ($p < 0.05$).

Impregnated samples were weighed until constant weight due to residual CO_2 desorption, which took approximately 10 minutes. This phenomenon was also reported by Goñi et al. (2016) and Goñi et al. (2017) after depressurization of semi-crystalline polyethylene-based films. The desorbed mass of CO_2 varied from 0.9 to 3.4 mg CO_2/g LLDPE, at atmospheric pressure and 25 °C, and it was not considered in calculations of impregnated CEO mass. The solubility of CO_2 in low-density polyethylene (LDPE, 922.5 kg m^{-3} density) is around 48 mg CO_2/g polymer at 150 bar/100 °C and reduces to approximately 1 mg CO_2/g polymer at 2 bar/100 °C (ČUČEK et al., 2013). Sarrasin et al. (2015) reported that CO_2 uptake in the amorphous phase of semi-crystalline polyethylene samples, with crystallinity near 50%, varied from 40-50 mg CO_2/g polymer at 150 bar/60 °C and reached values close to 1 mg CO_2/g polymer as pressure was reduced to atmospheric conditions. These values agree with observed results of CO_2 desorption from semi-crystalline LLDPE films in the present study, which crystallinity is around 50% determined by differential scanning calorimetry (MEDEIROS; FERREIRA; CARCIOFI, 2017).

4.3.2 Chemical, topographic and morphological characterization of films

The results of relative composition (integrated composition) of CEO impregnated in LLDPE films with the identified compounds after the two extractions with methanol are shown in Table 4.2. Three compounds were identified in all analyzed samples. Eugenol was the majoritarian compound, followed by β-caryophyllene and α-humulene.

Table 4.2. Relative composition, in % peak area, of impregnated CEO in LLDPE films after two extractions with methanol (Pressure = 150 bar, Depressurization rate = 100 bar min^{-1}).

Compound	RT[1] (min)	First extraction (% area)		Second extraction (% area)	
		25 ºC	32 ºC	25 ºC	32 ºC
Eugenol	14.59	65.1	66.6	-	-
β-caryophyllene	16.02	28.7	33.4	82.7	84.5
α-humulene	16.71	6.2	-	17.3	15.5

[1] RT: retention time.

The chromatogram of films processed at 150 bar, 25 °C, and 100 bar min^{-1} is similar to that of samples processed at 150 bar, 32 °C, and 100 bar min^{-1}. In the first extraction (Figure 4.2 A), samples processed in supercritical condition showed the highest relative amount of eugenol, but the peak relative to the α-humulene was not identified. The highest amount of eugenol, in this case, suggests that when the system is in supercritical condition, the interactions between eugenol and ethylene molecules are favored due to an increased diffusion rate of CEO in supercritical CO_2, as previously discussed. In the second extraction (Figure 4.2 B), no sample presented the peak relative to eugenol, indicating that this compound was completely extracted in 24 h in methanol. The presence of sesquiterpenes β-caryophyllene and α-humulene in CEO impregnated in polymer films indicate a potential synergistic effect of all components in antimicrobial and antioxidant activities. Literature reports that even minor compounds in essential oils contribute to the biological activities of such multicomponent active agents (BURT, 2004; CABRAL et al., 2013; GRINEVICIUS et al., 2017; MICHIELIN et al., 2009).

Figure 4.2. Chromatograms of CEO impregnated in LLDPE films from first (A) and second (B) extraction with methanol (P = 150 bar, T = 25 °C, DR = 100 bar min^{-1}).

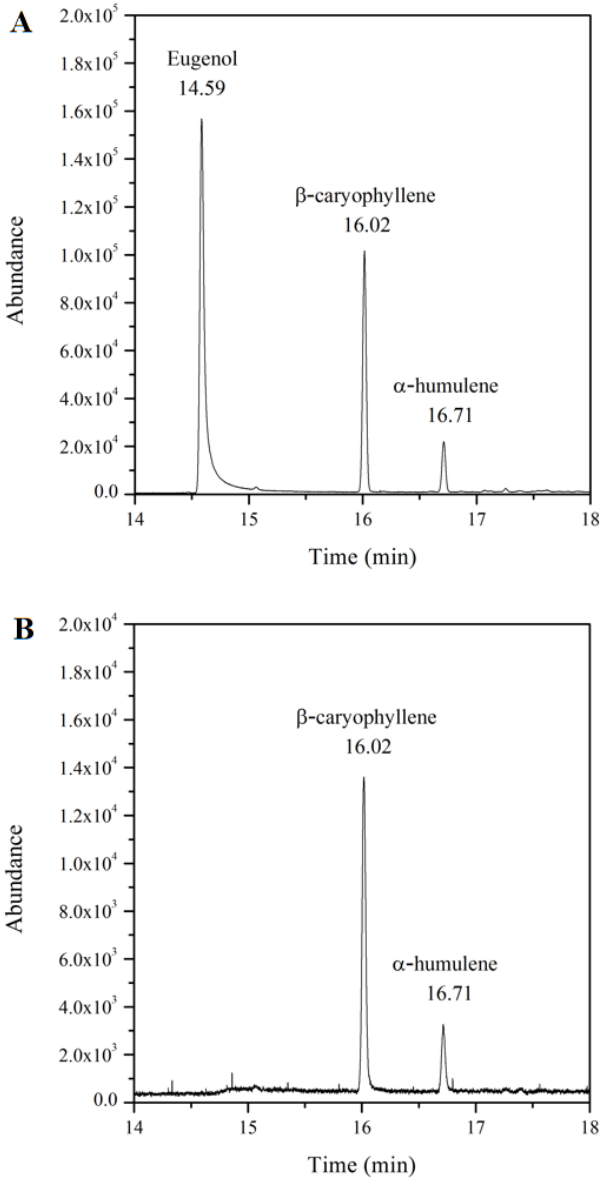

Thickness and opacity of films before and after impregnation are presented in Table 4.3, in which no significant difference was observed for thickness and opacity among samples processed at different operational conditions. In addition, no significant differences were found between film thickness before and after CEO incorporation, suggesting that the reversible swelling of high-pressure CO_2 in polymer samples did not cause modifications in film thickness after system depressurization. Measurements of film opacity at visible wavelength showed that LLDPE films become less transparent after active compound incorporation, attributed to a possible light scattering effect of the CEO in the polymer matrix, which can be advantageous when considering the development of light barrier packages. Similar results were reported after incorporation of CEO by surface coating in LLDPE films (MULLA et al., 2017).

Table 4.3. Thickness and opacity of films before and after CEO impregnation (Pressure = 150 bar and total impregnation time = 2 h).

T (°C)	DR (bar min^{-1})	Thickness (mm)[1]		Opacity[1]	
		Before	After	Before	After
25	10	0.307 ± 0.001	0.309 ± 0.001	1.34 ± 0.07	1.36 ± 0.07
	50	0.312 ± 0.003	0.311 ± 0.002	1.35 ± 0.06	1.41 ± 0.08
	100	0.309 ± 0.004	0.309 ± 0.004	1.37 ± 0.12	1.38 ± 0.14
32	10	0.314 ± 0.005	0.310 ± 0.000	1.30 ± 0.05	1.38 ± 0.06
	50	0.306 ± 0.005	0.313 ± 0.003	1.37 ± 0.04	1.39 ± 0.07
	100	0.307 ± 0.004	0.310 ± 0.000	1.35 ± 0.03	1.39 ± 0.06

[1] No statistical difference between values in the same column ($p > 0.05$).

Values of water contact angle, presented in Table 4.4, indicate that samples can be classified as hydrophobic films or with a non-wetting surface, as their contact angle values are above 90 ° (COSTA et al., 2010). CEO impregnation seems to enhance the hydrophobicity of impregnated films, but no statistical difference was observed between values. The effect of high-pressure processing on the surface roughness of LLDPE films is demonstrated in Figure 4.3. From the topographic images is possible to observe a slight increase of surface roughness of samples processed at 150 bar and 32 °C at maximum DR. Values of LLDPE average roughness (*R*a) are presented in Table 4.4. The CEO incorporation in supercritical medium augmented the average surface roughness of films, possibly because the swelling and plasticization of most polymers are favored at higher pressures/temperatures (BRAGA et al., 2008; DIAS et al., 2011). As a result, an increased polymer swelling in the supercritical condition coupled with a fast CO_2 removal in a short time prevented the polymer chain reorganization, inducing more variations in the topographic pattern of the film surface.

Table 4.4. Contact angle and average roughness of pure and CEO-impregnated LLDPE films.

Sample	T (°C)/DR (bar min^{-1})	Contact angle (°)[1]	R_a (μm)[1]
Pure LLDPE	-	89.6 ± 3.6^{a}	0.11 ± 0.03^{a}
LLDPE-CEO	25/10	95.1 ± 3.6^{a}	0.13 ± 0.03^{a}
	25/50	95.3 ± 3.3^{a}	0.23 ± 0.07^{ab}
	25/100	94.6 ± 3.0^{a}	0.20 ± 0.05^{ab}
	32/10	97.3 ± 0.3^{a}	0.24 ± 0.13^{ab}
	32/50	96.6 ± 1.3^{a}	0.27 ± 0.10^{ab}
	32/100	95.6 ± 2.1^{a}	0.33 ± 0.13^{b}

[1] Same letter indicates no statistical difference between values ($p < 0.05$).

Figure 4.3. Topographic images of LLDPE surfaces before and after CEO impregnation. (A) Control sample (non-impregnated); (B) impregnated at T = 25 °C and DR = 100 bar min^{-1}; (C) impregnated at T = 32 °C and DR = 100 bar min^{-1}.

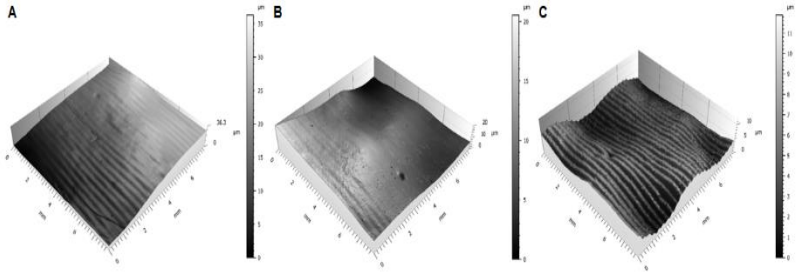

SEM micrographs of non-impregnated LLDPE film (control sample) compared to CO_2-treated and CEO-impregnated films (Figure 4.4) highlight the presence of pores on film surface after high-pressure processing. Structures similar to bubbles were observed on the surface of films processed in supercritical conditions at DR of 100 bar min^{-1} for samples with pure CO_2 (Figure 4.4, LLDPE-CO_2) and DR of 50 and 100 bar min^{-1} for samples impregnated with CEO (Figure 4.4, E and F). These structures were probably created during the rapid CO_2 removal from the swollen polymer phase, especially in amorphous regions near the surface. In fact, LLDPE as a semi-crystalline polymer possesses crystalline and amorphous domains and CO_2 is sorbed in the amorphous regions, as the crystallites in polyethylene are considered as impermeable domains (MICHAELS; BIXLER, 1961). The CO_2 adsorption in amorphous regions generates bubbles in superficial layers that are more susceptible to rupture during fast depressurization. As CO_2 is rapidly removed from the swollen polymer phase, it can prevent the polymer chain reorganization. This phenomenon favors the venting of CO_2 through paths in the amorphous domains, forming the structures observed in SEM images.

Figure 4.4. SEM micrographs of pure, CO_2-treated and CEO-impregnated LLDPE films.

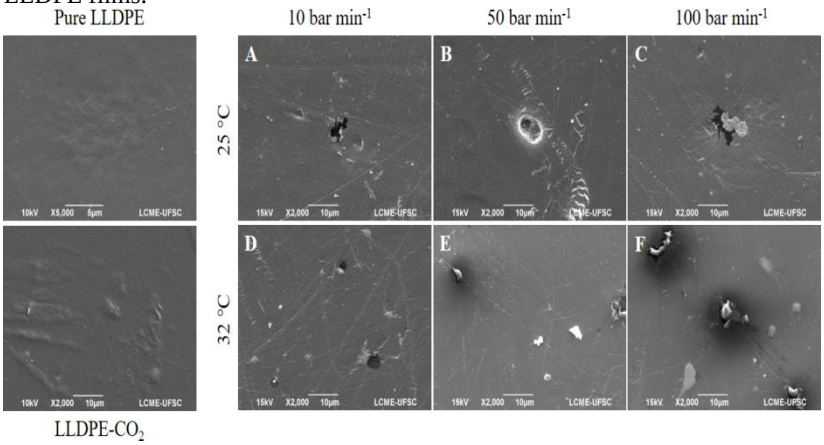

4.3.3 Thermomechanical properties

The effect of CEO impregnation on mechanical film properties is shown in Table 4.5. Considering the macroscopic behavior of LLDPE films during tensile tests, all samples showed neck formation in stress-strain curves, which is typical of semi-crystalline and flexible polymer materials (KONTOU; NIAOUNAKIS, 2006). It is important to highlight that the high-pressure processing with pure CO_2 in absence of CEO did not affect the mechanical behavior of LLDPE films (MEDEIROS; FERREIRA; CARCIOFI, 2017). Increasing temperature and DR, tensile strength reduced in all samples. Samples processed at 150 bar/32 °C at maximum DR (100 bar min^{-1}) presented the greatest difference on τ_b compared to pure LLDPE film. The increased surface roughness and the presence of bubbles on the film surface, evidenced by topographic and SEM images, probably weakened the mechanical resistance of these films.

CEO impregnation in LLDPE at high-pressure medium caused a reduction in film strength, evidenced by a reduction in τ_b parameter, due to an enhancement of polymer chain mobility after active compound incorporation. However, the original strength and stiffness of samples after migration assays in both food simulant fluids were maintained, as indicated by the mechanical parameters τ_b and E (Table 4.5). Despite this, control films (pure LLDPE) presented a film strength reduction after contacting both simulant fluids, which can be attributed to some degree

of interaction between pure film and ethanol solutions. To the best of our knowledge, there is no information regarding the mechanical behavior of polyethylene films after migration and contact with aqueous solutions of ethanol. It is known that plastic materials are able to interact with the surrounding environment, resulting in sorption, permeation, and migration of constituents, which may lead to changes in their mechanical resistance (SATISH et al., 2013; OTERO-PAZOS et al., 2016). Furthermore, no remarkable changes in ε_b, indicative of film ductility, were observed after CEO impregnation and migration from films to simulant fluids.

Table 4.5. Mechanical properties of pure and CEO-impregnated LLDPE films.

Sample	T (°C)/DR (bar min^{-1})	τ_b (MPa)[1]	ε_b (%)[1]	E (MPa)[1]
Pure LLDPE	-	42.0 ± 0.1^{a}	549 ± 4^{ab}	458 ± 31^{ab}
LLDPE-CEO	25/10	37.8 ± 1.2^{ab}	538 ± 8^{bc}	409 ± 40^{abcd}
	25/50	37.3 ± 1.8^{ab}	526 ± 9^{bc}	444 ± 49^{ab}
	25/100	37.9 ± 2.7^{ab}	530 ± 12^{bc}	427 ± 26^{abcd}
	32/10	38.4 ± 1.8^{ab}	541 ± 14^{bc}	416 ± 37^{abcd}
	32/50	37.0 ± 2.0^{ab}	532 ± 5^{bc}	443 ± 11^{abc}
	32/100	35.2 ± 1.4^{b}	505 ± 18^{c}	374 ± 45^{abcd}
Ethanol 10%[2]				
Pure LLDPE	-	34.9 ± 2.0^{b}	539 ± 9^{bc}	373 ± 20^{abcd}
LLDPE-CEO	25/10	38.5 ± 1.3^{ab}	564 ± 12^{ab}	350 ± 31^{abcd}
	25/50	36.4 ± 1.5^{ab}	563 ± 6^{ab}	312 ± 25^{cd}
	25/100	36.8 ± 0.2^{ab}	558 ± 6^{ab}	335 ± 53^{bcd}
	32/10	38.7 ± 1.8^{ab}	557 ± 4^{ab}	361 ± 42^{abcd}
	32/50	36.2 ± 3.9^{ab}	542 ± 9^{abc}	301 ± 40^{d}
	32/100	33.6 ± 1.8^{b}	535 ± 14^{bc}	345 ± 47^{bcd}

Ethanol 95%[2]				
Pure LLDPE	-	34.4 ± 0.9^{b}	532 ± 16^{bc}	495 ± 34^{a}
LLDPE-CEO	25/10	35.7 ± 1.6^{ab}	504 ± 16^{c}	444 ± 38^{abcd}
	25/50	36.6 ± 4.0^{ab}	555 ± 6^{ab}	406 ± 23^{abcd}
	25/100	35.2 ± 2.6^{ab}	583 ± 12^{a}	383 ± 53^{abcd}
	32/10	37.8 ± 3.1^{ab}	555 ± 13^{ab}	462 ± 29^{ab}
	32/50	34.0 ± 0.8^{b}	503 ± 19^{c}	452 ± 38^{abc}
	32/100	33.7 ± 1.1^{b}	534 ± 4^{bc}	356 ± 35^{abcd}

[1] Same letter indicates no statistical difference between values in the same column ($p < 0.05$).
[2] Samples analyzed after migration in food simulant fluids (ethanol 10 and 95%).

Curves of tan δ versus temperature are shown in Figure 4.5. LLDPE usually exhibits three transitions or relaxations in DMA analysis with decreasing temperature, called α-, β- and γ-transition. The α-transition is related to the motion of crystalline regions before the polymer melts and it is found from 20 to 100 °C. The β-transition originates from polymer chain relaxation in amorphous phase near the branching points. This transition can be obtained in E'' or in tan δ curves within a temperature range of -30 to 10 °C. The γ-transition is attributed to the motion of CH_2 units in the amorphous region, frequently associated with polyethylene glass transition. This transition can be detected from -150 to -120 °C (NIAOUNAKIS; KONTOU, 2005; PAN et al., 2006).

Figure 4.5. Tan δ curves of pure and CEO-impregnated LLDPE films.

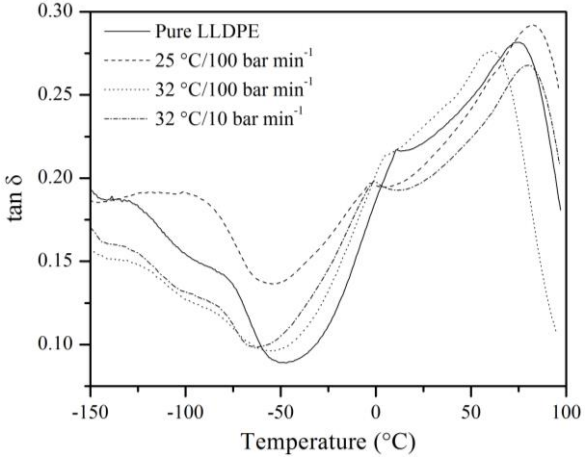

In the present work, γ-transition was observed as a shoulder at the temperature of -130 °C, but this transition was difficult to be detected for the sample processed at 25 °C/100 bar min^{-1}. The β-transition corresponded to the peaks observed at temperatures from -3 to 10 °C. This relaxation in the crystalline-amorphous interfacial region, typical of branched polymers as the polyethylene (QUENTAL; FELISBERTI, 2005), shifted to lower temperatures for CEO-impregnated samples compared with pure LLDPE films, indicating that the mobility of amorphous chains close to branching points increased with the presence of CEO, regardless of processing conditions. The α-transition of CEO-impregnated LLDPE films processed at 32 °C/100 bar min^{-1} occurred at the lowest temperature (60 °C) compared with pure LLDPE film (75 °C)

and other processed samples (close to 80 °C). However, this trend was not clear and no correlations could be established for the effect of CEO impregnation on the mobility and reorganization of crystalline domains.

4.3.4 Migration kinetics and transport properties

The CEO migrated from LLDPE films to simulant fluids was measured by UV-visible analysis and by gravimetric measurements of samples before and after release experiments. Similar results were observed for both techniques (Table 4.6). It suggests that the gravimetric method can be satisfactorily employed to determine the active compounds migration from polymers to fluids, as it is a simple and easy technique to be used for a great number of samples, also providing good results. Furthermore, no significant changes were observed for LLDPE film thickness before and after CEO release in both simulant fluids, which is in good agreement with the consideration of no polymer swelling and constant film thickness proposed in the diffusion-based model.

Table 4.6. Released amount of CEO by spectrophotometric and gravimetric methods and LLDPE thickness before and after release in ethanol 10 and 95% (v/v).

Food simulant	T (°C)/ DR (bar min^{-1})	Thickness (mm)		Released amount (%)	
		Before	After	Spectrophotometric	Gravimetric
Ethanol 10%	25/10	0.311 ± 0.010	0.313 ± 0.007	57.4 ± 0.6	60.4 ± 2.2
	25/50	0.307 ± 0.008	0.307 ± 0.009	56.8 ± 0.1	60.5 ± 0.1
	25/100	0.303 ± 0.005	0.297 ± 0.005	59.1 ± 0.3	59.7 ± 1.7
	32/10	0.316 ± 0.002	0.313 ± 0.004	54.4 ± 0.9	59.7 ± 0.1
	32/50	0.308 ± 0.007	0.310 ± 0.006	55.3 ± 0.0	60.4 ± 1.4
	32/100	0.307 ± 0.008	0.309 ± 0.006	56.1 ± 0.8	59.6 ± 0.2
Ethanol 95%	25/10	0.318 ± 0.000	0.319 ± 0.000	99.2 ± 2.0	101.7 ± 0.2
	25/50	0.314 ± 0.001	0.314 ± 0.001	102.4 ± 1.0	107.4 ± 0.1
	25/100	0.309 ± 0.007	0.303 ± 0.014	101.7 ± 0.7	102.0 ± 3.2
	32/10	0.315 ± 0.001	0.316 ± 0.004	99.7 ± 1.2	104.9 ± 0.1
	32/50	0.310 ± 0.001	0.313 ± 0.000	100.5 ± 0.8	104.1 ± 0.0
	32/100	0.309 ± 0.004	0.310 ± 0.004	101.9 ± 1.2	103.1 ± 4.3

Overall migration of CEO from LLDPE films to food simulant fluids is presented in Figure 4.6. The release profiles of CEO-impregnated LLDPE samples in both simulant fluids were similar, but the total cumulative mass fraction of CEO released in ethanol 95% was higher than in ethanol 10%, as shown in Table 4.6. Samples in contact with ethanol 95% exhibited a complete release in 12 hours as consequence of high CEO solubility in this fatty food simulant. On the other hand, samples in ethanol 10% reached equilibrium after 24 hours. Experiments with this fluid were conducted for further 6 days, but samples showed no additional release. It is worth mentioning that CEO concentration remained below 4% of saturation value in both simulant fluids during the entire period of release. As an example, samples processed at 32 °C/10 bar min^{-1}, the condition of maximum active compound impregnation, in contact with aqueous food simulant fluid presented a maximum release of 55 µg CEO mL^{-1}. This value represents approximately 3% of eugenol solubility in ethanol 5% (v:v), equal to 1.63 mg eugenol mL^{-1} (CHEN; DAVIDSON; ZHONG, 2014). Considering that, in this case, migration assays were performed in ethanol 10%, the CEO (and eugenol) solubility can be even higher, which means that the CEO solubility in aqueous food simulant was not a limiting factor for its incomplete release. For these samples, interactions between CEO and LLDPE were probably strengthened when films were in aqueous food simulant due to a low affinity of CEO with the surrounding aqueous medium. Similar results were reported for nonpolar active compound migration from LLDPE films in the aqueous solution of ethanol 10% (v:v) (ROJAS et al., 2015).

The higher CEO migration in fatty than in aqueous food simulant evidences the influence of active compound solubility in release medium. Moreover, it can be assumed that a certain amount of simulant fluid, mainly ethanol 95%, will be sorbed at the film surface, enhancing the mobility of active compound in polymer network and facilitating its release. This mechanism of fluid sorption at film surface has been suggested for nonpolar active compounds migration from polyolefins to fatty food simulants (VITRAC; MOUGHARBEL; FEIGENBAUM, 2007; CRAN et al., 2010; RAMOS et al., 2014). In fact, when a polymer matrix containing an active agent is immersed in a nonpolar fluid, the surrounding medium starts to solubilize the active agent, promoting its diffusion out of polymer. Therefore, the diffusion rate will depend on the chemical nature of the fluid, the solubility of the active agent in this fluid and interactions between the active agent and polymer matrix (MILOVANOVIC et al., 2015).

Figure 4.6. CEO release from LLDPE films in ethanol 10% (gray) and ethanol 95% (black). Symbols: experimental data; Line: diffusive model. Processing conditions: P = 150 bar; T = 25 °C (A) and 32 °C (B); DR = 10 bar min^{-1} (Δ, dotted line), 50 bar min^{-1} (□, dashed line) and 100 bar min^{-1} (○, solid line).

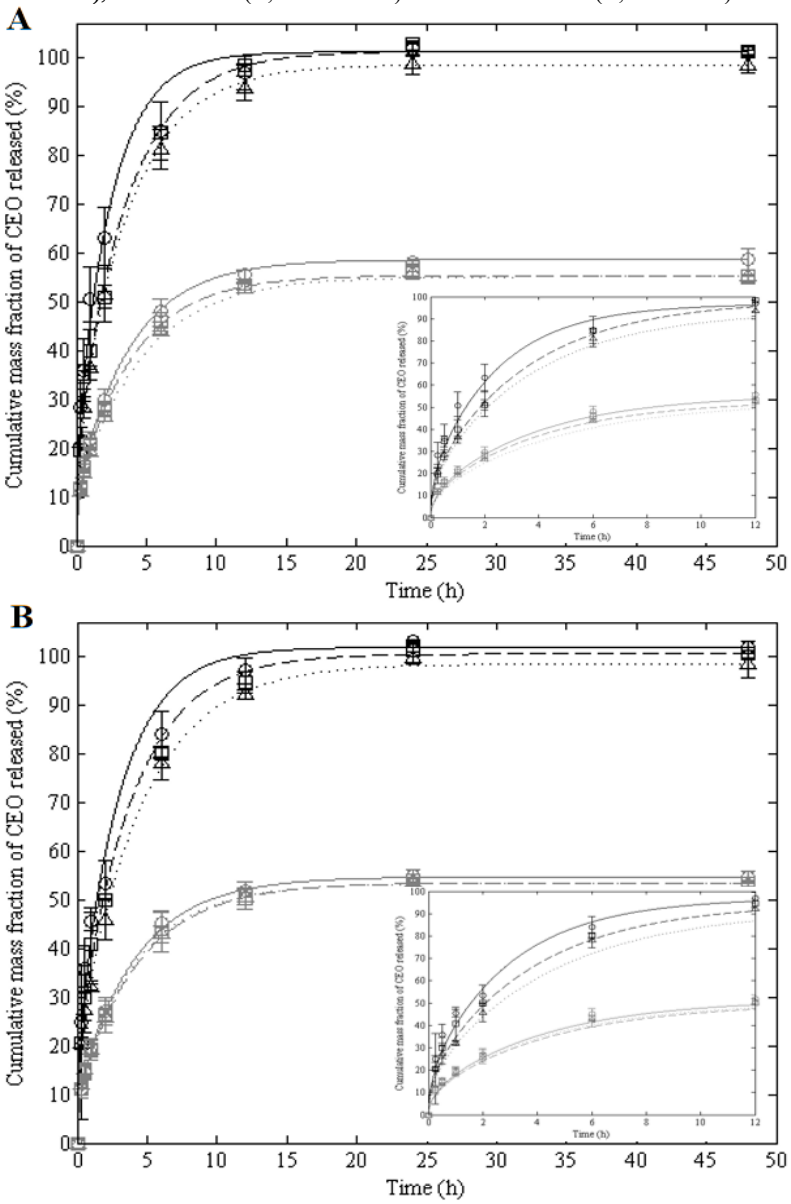

In addition, CEO migration in fluids seems to be faster for samples processed at 100 bar min^{-1} in liquid and supercritical conditions. This tendency is best viewed by fitting the diffusive mathematical model to experimental migration data (Figure 4.6). The mathematical model adequately described the release profile of CEO migration from LLDPE films in both simulant fluids, despite an overestimation in some regions for samples in ethanol 95%. The parameters of numerical solution, R^2 and root mean square error (RMSE), presented in Table 4.7, reinforce the good agreement between theory and experimental data.

Table 4.7. Effective diffusion coefficient of CEO in LLDPE films and parameters of numerical solution.

Food simulant	T (°C)/ DR (bar min^{-1})	$\bar{D}$ (m^2 s^{-1})[1]	R^2	RMSE
Ethanol 10%	25/10	5.4×10^{-13} b	0.996	0.013
	25/50	6.2×10^{-13} ab	0.997	0.011
	25/100	6.5×10^{-13} ab	0.998	0.010
	32/10	5.9×10^{-13} ab	0.996	0.012
	32/50	5.7×10^{-13} ab	0.997	0.012
	32/100	6.0×10^{-13} ab	0.998	0.009
Ethanol 95%	25/10	6.7×10^{-13} ab	0.998	0.016
	25/50	6.9×10^{-13} ab	0.993	0.031
	25/100	1.0×10^{-12} a	0.988	0.038
	32/10	5.6×10^{-13} ab	0.997	0.021
	32/50	6.5×10^{-13} ab	0.985	0.045
	32/100	8.4×10^{-13} ab	0.981	0.048

[1] Average value determined by the numerical solution of diffusive model. Same letter indicates no statistical difference between values ($p < 0.05$).

Average values of the effective diffusion coefficient of CEO in LLDPE, for each operational condition and simulant fluid, ranged from 5.4×10^{-13} to 6.5×10^{-13} m^2 s^{-1} for samples in ethanol 10%, while for films in ethanol 95%, it varied from 5.6×10^{-13} to 1.0×10^{-12} m^2 s^{-1} (Table 4.7).

Values of this parameter for similar active agents (nonpolar compounds) in LLDPE are in the same order of magnitude (DHOOT et al., 2009). The observed trend of faster diffusion rates as a function of DR was not statistically significant between samples evaluated with the same food simulant fluid. Therefore, these results suggest that the effective diffusion coefficient of the system CEO-LLDPE is not dependent on operational parameters of active compound incorporation in polymer matrices by means of high-pressure CO_2 impregnation.

4.4 Conclusions

High-pressure CO_2 impregnation was a suitable technique to incorporate clove essential oil in LLDPE films. Above the CO_2 supercritical condition, higher impregnated amount was achieved. A slower depressurization rate favors the active compound retention in the polymer matrix, also contributing to higher impregnation amounts. An increased surface roughness and presence of bubbles on film surface were observed for samples processed in supercritical conditions at maximum depressurization rate, assigned to the fast CO_2 removal from the swollen polymer phase. CEO impregnation affects the film strength due to an enhancement of polymer chain mobility and, after migration, the original strength and stiffness of impregnated samples were maintained. Diffusion is the main mechanism of mass transfer that governs CEO migration from LLDPE films to food simulant fluids. The operational parameters temperature and depressurization rate exert no significant influence on the effective diffusion coefficient of the system CEO-LLDPE. The CEO impregnated LLDPE films are promising materials for antioxidant and antimicrobial active food packaging.

Acknowledgments

The authors acknowledge Videplast (Brazil) for supplying LLDPE pellets and Brazilian governmental agencies CNPq (project number 473153/2012-2), FAPESC (project number 6342/2011-8), and CAPES for the financial support and G. R. Medeiros scholarship. The authors also thank the laboratories from UFSC for technical support: Laboratório Central de Microscopia Eletrônica (LCME) (SEM analyses), Central de Análises (contact angle and tensile analyses) and Laboratório de Materiais (LabMat) (optical interferometry and DMA analyses).

Chapter 5: Conclusions and suggestions for future research

5.1 Conclusions

Impregnations assisted by CO_2 at near-critical and supercritical conditions promote a reversible swelling of LLDPE films, which favors the retention of CEO in the polymer film compared to the conventional method of immersion without pressure. The CEO incorporation is more effective when the system is in supercritical conditions than in near-critical conditions (as pressurized liquid).

The impregnated amount of CEO in LLDPE films is dependent on processing parameters. The highest impregnation can be achieved with increasing CEO:CO_2 mass ratio (the driving force for impregnation), increasing temperature (increase of diffusion rate and kinetic energy of molecules), reducing pressure (reduction of CO_2 density and its solubilization power to favor the interaction CEO-LLDPE), and reducing depressurization rate (reduction of mass transfer rate from polymer to vapor phase). In addition, the amount of impregnated CEO reaches its maximum at 2 hours of processing.

The high-pressure processing with pure CO_2 does not change thermal and mechanical properties of LLDPE films. After system depressurization, CEO remains impregnated in films due to molecular interactions, as van der Waals forces, between eugenol and ethylene molecules in the active sites of polymer chains. The CEO impregnation increases the polymer chain mobility, also reducing the tensile strength of films. After CEO migration from LLDPE to food simulant fluids, the original strength and stiffness of films are maintained.

The CEO incorporation in supercritical medium followed by the maximum depressurization rate augmented the average surface roughness of films. This phenomenon can be attributed to the polymer swelling in the amorphous region, which is favored in supercritical condition, along with a fast CO_2 removal in a short time that prevented the polymer chain reorganization, causing variations in the topographic pattern of the film surface.

The CEO migration from LLDPE films in aqueous and fatty food simulants is governed by the diffusive mechanism of mass transfer. The effective diffusion coefficient of the CEO in LLDPE is not dependent on the operational parameters (temperature and depressurization rate) of the system.

The CEO impregnation in LLDPE films is mainly dependent on the CO_2 density, as in lower densities the interactions between CEO and

LLDPE are favored, contributing to higher impregnation amounts. In general, the operational parameters can be adjusted to enhance CEO incorporation, but they present negligible effect over the CEO diffusivity in LLDPE as well as on thermal and mechanical properties of films. The high-pressure CO_2 impregnation is an emerging and innovative technology to incorporate multicomponent active agents in polymer matrices to develop active food packaging materials.

5.2 Suggestions for future research

This study has significantly advanced the knowledge and design of active packaging systems produced by high-pressure CO_2 impregnation containing multicomponent active agents. The following suggestions may contribute to further studies:

- To evaluate the effect of film thickness and polymer chain orientation of films produced by blown extrusion, since this parameter, especially in thinner samples, may influence the resulting transport properties;
- To perform impregnation assays with cycles of pressurization-and-depressurization of the system, as they can favor active compound impregnation;
- To evaluate the released volatiles of CEO from LLDPE films to simulate migration into the headspace;
- To use a cosolvent, as ethanol, in impregnation experiments, as the presence of a cosolvent in high-pressure medium may enhance interactions of the mixture CEO-CO_2 with LLDPE;
- To study sealing properties of CEO-impregnated films because they may be affected after CEO incorporation and/or migration;
- To analyze barrier properties to moisture and gases of CEO-impregnated LLDPE films;
- To evaluate antioxidant and antimicrobial activities of CEO-impregnated LLDPE films to understand their biological action;
- To study the effect of encapsulating CEO in nano/microparticles before incorporation in polymer films. This procedure can reduce the CEO diffusion rate from packaging to food, also minimizing sensory modifications of packaged products;
- To evaluate the retention of impregnated CEO in LLDPE films under different storage conditions (temperature and presence/absence of visible light).

References

21 CFR-PART 184. Code of Federal Regulations. Title 21 - Food and Drugs. Chapter I - Food and Drug Administration: Department of Health and Human Services. Subchapter B - Food for Human Consumption. Part 184 - Direct food substances affirmed as Generally Recognized As Safe. Subpart B: Listing of specific substances affirmed as GRAS. Washington: U. S. Government Publishing Office, 2017. v. 3

ABBASZADEH, S.; SHARIFZADEH, A.; SHOKRI, H.; KHOSRAVI, A. R.; ABBASZADEH, A. Antifungal efficacy of thymol, carvacrol, eugenol and menthol as alternative agents to control the growth of food-relevant fungi. Journal de Mycologie Médicale / Journal of Medical Mycology, v. 24, n. 2, p. e51–e56, jun. 2014.

ABDALI, H.; AJJI, A. Development of antibacterial structures and films using clove bud powder. Industrial Crops and Products, Special issue derived from International Conference on Bio-based Materials and Composites. v. 72, p. 214–219, 15 out. 2015.

AFFONSO, R. S.; LESSA, B.; SLANA, G. B. C. A.; BARBOZA, L. L.; ALMEIDA, F. V. de; LIMA, A. L. S.; SOUZA, F. R. de; FRANÇA, T. C. C. Quantificação e caracterização dos principais componentes do extrato etanólico de cravo-da-Índia Syzygium aromaticum [l] Merr. et Perry. Revista Virtual de Química, v. 6, n. 5, p. 1316–1331, 2014.

AGHEL, N.; YAMINI, Y.; HADJIAKHOONDI, A.; POURMORTAZAVI, S. M. Supercritical carbon dioxide extraction of Mentha pulegium L. essential oil. Talanta, v. 62, n. 2, p. 407–411, 6 fev. 2004.

AMIRI, A.; DUGAS, R.; PICHOT, A. L.; BOMPEIX, G. In vitro and in vitro activity of eugenol oil (Eugenia caryophylata) against four important postharvest apple pathogens. International Journal of Food Microbiology, v. 126, n. 1–2, p. 13–19, 15 ago. 2008.

APPENDINI, P.; HOTCHKISS, J. H. Review of antimicrobial food packaging. Innovative Food Science & Emerging Technologies, v. 3, n. 2, p. 113–126, jun. 2002.

ASTM D882-12. Standard test method for tensile properties of thin plastic sheeting. West Conshohocken: ASTM International, 2012. . Disponível em: <http://www.astm.org/Standards/D882.htm>. Acesso em: 9 jun. 2015.

ASTM D3418-12. Standard test method for transition temperatures and enthalpies of fusion and crystallization of polymers by differential scanning calorimetry. West Conshohocken: ASTM International, 2012. . Disponível em: <http://www.astm.org/Standards/D3418.htm>. Acesso em: 9 jun. 2015.

ASTM D4754-11. Standard test method for two-sided liquid extraction of plastic materials using FDA migration cell. West Conshohocken: ASTM International, 2011. . Disponível em: <http://www.astm.org/Standards/D4754.htm>. Acesso em: 9 jun. 2015.

AVISON, S. J.; GRAY, D. A.; DAVIDSON, G. M.; TAYLOR, A. J. Infusion of volatile flavor compounds into low-density polyethylene. Journal of Agricultural and Food Chemistry, v. 49, n. 1, p. 270–275, 2001.

BACHU, S. CO2 storage in geological media: Role, means, status and barriers to deployment. Progress in Energy and Combustion Science, v. 34, n. 2, p. 254–273, 1 abr. 2008.

BAKKALI, F.; AVERBECK, S.; AVERBECK, D.; IDAOMAR, M. Biological effects of essential oils – a review. Food and Chemical Toxicology, v. 46, n. 2, p. 446–475, fev. 2008.

BANCHERO, M. Supercritical Fluid Dyeing of Synthetic and Natural Textiles – a Review. Coloration Technology, v. 129, n. 1, p. 2–17, 1 fev. 2013.

BEN, A. A.; CHALIER, P.; GONTARD, N.; PREZIOSI-BELLOY, L. Materials based on a woven or non-woven textile substrate coated with a matrix, containing at least one antimicrobial agent and method for making same, 24 jan. 2008. Disponível em: <http://www.google.com/patents/WO2007135273A3>.

BENELLI, P.; ROSSO COMIM, S. R.; VLADIMIR OLIVEIRA, J.; PEDROSA, R. C.; FERREIRA, S. R. S. Phase equilibrium data of guaçatonga (Casearia sylvestris) extract + ethanol + CO2 system and encapsulation using a supercritical anti-solvent process. The Journal of Supercritical Fluids, III Iberoamerican Conference on Supercritical Fluids - PROSCIBA 2013. v. 93, p. 103–111, set. 2014.

BHUNIA, K.; SABLANI, S. S.; TANG, J.; RASCO, B. Migration of Chemical Compounds from Packaging Polymers during Microwave, Conventional Heat Treatment, and Storage. Comprehensive Reviews in Food Science and Food Safety, v. 12, n. 5, p. 523–545, 1 set. 2013.

BIERHALZ, A. C. K.; DA SILVA, M. A.; DE SOUSA, H. C.; BRAGA, M. E. M.; KIECKBUSCH, T. G. Influence of natamycin loading methods on the

physical characteristics of alginate active films. The Journal of Supercritical Fluids, v. 76, p. 74–82, 1 abr. 2013.

BOULEDJOUIDJA, A.; MASMOUDI, Y.; SERGENT, M.; TRIVEDI, V.; MENIAI, A.; BADENS, E. Drug loading of foldable commercial intraocular lenses using supercritical impregnation. International Journal of Pharmaceutics, v. 500, n. 1, p. 85–99, 16 mar. 2016.

BOYÈRE, C.; JÉRÔME, C.; DEBUIGNE, A. Input of supercritical carbon dioxide to polymer synthesis: an overview. European Polymer Journal, v. 61, p. 45–63, 1 dez. 2014.

BRAGA, M. E. M.; PATO, M. T. V.; SILVA, H. S. R. C.; FERREIRA, E. I.; GIL, M. H.; DUARTE, C. M. M.; DE SOUSA, H. C. Supercritical solvent impregnation of ophthalmic drugs on chitosan derivatives. The Journal of Supercritical Fluids, v. 44, n. 2, p. 245–257, 1 mar. 2008.

BRASIL. ANVISA. Agência Nacional de Vigilância Sanitária. Resolução RDC nº 51, de 26 de novembro de 2010. Dispõe sobre migração em materiais, embalagens e equipamentos plásticos destinados a entrar em contato com alimentos. Brasília: Diário Oficial da União - Ministério da Saúde, 2010.

BRASIL. ANVISA. Agência Nacional de Vigilância Sanitária. Resolução RDC nº 56, de 16 de novembro de 2012. Dispõe sobre a lista positiva de monômeros, outras substâncias iniciadoras e polímeros autorizados para a elaboração de embalagens e equipamentos plásticos em contato com alimentos. Brasília: Diário Oficial da União - Ministério da Saúde, 2012.

BRUNNER, G. Gas extraction: an introduction to fundamentals of supercritical fluids and the application to separation processes. Darmstadt/New York: Steinkopff/Springer, 1994. v. 4

BURT, S. Essential oils: their antibacterial properties and potential applications in foods – a review. International Journal of Food Microbiology, v. 94, n. 3, p. 223–253, 1 ago. 2004.

CABRAL, L. da C.; PINTO, V. F.; PATRIARCA, A. Application of plant derived compounds to control fungal spoilage and mycotoxin production in foods. International Journal of Food Microbiology, v. 166, n. 1, p. 1–14, 16 ago. 2013.

CARCIOFI, B. A. M.; FAISTEL, J.; ARAGÃO, G. M. F.; LAURINDO, J. B. Determination of thermal diffusivity of mortadella using actual cooking process data. Journal of Food Engineering, v. 55, n. 1, p. 89–94, 2002.

CASKEY, T.; LESSER, A. J.; MCCARTHY, T. J. Supercritical CO2 Welding of Laminated Linear Low Density Polyethylene Films. Polymer Engineering & Science, v. 41, n. 12, p. 2259–2265, 1 dez. 2001.

CHAIEB, K.; HAJLAOUI, H.; ZMANTAR, T.; KAHLA-NAKBI, A. B.; ROUABHIA, M.; MAHDOUANI, K.; BAKHROUF, A. The Chemical Composition and Biological Activity of Clove Essential Oil, Eugenia Caryophyllata (Syzigium Aromaticum L. Myrtaceae): A Short Review. Phytotherapy Research, v. 21, n. 6, p. 501–506, 1 jun. 2007.

CHAMPEAU, M.; THOMASSIN, J.-M.; JÉRÔME, C.; TASSAING, T. In situ FTIR micro-spectroscopy to investigate polymeric fibers under supercritical carbon dioxide: CO2 sorption and swelling measurements. The Journal of Supercritical Fluids, v. 90, p. 44–52, 1 jun. 2014.

CHAMPEAU, M.; THOMASSIN, J.-M.; TASSAING, T.; JÉRÔME, C. Drug Loading of Polymer Implants by Supercritical CO2 Assisted Impregnation: A Review. Journal of Controlled Release: Official Journal of the Controlled Release Society, v. 209, p. 248–259, 10 jul. 2015.

CHEN, H.; DAVIDSON, P. M.; ZHONG, Q. Impacts of Sample Preparation Methods on Solubility and Antilisterial Characteristics of Essential Oil Components in Milk. Applied and Environmental Microbiology, v. 80, n. 3, p. 907–916, 1 fev. 2014.

CHEN, Z.; CAO, K.; YAO, Z.; HUANG, Z. Modeling solubilities of subcritical and supercritical fluids in polymers with cubic and non-cubic equations of state. The Journal of Supercritical Fluids, v. 49, n. 2, p. 143–153, jun. 2009.

CHENG, K.-W.; KUO, S.-J.; TANG, M.; CHEN, Y.-P. Vapor–liquid equilibria at elevated pressures of binary mixtures of carbon dioxide with methyl salicylate, eugenol, and diethyl phthalate. The Journal of Supercritical Fluids, v. 18, n. 2, p. 87–99, 10 set. 2000.

CHOI, J. H.; CHOI, W. Y.; CHA, D. S.; CHINNAN, M. J.; PARK, H. J.; LEE, D. S.; PARK, J. M. Diffusivity of potassium sorbate in κ-carrageenan based antimicrobial film. LWT - Food Science and Technology, v. 38, n. 4, p. 417–423, jun. 2005.

CORTÉS-ROJAS, D. F.; DE SOUZA, C. R. F.; OLIVEIRA, W. P. Clove (Syzygium aromaticum): a precious spice. Asian Pacific Journal of Tropical Biomedicine, v. 4, n. 2, p. 90–96, fev. 2014.

COSTA, V. P.; BRAGA, M. E. M.; DUARTE, C. M. M.; ALVAREZ-LORENZO, C.; CONCHEIRO, A.; GIL, M. H.; DE SOUSA, H. C. Anti-glaucoma drug-loaded contact lenses prepared using supercritical solvent impregnation. The Journal of Supercritical Fluids, Selected papers from the 9th International Symposium on Supercritical Fluids (ISSF 2009) - New Trends in Supercritical Fluids: Energy, Materials, Processing, Arcachon, France, May 18-20, 2009. v. 53, n. 1–3, p. 165–173, jun. 2010.

COUTINHO, F. M. B.; MELLO, I. L.; MARIA, S.; DE, L. C. Polyethylene: main types, properties and applications. Polímeros, v. 13, n. 1, p. 01-13, jan. 2003.

CRAN, M. J.; RUPIKA, L. a. S.; SONNEVELD, K.; MILTZ, J.; BIGGER, S. W. Release of Naturally Derived Antimicrobial Agents from LDPE Films. Journal of Food Science, v. 75, n. 2, p. E126-133, mar. 2010.

CRANK, J. The mathematics of diffusion. 2nd. ed. Oxford: Clarendon Press, 1975.

ČUČEK, D.; PERKO, T.; ILIĆ, L.; ZNOJ, B.; VENTURINI, P.; KNEZ, Ž.; ŠKERGET, M. Phase equlibiria and diffusivity of dense gases in various polyethylenes. The Journal of Supercritical Fluids, v. 78, p. 54–62, jun. 2013.

CUSSLER, E. L. Diffusion: mass transfer in fluid systems. 3rd. ed. New York: Cambridge University Press, 2009.

DARR, J. A.; POLIAKOFF, M. New directions in inorganic and metal-organic coordination chemistry in supercritical fluids. Chemical Reviews, v. 99, p. 495–541, 1999.

DEBIAGI, F.; KOBAYASHI, R. K. T.; NAKAZATO, G.; PANAGIO, L. A.; MALI, S. Biodegradable active packaging based on cassava bagasse, polyvinyl alcohol and essential oils. Industrial Crops and Products, v. 52, p. 664–670, jan. 2014.

DHOOT, G.; AURAS, R.; RUBINO, M.; DOLAN, K.; SOTO-VALDEZ, H. Determination of eugenol diffusion through LLDPE using FTIR-ATR flow cell and HPLC techniques. Polymer, v. 50, n. 6, p. 1470–1482, 6 mar. 2009.

DIAS, A. M. A.; BRAGA, M. E. M.; SEABRA, I. J.; FERREIRA, P.; GIL, M. H.; DE SOUSA, H. C. Development of Natural-Based Wound Dressings Impregnated with Bioactive Compounds and Using Supercritical Carbon Dioxide. International Journal of Pharmaceutics, v. 408, n. 1–2, p. 9–19, 15 abr. 2011.

DÍEZ-MUNICIO, M.; MONTILLA, A.; HERRERO, M.; OLANO, A.; IBÁÑEZ, E. Supercritical CO2 impregnation of lactulose on chitosan: A comparison between scaffolds and microspheres form. The Journal of Supercritical Fluids, v. 57, n. 1, p. 73–79, maio 2011.

DOHRN, R.; BRUNNER, G. High-pressure fluid-phase equilibria: experimental methods and systems investigated (1988–1993). Fluid Phase Equilibria, v. 106, n. 1, p. 213–282, 1 maio 1995.

DONSÌ, F.; CUOMO, A.; MARCHESE, E.; FERRARI, G. Infusion of essential oils for food stabilization: unraveling the role of nanoemulsion-based delivery systems on mass transfer and antimicrobial activity. Innovative Food Science & Emerging Technologies, v. 22, p. 212–220, abr. 2014.

DUARTE, A. R. C.; SIMPLICIO, A. L.; VEGA-GONZÁLEZ, A.; SUBRA-PATERNAULT, P.; COIMBRA, P.; GIL, M. H.; DE SOUSA, H. C.; DUARTE, C. M. M. Supercritical fluid impregnation of a biocompatible polymer for ophthalmic drug delivery. The Journal of Supercritical Fluids, Selected Papers from the 8th Conference on Supercritical Fluids and Their Applications Ischia, Naples, Italy, May 28-31, 2006. v. 42, n. 3, p. 373–377, 1 out. 2007.

EC. Commission Regulation (European Union) nº 10/2011 of 14 January 2011 on plastic materials and articles intended to come into contact with food. Official Journal of the European Union, p. 2–89, 2011.

EN 1186-1. Materials and articles in contact with foodstuffs. Plastics. Part 1: guide to the selection of conditions and test methods for overall migration. Brussels: European Committee for Standardization, 2002.

EN 1186-3. Materials and articles in contact with foodstuffs. Plastics. Part 3: test methods for overall migration into aqueous food simulants by total immersion. Brussels: European Committee for Standardization, 2002.

EN 1186-14. Materials and articles in contact with foodstuffs. Plastics. Part 14: test methods for substitute tests for overall migration from plastics intended to come into contact with fatty foodstuffs using test media isooctane and 95% ethanol. Brussels: European Committee for Standardization, 2002.

FANG, Z.; ZHAO, Y.; WARNER, R. D.; JOHNSON, S. K. Active and intelligent packaging in meat industry. Trends in Food Science & Technology, v. 61, p. 60–71, mar. 2017.

FRANCESCHI, E.; KUNITA, M. H.; RUBIRA, A. F.; MUNIZ, E. C.; CORAZZA, M. L.; OLIVEIRA, J. V.; DARIVA, C. Phase behavior of binary and

ternary systems involving carbon dioxide, propane, and glycidyl methacrylate at high pressure. Journal of Chemical & Engineering Data, v. 51, n. 2, p. 686–690, 1 mar. 2006.

FRANZ, R. Migration Modelling from Food-Contact Plastics into Foodstuffs as a New Tool for Consumer Exposure Estimation. Food Additives and Contaminants, v. 22, n. 10, p. 920–937, out. 2005.

GARCIA, R. Essential oils in plastic film, 19 fev. 2004. Disponível em: <http://www.google.com/patents/US20040034149>.

GÓMEZ-ESTACA, J.; LÓPEZ-DE-DICASTILLO, C.; HERNÁNDEZ-MUÑOZ, P.; CATALÁ, R.; GAVARA, R. Advances in antioxidant active food packaging. Trends in Food Science & Technology, v. 35, n. 1, p. 42–51, jan. 2014.

GOÑI, M. L.; GAÑÁN, N. A.; HERRERA, J. M.; STRUMIA, M. C.; ANDREATTA, A. E.; MARTINI, R. E. Supercritical CO2 iof LDPE films with terpene ketones as biopesticides against corn weevil (Sitophilus zeamais). The Journal of Supercritical Fluids, v. 122, p. 18–26, abr. 2017.

GOÑI, M. L.; GAÑÁN, N. A.; MARTINI, R. E.; ANDREATTA, A. E. Carvone-Loaded LDPE Films for Active Packaging: Effect of Supercritical CO2-Assisted Impregnation on Loading, Mechanical and Transport Properties of the Films. The Journal of Supercritical Fluids, v. 133, p. 278–290, 1 mar. 2018.

GOÑI, M. L.; GAÑÁN, N. A.; STRUMIA, M. C.; MARTINI, R. E. Eugenol-loaded LLDPE films with antioxidant activity by supercritical carbon dioxide impregnation. The Journal of Supercritical Fluids, v. 111, p. 28–35, maio 2016.

GONZÁLEZ, L. M.; BUENO, J. L.; MEDINA, I. Determination of binary diffusion coefficients of anisole, 2,4-dimethylphenol, and nitrobenzene in supercritical carbon dioxide. Industrial & Engineering Chemistry Research, v. 40, n. 16, p. 3711–3716, 1 ago. 2001.

GRINEVICIUS, V. M. A. S.; ANDRADE, K. S.; OURIQUE, F.; MICKE, G. A.; FERREIRA, S. R. S.; PEDROSA, R. C. Antitumor activity of conventional and supercritical extracts from Piper nigrum L. cultivar Bragantina through cell cycle arrest and apoptosis induction. The Journal of Supercritical Fluids, v. 128, n. Supplement C, p. 94–101, 1 out. 2017.

GUAN, W.; LI, S.; YAN, R.; TANG, S.; QUAN, C. Comparison of essential oils of clove buds extracted with supercritical carbon dioxide and other three traditional extraction methods. Food Chemistry, v. 101, n. 4, p. 1558–1564, 2007.

HAYNES, W. M. Handbook of chemistry and physics. 91st. ed. Boca Raton: CRC Press, 2010.

HERNÁNDEZ-OCHOA, L.; MACÍAS-CASTAÑEDA, C. A.; NEVÁREZ-MOORILLÓN, G. V.; SALAS-MUÑOZ, E.; SANDOVAL-SALAS, F. Antimicrobial activity of chitosan-based films including spices' essential oils and functional extracts. CyTA - Journal of Food, v. 10, n. 2, p. 85–91, 1 maio 2012.

HIROSE, T.; MIZOGUCHI, K.; KAMIYA, Y. Dilation of Polyethylene by Sorption of Carbon Dioxide. Journal of Polymer Science Part B: Polymer Physics, v. 24, n. 9, p. 2107–2115, 1 set. 1986.

HOSSEINI, M. h.; RAZAVI, S. h.; MOUSAVI, M. a. Antimicrobial, Physical and Mechanical Properties of Chitosan-Based Films Incorporated with Thyme, Clove and Cinnamon Essential Oils. Journal of Food Processing and Preservation, v. 33, n. 6, p. 727–743, 1 dez. 2009.

HOTCHKISS, J. H. Food-Packaging Interactions Influencing Quality and Safety. Food Additives and Contaminants, v. 14, n. 6–7, p. 601–607, out. 1997.

HUSSAIN, Y. A.; GRANT, C. S. Ibuprofen impregnation into submicron polymeric films in supercritical carbon dioxide. The Journal of Supercritical Fluids, v. 71, p. 127–135, nov. 2012.

HYLDGAARD, M.; MYGIND, T.; MEYER, R. L. Essential Oils in Food Preservation: Mode of Action, Synergies, and Interactions with Food Matrix Components. Frontiers in Microbiology, v. 3, p. 12, 2012.

IBÁÑEZ, E.; OCA, A.; DE MURGA, G.; LÓPEZ-SEBASTIÁN, S.; TABERA, J.; REGLERO, G. Supercritical fluid extraction and fractionation of different preprocessed rosemary plants. Journal of Agricultural and Food Chemistry, v. 47, n. 4, p. 1400–1404, 1 abr. 1999.

IVANOVIC, J.; DIMITRIJEVIC-BRANKOVIC, S.; MISIC, D.; RISTIC, M.; ZIZOVIC, I. Evaluation and improvement of antioxidant and antibacterial activities of supercritical extracts from clove buds. Journal of Functional Foods, v. 5, n. 1, p. 416–423, jan. 2013.

IVANOVIC, J.; KNAUER, S.; FANOVICH, A.; MILOVANOVIC, S.; STAMENIC, M.; JAEGER, P.; ZIZOVIC, I.; EGGERS, R. Supercritical CO2 sorption kinetics and thymol impregnation of PCL and PCL-HA. The Journal of Supercritical Fluids, v. 107, p. 486–498, jan. 2016.

IVERSEN, S. B.; LARSEN, T.; HENRIKSEN, O.; FELSVANG, K. The world's first commercial supercritical wood treatment plant. Presented at the 6th International Symposium on Supercritical Fluids, Versailles, France, 2003.

JIROVETZ, L.; BUCHBAUER, G.; STOILOVA, I.; STOYANOVA, A.; KRASTANOV, A.; SCHMIDT, E. Chemical composition and antioxidant properties of clove leaf essential oil. Journal of Agricultural and Food Chemistry, v. 54, n. 17, p. 6303–6307, 1 ago. 2006.

JOERGER, R. D. Antimicrobial Films for Food Applications: A Quantitative Analysis of Their Effectiveness. Packaging Technology and Science, v. 20, n. 4, p. 231–273, 1 jul. 2007.

KEITH, L. H.; WALTERS, D. B. National toxicology program's: chemical, solubility and compendium. Chelsea: Lewis Publishers, Inc., 1992.

KEMMERE, M. F. Supercritical carbon dioxide for sustainable polymer processes. In: KEMMERE, IR ARTJE F.; MEYER, T. (Ed.). Supercritical carbon dioxide in polymer reaction engineering. Weinheim: Wiley-VCH Verlag GmbH & Co., 2005. p. 1–14.

KHONAKDAR, H. A. Dynamic mechanical analysis and thermal properties of LLDPE/EVA/modified silica nanocomposites. Composites Part B: Engineering, v. 76, p. 343–353, jul. 2015.

KIKIC, I.; VECCHIONE, F. Supercritical impregnation of polymers. Current Opinion in Solid State and Materials Science, v. 7, n. 4–5, p. 399–405, ago. 2003.

KIRAN, E. Polymer miscibility, phase separation, morphological modifications and polymorphic transformations in dense fluids. The Journal of Supercritical Fluids, 20th Year Anniversary Issue of the Journal of Supercritical Fluids. v. 47, n. 3, p. 466–483, 1 jan. 2009.

KONTOU, E.; NIAOUNAKIS, M. Thermo-mechanical properties of LLDPE/SiO2 nanocomposites. Polymer, v. 47, n. 4, p. 1267–1280, 8 fev. 2006.

LABUZA, T. P.; BREENE, W. M. Applications of "active Packaging" for Improvement of Shelf-Life and Nutritional Quality of Fresh and Extended Shelf-Life Foods. Journal of Food Processing and Preservation, v. 13, n. 1, p. 1–69, 1 fev. 1989.

LEI, Z.; OHYABU, H.; SATO, Y.; INOMATA, H.; SMITH JR., R. L. Solubility, swelling degree and crystallinity of carbon dioxide–polypropylene system. The Journal of Supercritical Fluids, v. 40, n. 3, p. 452–461, abr. 2007.

LEMMON, E. W.; MCLINDEN, M. O.; FRIEND, D. G. Thermophysical properties of fluid systems. In: NIST Chemistry WebBook. NIST Standard Reference Database Number 69. Gaithersburg: National Institute of Standards and Technology, 2001.

LÓPEZ, P.; SÁNCHEZ, C.; BATLLE, R.; NERÍN, C. Development of flexible antimicrobial films using essential oils as active agents. Journal of Agricultural and Food Chemistry, v. 55, n. 21, p. 8814–8824, 1 out. 2007.

MAJID, I.; AHMAD NAYIK, G.; MOHAMMAD DAR, S.; NANDA, V. Novel food packaging technologies: innovations and future prospective. Journal of the Saudi Society of Agricultural Sciences, 23 nov. 2016. Disponível em: <http://www.sciencedirect.com/science/article/pii/S1658077X16300765>.

MANNA, L.; BANCHERO, M.; SOLA, D.; FERRI, A.; RONCHETTI, S.; SICARDI, S. Impregnation of PVP microparticles with ketoprofen in the presence of supercritical CO2. The Journal of Supercritical Fluids, Selected Papers from the 8th Conference on Supercritical Fluids and Their Applications Ischia, Naples, Italy, May 28-31, 2006 Ischia Special Issue. v. 42, n. 3, p. 378–384, out. 2007.

MANZANAREZ-LÓPEZ, F.; SOTO-VALDEZ, H.; AURAS, R.; PERALTA, E. Release of α-tocopherol from poly(lactic acid) films, and its effect on the oxidative stability of soybean oil. Journal of Food Engineering, v. 104, n. 4, p. 508–517, jun. 2011.

MCEWEN ASSOCIATES. The value of flexible packaging in extending shelf life and reducing food waste. Maryland: Flexible Packaging Association, 2014.

MCHUGH, M. A.; KRUKONIS, V. J. (ed.). Supercritical fluid extraction: principles and practice. 2nd. ed. Boston: Butterworth-Heinemann, 1994.

MEDEIROS, G. R.; FERREIRA, S. R. S.; CARCIOFI, B. A. M. High pressure carbon dioxide for impregnation of clove essential oil in LLDPE films. Innovative Food Science & Emerging Technologies, v. 41, p. 206–215, jun. 2017.

MEDINA, I. Determination of diffusion coefficients for supercritical fluids. Journal of Chromatography A, Supercritical Fluid Extraction and Chromatography. v. 1250, p. 124–140, 10 ago. 2012.

MEZZOMO, N.; ROSSO COMIM, S. R.; CAMPOS, C. E. M.; FERREIRA, S. R. S. Nanosizing of sodium ibuprofen by SAS method. Powder Technology, v. 270, Part A, p. 378–386, jan. 2015.

MICHAELS, A. S.; BIXLER, H. J. Solubility of Gases in Polyethylene. Journal of Polymer Science, v. 50, n. 154, p. 393–412, 1 abr. 1961.

MICHIELIN, E. M. Z.; SALVADOR, A. A.; RIEHL, C. A. S.; SMÂNIA JR., A.; SMÂNIA, E. F. A.; FERREIRA, S. R. S. Chemical composition and antibacterial activity of Cordia verbenacea extracts obtained by different methods. Bioresource Technology, v. 100, n. 24, p. 6615–6623, dez. 2009.

MILOVANOVIC, S.; STAMENIC, M.; MARKOVIC, D.; IVANOVIC, J.; ZIZOVIC, I. Supercritical impregnation of cellulose acetate with thymol. The Journal of Supercritical Fluids, v. 97, p. 107–115, fev. 2015.

MILTZ, J.; BIGGER, S. W.; SONNEVELD, C.; SUPPAKUL, P. Antimicrobial packaging material, 5 jan. 2006. Disponível em: <http://www.google.com.br/patents/WO2006000032A1>.

MIN, A. M.; CHUAH, T. G.; CHANTARA, T. R. Thermal and dynamic mechanical analysis of polyethylene modified with crude palm oil. Materials & Design, v. 29, n. 5, p. 992–999, 1 jan. 2008.

MIR, S. A.; SHAH, M. A.; DAR, B. N.; WANI, A. A.; GANAI, S. A.; NISHAD, J. Supercritical Impregnation of Active Components into Polymers for Food Packaging Applications. Food and Bioprocess Technology, v. 10, n. 9, p. 1749–1754, 1 set. 2017.

MULLA, M.; AHMED, J.; AL-ATTAR, H.; CASTRO-AGUIRRE, E.; ARFAT, Y. A.; AURAS, R. Antimicrobial efficacy of clove essential oil infused into chemically modified LLDPE film for chicken meat packaging. Food Control, v. 73, Part B, p. 663–671, mar. 2017.

MUPPALLA, S. R.; KANATT, S. R.; CHAWLA, S. P.; SHARMA, A. Carboxymethyl cellulose–polyvinyl alcohol films with clove oil for active packaging of ground chicken meat. Food Packaging and Shelf Life, v. 2, n. 2, p. 51–58, dez. 2014.

NADDEO, C.; GUADAGNO, L.; DE LUCA, S.; VITTORIA, V.; CAMINO, G. Mechanical and transport properties of irradiated linear low density polyethylene (LLDPE). Polymer Degradation and Stability, v. 72, n. 2, p. 239–247, maio 2001.

NALAWADE, S. P.; PICCHIONI, F.; JANSSEN, L. P. B. M. Supercritical carbon dioxide as a green solvent for processing polymer melts: Processing aspects and applications. Progress in Polymer Science, v. 31, n. 1, p. 19–43, jan. 2006.

NARAYANAN, A.; NEERA; MALLESHA; RAMANA, K. V. Synergized Antimicrobial Activity of Eugenol Incorporated Polyhydroxybutyrate Films against Food Spoilage Microorganisms in Conjunction with Pediocin. Applied Biochemistry and Biotechnology, v. 170, n. 6, p. 1379–1388, jul. 2013.

NIAOUNAKIS, M.; KONTOU, E. Effect of LDPE on the Thermomechanical Properties of LLDPE-Based Films. Journal of Polymer Science Part B: Polymer Physics, v. 43, n. 13, p. 1712–1727, 1 jul. 2005.

O'NEIL, M. J.; HECKELMAN, P. E.; KOCH, C. B.; ROMAN, K. J. The Merck Index: an encyclopedia of chemicals, drugs, and biologicals. 14th. ed. Hoboken: John Wiley & Sons, Inc., 2006.

OPDYKE, D. L. J. Monographs on fragrance raw materials: eugenol. Food and Cosmetics Toxicology, v. 13, n. 5, p. 545–547, out. 1975.

OTERO-PAZOS, P.; SENDÓN, R.; BLANCO-FERNANDEZ, B.; BLANCO-DORADO, S.; ALVAREZ-LORENZO, C.; CONCHEIRO, A.; ANGULO, I.; PASEIRO-LOSADA, P.; RODRÍGUEZ-BERNALDO DE QUIRÓS, A. Preparation of Antioxidant Active Films Based on Chitosan: Diffusivity Study of α-Tocopherol into Food Simulants. Journal of Food Science and Technology, v. 53, n. 6, p. 2817–2826, jun. 2016.

PAN, L.; LIU, Y.; ZHANG, K.; BO, S.; LI, Y. Investigation of the effect of branched structure on the performances of the copolymers synthesized from ethylene and α-olefin with rac-Et(Ind)2ZrCl2/MMAO catalyst system. Polymer, v. 47, n. 4, p. 1465–1472, 8 fev. 2006.

PARK, H.-Y.; KIM, S.-J.; KIM, K. M.; YOU, Y.-S.; KIM, S. Y.; HAN, J. Development of Antioxidant Packaging Material by Applying Corn-Zein to LLDPE Film in Combination with Phenolic Compounds. Journal of Food Science, v. 77, n. 10, p. E273-279, out. 2012.

PEELMAN, N.; RAGAERT, P.; DE MEULENAER, B.; ADONS, D.; PEETERS, R.; CARDON, L.; VAN IMPE, F.; DEVLIEGHERE, F. Application of bioplastics for food packaging. Trends in Food Science & Technology, v. 32, n. 2, p. 128–141, 1 ago. 2013.

PEREDA, S.; BOTTINI, S.; BRIGNOLE, E. Fundamentals of supercritical fluid technology. In: Supercritical fluid extraction of nutraceuticals and bioactive compounds. [s.l.] CRC Press, 2007. p. 1–24.

PEYCHÈS-BACH, A.; MOUTOUNET, M.; PEYRON, S.; CHALIER, P. Factors determining the transport coefficients of aroma compounds through polyethylene films. Journal of Food Engineering, v. 95, n. 1, p. 45–53, nov. 2009.

PIRES, M. L.; PETZHOLD, C. L.; SANTOS, R. V.; PERÃO, L. H.; CHIES, A. P. Efeito da migração de composto antimicrobiano nas propriedades finais de selagem de filme poliolefínico. Polímeros, v. 24, n. 2, p. 237–242, 2014.

PORCIUNCULA, B. D. A.; ZOTARELLI, M. F.; CARCIOFI, B. A. M.; LAURINDO, J. B. Determining the effective diffusion coefficient of water in banana (Prata variety) during osmotic dehydration and its use in predictive models. Journal of Food Engineering, v. 119, n. 3, p. 490–496, dez. 2013.

PREEDY, V. R. Essential oils in food preservation, flavor and safety. 1st. ed. London: Academic Press, 2016.

QUENTAL, A. C.; FELISBERTI, M. I. Phase behavior of blends of linear low density polyethylene and poly(ethene-propene-1-butene). European Polymer Journal, v. 41, n. 5, p. 894–902, 1 maio 2005.

QUINTAVALLA, S.; VICINI, L. Antimicrobial food packaging in meat industry. Meat Science, v. 62, n. 3, p. 373–380, 1 nov. 2002.

RAJA, M. R. C.; SRINIVASAN, V.; SELVARAJ, S.; MAHAPATRA, S. K. Versatile and synergistic potential of eugenol: a review. Pharmaceutica Analytica Acta, 6 maio 2015. Disponível em: <https://www.omicsonline.org/open-access/versatile-and-synergistic-potential-of-eugenol-a-review-2153-2435-1000367.php?aid=53182>. Acesso em: 3 ago. 2017.

RAMOS, M.; BELTRÁN, A.; PELTZER, M.; VALENTE, A. J. M.; GARRIGÓS, M. del C. Release and antioxidant activity of carvacrol and thymol from polypropylene active packaging films. LWT - Food Science and Technology, v. 58, n. 2, p. 470–477, out. 2014.

RAMOS, M.; JIMÉNEZ, A.; PELTZER, M.; GARRIGÓS, M. C. Characterization and antimicrobial activity studies of polypropylene films with carvacrol and thymol for active packaging. Journal of Food Engineering, v. 109, n. 3, p. 513–519, abr. 2012.

REBELATTO, E. A.; BENDER, J. P.; CORAZZA, M. L.; FERREIRA, S. R. S.; VLADIMIR OLIVEIRA, J.; LANZA, M. High-pressure phase equilibrium data for the (carbon dioxide + l-lactide + ethanol) system. The Journal of Chemical Thermodynamics, v. 86, p. 37–42, jul. 2015.

REID, R. C.; PRAUSNITZ, J. M.; POLING, B. E. The properties of gases and liquids. 4th. ed. New York: McGraw-Hill, 1987.

REVERCHON, E.; MARRONE, C. Supercritical extraction of clove bud essential oil: isolation and mathematical modeling. Chemical Engineering Science, v. 52, n. 20, p. 3421–3428, 1 out. 1997.

RIBEIRO-SANTOS, R.; ANDRADE, M.; DE MELO, N. R.; DOS SANTOS, F. R.; NEVES, I. de A.; DE CARVALHO, M. G.; SANCHES-SILVA, A. Biological activities and major components determination in essential oils intended for a biodegradable food packaging. Industrial Crops and Products, v. 97, p. 201–210, mar. 2017a.

RIBEIRO-SANTOS, R.; ANDRADE, M.; MELO, N. R. de; SANCHES-SILVA, A. Use of essential oils in active food packaging: recent advances and future trends. Trends in Food Science & Technology, v. 61, p. 132–140, 1 mar. 2017b.

RODRIGUES, V. M.; SOUSA, E. M. B. D.; MONTEIRO, A. R.; CHIAVONE-FILHO, O.; MARQUES, M. O. M.; MEIRELES, M. A. A. Determination of the solubility of extracts from vegetable raw material in pressurized CO2: a pseudo-ternary mixture formed by cellulosic structure+solute+solvent. The Journal of Supercritical Fluids, v. 22, n. 1, p. 21–36, jan. 2002.

ROJAS, A.; CERRO, D.; TORRES, A.; GALOTTO, M. J.; GUARDA, A.; ROMERO, J. Supercritical impregnation and kinetic release of 2-nonanone in LLDPE films used for active food packaging. The Journal of Supercritical Fluids, v. 104, p. 76–84, set. 2015.

ROSSO, S. R. C.; BIANCHIN, E.; DE OLIVEIRA, D.; OLIVEIRA, J. V.; FERREIRA, S. R. S. Enzymatic synthesis of poly(ε-caprolactone) in supercritical carbon dioxide medium by means of a variable-volume view reactor. The Journal of Supercritical Fluids, Special Issue – 10th International Symposium on Supercritical Fluids Special Issue – 10th International Symposium on Supercritical Fluids. v. 79, p. 133–141, jul. 2013.

SABEHAT, A. Active materials incorporating micro-porous solids and essential oils, 6 jun. 2008. Disponível em: <http://www.google.com/patents/WO2008149232A2>.

SAND, M. L. Method for impregnating a thermoplastic polymer, 1 jul. 1986. Disponível em: <http://www.google.com/patents/US4598006>.

SARRASIN, F.; MEMARI, P.; KLOPFFER, M. H.; LACHET, V.; TARAVEL CONDAT, C.; ROUSSEAU, B.; ESPUCHE, E. Influence of high pressures on

CH4, CO2 and H2S solubility in polyethylene: Experimental and molecular simulation approaches for pure gas and gas mixtures. Modelling of the sorption isotherms. Journal of Membrane Science, v. 490, p. 380–388, 15 set. 2015.

SATISH, A.; LASYA, M.; HARINI, S. T.; PADMAVATHI, S.; BALDEV, R. Migration aspects for food contact materials with aqueous food simulating solvents as per different international standards. Journal of Agroalimentary Processes and Technologies, v. 19, n. 4, p. 399–404, 2013.

SATO, Y.; FUJIWARA, K.; TAKIKAWA, T.; SUMARNO; TAKISHIMA, S.; MASUOKA, H. Solubilities and diffusion coefficients of carbon dioxide and nitrogen in polypropylene, high-density polyethylene, and polystyrene under high pressures and temperatures. Fluid Phase Equilibria, v. 162, n. 1–2, p. 261–276, ago. 1999.

SCOPEL, R.; FALCÃO, M. A.; LUCAS, A. M.; ALMEIDA, R. N.; GANDOLFI, P. H. K.; CASSEL, E.; VARGAS, R. M. F. Supercritical fluid extraction from Syzygium aromaticum buds: Phase equilibrium, mathematical modeling and antimicrobial activity. The Journal of Supercritical Fluids, v. 92, p. 223–230, ago. 2014.

SEGUELA, R.; RIETSCH, F. Tensile drawing behaviour of a linear low-density polyethylene: Changes in physical and mechanical properties. Polymer, v. 27, n. 4, p. 532–536, abr. 1986.

SEILER, A.; BACH, A.; DRIFFIELD, M.; PASEIRO LOSADA, P.; MERCEA, P.; TOSA, V.; FRANZ, R. Correlation of Foodstuffs with Ethanol-Water Mixtures with Regard to the Solubility of Migrants from Food Contact Materials. Food Additives & Contaminants. Part A, Chemistry, Analysis, Control, Exposure & Risk Assessment, v. 31, n. 3, p. 498–511, 2014.

SEOW, Y. X.; YEO, C. R.; CHUNG, H. L.; YUK, H.-G. Plant Essential Oils as Active Antimicrobial Agents. Critical Reviews in Food Science and Nutrition, v. 54, n. 5, p. 625–644, 2014.

SHINE, A. D. Polymers and supercritical fluids. In: Physical properties of polymers handbook. New York: Springer, 2007. p. 319–338.

SIEPMANN, J.; SIEPMANN, F. Mathematical modeling of drug delivery. International Journal of Pharmaceutics, v. 364, n. 2, p. 328–343, 2008.

SIMANKE, A. G.; DE LEMOS, C.; PIRES, M. Linear low density polyethylene: microstructure and sealing properties correlation. Polymer Testing, v. 32, n. 2, p. 279–290, abr. 2013.

SIMONEAU, C. Applicability of generally recognised diffusion models for the estimation of specific migration in support of EU Directive 2002/72/EC. Luxembourg: Publication Office of the European Union, 2010.

SOUZA, A. C.; DIAS, A. M. A.; SOUSA, H. C.; TADINI, C. C. Impregnation of Cinnamaldehyde into Cassava Starch Biocomposite Films Using Supercritical Fluid Technology for the Development of Food Active Packaging. Carbohydrate Polymers, v. 102, p. 830–837, 15 fev. 2014.

SOUZA, A. T.; CORAZZA, M. L.; CARDOZO-FILHO, L.; GUIRARDELLO, R.; MEIRELES, M. A. A. Phase equilibrium measurements for the system clove (Eugenia caryophyllus) oil + CO2. Journal of Chemical & Engineering Data, v. 49, n. 2, p. 352–356, 1 mar. 2004.

SOVOVÁ, H. Apparent solubility of natural products extracted with near-critical carbon dioxide. American Journal of Analytical Chemistry, v. 3, p. 958–965, 2012.

SUÁREZ-IGLESIAS, O.; MEDINA, I.; PIZARRO, C.; BUENO, J. L. Limiting diffusion coefficients of ethyl benzoate, benzylacetone, and eugenol in carbon dioxide at supercritical conditions. Journal of Chemical & Engineering Data, v. 53, n. 3, p. 779–784, 1 mar. 2008.

SUNG, S.-Y.; SIN, L. T.; TEE, T.-T.; BEE, S.-T.; RAHMAT, A. R.; RAHMAN, W. A. W. A.; TAN, A.-C.; VIKHRAMAN, M. Antimicrobial agents for food packaging applications. Trends in Food Science & Technology, v. 33, n. 2, p. 110–123, out. 2013.

SUPPAKUL, P.; MILTZ, J.; SONNEVELD, K.; BIGGER, S. W. Active packaging technologies with an emphasis on antimicrobial packaging and its applications. Journal of Food Science, v. 38, n. 2, p. 408–420, 2003.

SUPPAKUL, P.; SONNEVELD, K.; BIGGER, S. W.; MILTZ, J. Diffusion of linalool and methylchavicol from polyethylene-based antimicrobial packaging films. LWT - Food Science and Technology, v. 44, n. 9, p. 1888–1893, nov. 2011.

TEIXEIRA, B.; MARQUES, A.; PIRES, C.; RAMOS, C.; BATISTA, I.; SARAIVA, J. A.; NUNES, M. L. Characterization of fish protein films incorporated with essential oils of clove, garlic and origanum: Physical, antioxidant and antibacterial properties. LWT - Food Science and Technology, v. 59, n. 1, p. 533–539, nov. 2014.

TOMASKO, D. L.; LI, H.; LIU, D.; HAN, X.; WINGERT, M. J.; LEE, L. J.; KOELLING, K. W. A review of CO2 applications in the processing of polymers.

Industrial & Engineering Chemistry Research, v. 42, n. 25, p. 6431–6456, 1 dez. 2003.

TORLAK, E.; NIZAMLIOĞLU, M. Antimicrobial Effectiveness of Chitosan-Essential Oil Coated Plastic Films against Foodborne Pathogens. Journal of Plastic Film and Sheeting, v. 27, n. 3, p. 235–248, 1 jul. 2011.

TORRES, A.; ILABACA, E.; ROJAS, A.; RODRÍGUEZ, F.; GALOTTO, M. J.; GUARDA, A.; VILLEGAS, C.; ROMERO, J. Effect of processing conditions on the physical, chemical and transport properties of polylactic acid films containing thymol incorporated by supercritical impregnation. European Polymer Journal, v. 89, p. 195–210, abr. 2017.

TORRES, A.; ROMERO, J.; MACAN, A.; GUARDA, A.; GALOTTO, M. J. Near critical and supercritical impregnation and kinetic release of thymol in LLDPE films used for food packaging. The Journal of Supercritical Fluids, v. 85, p. 41–48, jan. 2014.

TUREK, C.; STINTZING, F. C. Stability of Essential Oils: A Review. Comprehensive Reviews in Food Science and Food Safety, v. 12, n. 1, p. 40–53, 1 jan. 2013.

VAN ROON, A.; PARSONS, J. R.; TE KLOEZE, A.-M.; GOVERS, H. A. J. Fate and transport of monoterpenes through soils. Part I: prediction of temperature dependent soil fate model input-parameters. Chemosphere, v. 61, n. 5, p. 599–609, 1 nov. 2005.

VARONA, S.; RODRÍGUEZ-ROJO, S.; MARTÍN, Á.; COCERO, M. J.; DUARTE, C. M. M. Supercritical impregnation of lavandin (Lavandula hybrida) essential oil in modified starch. The Journal of Supercritical Fluids, v. 58, n. 2, p. 313–319, set. 2011.

VARTIAINEN, J.; SKYTTA, E.; AHVENAINEN-RANTALA, R.; ENQVIST, J. Antimicrobial and Barrier Properties of LDPE Films Containing Imazalil and EDTA. Journal of Plastic Film and Sheeting, v. 19, n. 4, p. 249–261, 1 out. 2003.

VITRAC, O.; MOUGHARBEL, A.; FEIGENBAUM, A. Interfacial mass transport properties which control the migration of packaging constituents into foodstuffs. Journal of Food Engineering, v. 79, n. 3, p. 1048–1064, 1 abr. 2007.

WANG, L.; LIU, F.; JIANG, Y.; CHAI, Z.; LI, P.; CHENG, Y.; JING, H.; LENG, X. Synergistic antimicrobial activities of natural essential oils with chitosan films. Journal of Agricultural and Food Chemistry, v. 59, n. 23, p. 12411–12419, 14 dez. 2011.

WATTANANAWINRAT, K.; THREEPOPNATKUL, P.; KULSETTHANCHALEE, C. Morphological and thermal properties of LDPE/EVA blended films and development of antimicrobial activity in food packaging film. Energy Procedia, 11th Eco-Energy and Materials Science and Engineering (11th EMSES). v. 56, p. 1–9, 2014.

WENG, Y.-M.; HOTCHKISS, J. H. Anhydrides as Antimycotic Agents Added to Polyethylene Films for Food Packaging. Packaging Technology and Science, v. 6, n. 3, p. 123–128, 1 maio 1993.

WHO. Food safety and foodborne illness. World Health Organization - Fact sheet N° 237, 2007.

WRIGHT, B. W.; FULTON, J. L.; KOPRIVA, A. J.; SMITH, R. D. Analytical supercritical fluid extraction methodologies. In: Supercritical fluid extraction and chromatography. ACS Symposium Series. [s.l.] American Chemical Society, 1988. 366p. 44–62.

YAÑEZ, F.; MARTIKAINEN, L.; BRAGA, M. E. M.; ALVAREZ-LORENZO, C.; CONCHEIRO, A.; DUARTE, C. M. M.; GIL, M. H.; DE SOUSA, H. C. Supercritical fluid-assisted preparation of imprinted contact lenses for drug delivery. Acta Biomaterialia, v. 7, n. 3, p. 1019–1030, 1 mar. 2011.

YOKOZAKI, Y.; SAKABE, J.; NG, B.; SHIMOYAMA, Y. Effect of temperature, pressure and depressurization rate on release profile of salicylic acid from contact lenses prepared by supercritical carbon dioxide impregnation. Chemical Engineering Research and Design, v. 100, p. 89–94, ago. 2015.

ZHANG, N.; GIVEN, P. S. Releasably encapsulated aroma, 7 mar. 2013. Disponível em: <http://www.google.tl/patents/WO2013032631A1>.

ZIANI, K.; BARISH, J. A.; MCCLEMENTS, D. J.; GODDARD, J. M. Manipulating interactions between functional colloidal particles and polyethylene surfaces using interfacial engineering. Journal of Colloid and Interface Science, v. 360, n. 1, p. 31–38, 1 ago. 2011.

Appendix A: Complementary data and discussion

This chapter addresses a general discussion of employed methods in this study, including complementary data that were not presented in Chapters 3 and 4.

A.1 Film formation

In this study, pellets of LLDPE were compression-molded to produce transparent, flexible and homogeneous films without trapped air bubbles. A polyester film of 250 μm thickness was used as a frame for producing films with 300 μm average thickness. This frame was sandwiched between two sheets of polyester films (15 x 20 cm) to avoid adhesion of melted LLDPE pellets to the heated platen press, as schematized in Figure A.1. The advantage of using thicker films in comparison with commercial samples, which are usually thinner, is the ability to enhance the active compound incorporation, increasing the accuracy of analytical measurements to quantify the CEO impregnation in LLDPE films.

Figure A.1. Scheme of compression molding of polymeric films.

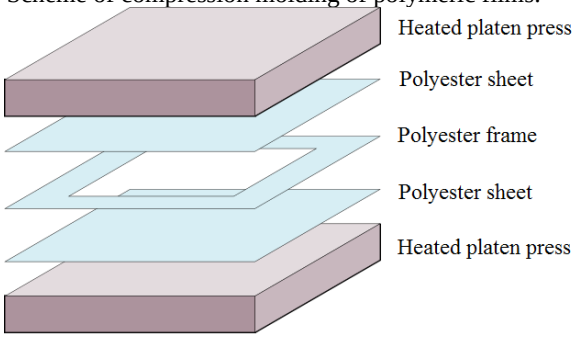

A.2 Thermophysical properties of eugenol, CO_2 and their mixture

The CEO is a multicomponent active agent naturally rich in eugenol. The thermophysical properties of eugenol (major component of CEO), CO_2 and the mixture eugenol:CO_2 in the two mass ratio used in this study are presented in Table A.1. The thermophysical properties of pure components (eugenol and CO_2), including P_C and T_C, were obtained from phase equilibrium data reported by Cheng et al. (2000) and Souza et

al. (2004). The pseudocritical pressure (P_{Cm}) and pseudocritical temperature (T_{Cm}) of the mixture eugenol:CO_2 in the two mass ratio, with equivalence of CEO:CO_2 mixtures at 2 and 10%, were calculated using a simple mole fraction average, also called Kay's mixing rule, shown in Equations A.1 and A.2 (REID; PRAUSNITZ; POLING, 1987).

$$P_{Cm} = \sum_i x_i P_{C,i} \quad \text{(A.1)}$$

$$T_{Cm} = \sum_i x_i T_{C,i} \quad \text{(A.2)}$$

in which x_i is the mole fraction of each pure component, $P_{C,i}$ and $T_{C,i}$ represents critical pressure and critical temperature of pure components, respectively. Values of pseudocritical properties for the mixture eugenol:CO_2 are very close to the values of CO_2 critical properties, as CO_2 is major component in the mixture. The use of Equation A.1 is satisfactory when components have similar critical pressures. Differences between T_{Cm} values from Equation A.2 with values from more complex mixing rules are of approximately 2% (REID; PRAUSNITZ; POLING, 1987). Therefore, Equation A.2 is considered suitable for this study.

Table A.1. Thermophysical properties of pure components (eugenol and CO_2)[1] and their mixtures equivalent to 2 and 10% CEO:CO_2 mass ratio.

	Mass fraction	MW (kg kmol^{-1})	Mole fraction	P_C (bar)	T_C (°C)
Eugenol	0.02	164.2	0.005	41.05	505.55
CO_2	0.98	44.01	0.995	73.82	31.04
Mixture eug:CO_2	1	-	1	73.64	33.62
Eugenol	0.10	164.2	0.029	41.05	505.55
CO_2	0.90	44.01	0.971	73.82	31.04
Mixture eug:CO_2	1	-	1	72.87	44.76

[1] Cheng et al. (2000) and Souza et al. (2004).

A.3 Retention of CEO in LLDPE films after 1 year of storage

After 1 year of storage, the mass of LLDPE samples produced in Chapter 3 (stored at -18 °C) were measured in an analytical balance (AUY 220, Shimadzu, Philippines, ± 0.0001 g accuracy) and results are listed in Table A.2. The differences between initial and final masses of films varied from 0.0001 to 0.0009 g, suggesting that the process of high-pressure impregnation is stable and the CEO remains incorporated in LLDPE films when stored at these conditions.

Table A.2. Impregnated mass of CEO in LLDPE films under different operational conditions of P, T and CEO:CO_2 mass ratio after 1 year of storage.

P (bar)	T (°C)	Mass ratio (%)	Initial mass of impregnated film (mg g^{-1})	Mass of film after 1 year (mg g^{-1})
150	25	2	0.2898	0.2897
250			0.2757	0.2755
150	35		0.2752	0.2748
250			0.3158	0.3156
150	45		0.2927	0.2919
250			0.2799	0.2794
150	25	10	0.2900	0.2898
250			0.2901	0.2898
150	35		0.2825	0.2817
250			0.2922	0.2921
150	45		0.2834	0.2829
250			0.2905	0.2896

A.4 Isochoric data of the system

For impregnation experiments, the high-pressure cell was loaded with 15 g of CO_2 for both experiments: without the active agent (pure CO_2) or the mixture of CEO and CO_2 in two different proportions (2 or 10%). The cell has a total volume of 24.95 mL, considering the volume of cell + tubing (Table A.6 in Appendix B.3). Then, dividing the total mass by the total volume of the system, the mass to volume ratio becomes equal to 0.6012 g mL^{-1}. Figure A.2 shows the pressure versus temperature diagram of pure CO_2 for isochoric data (specific mass at constant volume) at 0.6012 g mL^{-1}, showing the phase transitions of the system from 25 to 45 °C.

Figure A.2. P *x* T diagram of CO_2 for isochoric data at 0.6012 g mL^{-1}.

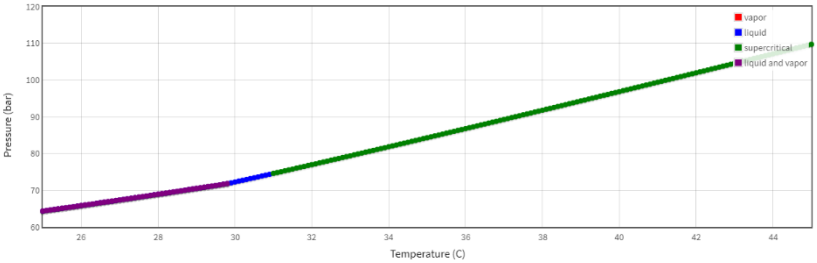

Source: NIST Chemistry Webbook (LEMMON; MCLINDEN; FRIEND, 2001).

The values of pressure for each temperature used in this study are presented in Table A.3. The variation of pressure inside the high-pressure cell is caused by a variation of its internal volume. This volume variation is consequence of piston displacement inside the cell, which in turn is controlled by the syringe pump once the back valve is opened (NV3, Figures A.8 and A.9 in Appendix B). Experiments with controlled depressurization rate presented in Chapter 4 were performed by the syringe pump operation. The system depressurization initiates by reducing the pressure of apparatus tubing, causing the displacement of cell piston until its original position, at the back of high-pressure cell. The content of high-pressure cell is still pressurized at a pressure that depends on system temperature, as exemplified in Table A.3. The cell content needs to be directly connected to the syringe pump by means of feed valve (NV2, Figures A.8 and A.9 in Appendix B) until reaching the atmospheric pressure to reduce the cell inner pressure in a controlled manner. The detailed procedure of apparatus operation in pressurization and depressurization modes is described in Appendices B.1, B.2 and B.3.

Table A.3. Values of temperature, pressure and physical state of system containing pure CO_2 for isochoric data at 0.6012 and 0.3006 g mL^{-1}.

T (°C)	0.6012 (g mL^{-1})		0.3006 (g mL^{-1})	
	P (bar)	Physical state	P (bar)	Physical State
25	64.34	VL	64.34	VL
32	76.98	SCF	73.51	V
35	84.31	SCF	76.67	SCF
45	109.73	SCF	86.88	SCF

Source: NIST Chemistry Webbook (LEMMON; MCLINDEN; FRIEND, 2001).

At the second step of depressurization, that is, when the cell is directly connected to the syringe pump (by means of NV2 aperture), the vapor phase of the cell must contain only CO_2 to be pumped back to the syringe pump, since this equipment operates exclusively with pure CO_2. When the cell is loaded with a total mass of 15 g, giving a mass to volume ratio equal to 0.6012 g mL^{-1}, the system is in the supercritical state at all temperatures covered in this study, except at 25 °C (Table A.3), thus hindering the direct connection of the cell to the syringe pump due to a fraction of CEO that remains solubilized in SC-CO_2. On the other hand, when the cell is loaded with half of its initial content, that is, with 7.5 g of total mass, the new mass to volume ratio is equal to 0.3006 g mL^{-1}. Figure A.3 presents the pressure versus temperature diagram of pure CO_2 for isochoric data at 0.3006 g mL^{-1} with the phase transitions of the system from 25 to 45 °C. The values of pressure for each temperature are listed in Table A.3.

Figure A.3. P *x* T diagram of CO_2 for isochoric data at 0.3006 g mL^{-1}.

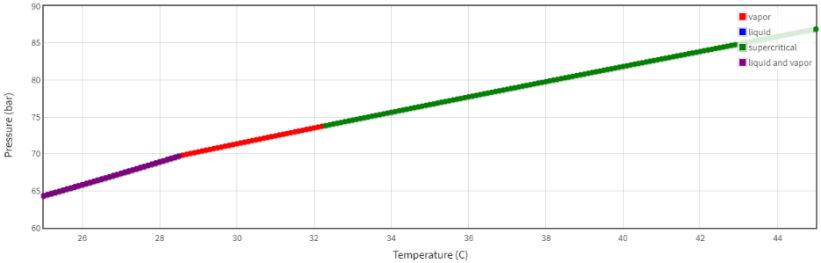

Source: NIST Chemistry Webbook (LEMMON; MCLINDEN; FRIEND, 2001).

The high-pressure cell was loaded with 7.5 g of total mass at the temperature of 32 °C to evaluate the effect of controlled depressurization from supercritical to atmospheric pressure on mechanical and surface properties of impregnated samples. At this temperature, the system is in vapor state (Table A.3), thus allowing the direct cell connection to the syringe pump, once the CEO is not soluble in gaseous CO_2. It is important to note that the amount of CEO in equilibrium with CO_2 after 50% reduction of total mass in the cell reduced from 9.97% to 9.90%, a small variation that is not expected to affect the impregnated amount of CEO in LLDPE film as well as the sensitivity of measurements.

The system depressurization with 50% of its initial content, considering an operation with pure CO_2, from 150 bar to the atmospheric pressure at temperatures of 25 and 32 °C is schematized in Figures A.4 and A.5. The pressure-temperature phase diagram of pure CO_2 (Figure

A.6) also shows the system phase transitions during depressurization at constant temperatures of 25 and 32 °C.

Figure A.4. Isothermal data of CO_2 at 25 °C from 150 bar to atmospheric pressure.

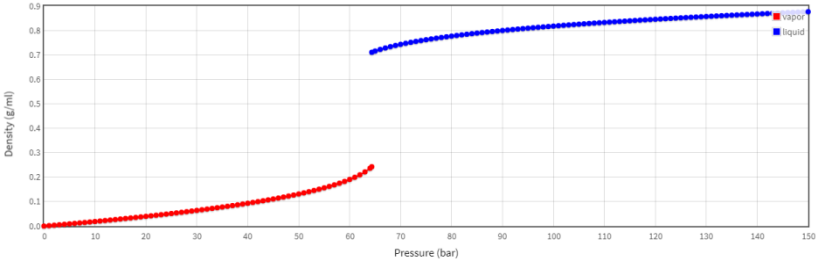

Source: NIST Chemistry Webbook (LEMMON; MCLINDEN; FRIEND, 2001).

Figure A.5. Isothermal data of CO_2 at 32 °C from 150 bar to atmospheric pressure.

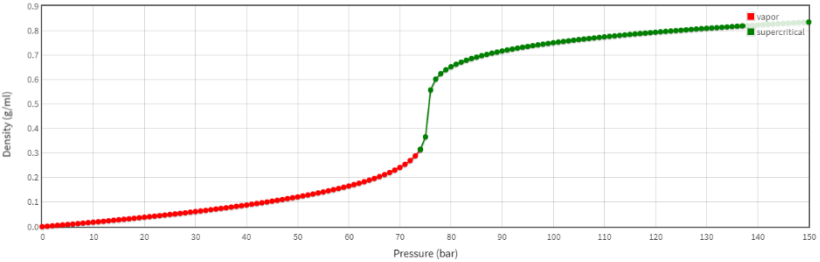

Source: NIST Chemistry Webbook (LEMMON; MCLINDEN; FRIEND, 2001).

Figure A.6. Pressure-temperature diagram of CO_2 with the respective phases during system depressurization at 25 and 32 °C.

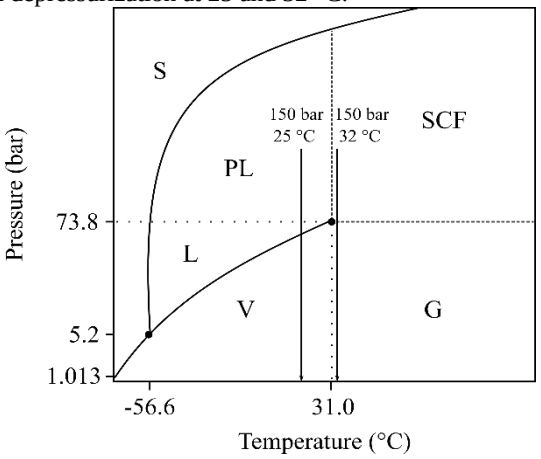

At 25 °C and 150 bar, the system is in the region of pressurized liquid, as $T < T_C$ and $P > P_C$ of CO_2. The pressure is gradually reduced at constant temperature until reaching the two-phase boundary line (liquid and vapor in equilibrium), in which the CO_2 in liquid and vapor state coexist at constant pressure and temperature. With further pressure reduction, the remaining CO_2 in liquid phase is converted to vapor phase up to the atmospheric pressure (Figures A.4 and A.6). On the other hand, at 32 °C and 150 bar the system is in the supercritical region, as $T > T_C$ and $P > P_C$ of CO_2. As the system undergoes a pressure reduction at constant temperature, the supercritical CO_2 is decompressed to the gaseous state without visible change of phases (Figures A.5 and A.6). Therefore, this study evaluated a depressurization with phase transition (from liquid to vapor phase, at 25 °C) and without phase transition (from supercritical to gas phase, at 32 °C), as presented in Chapter 4.

A.5 Calculation of depressurization time

Figure A.7 schematizes the pressure variation as function of time during pressurization from atmospheric pressure to 150 bar, the constant pressure during an experimental time of 2 hours, and the depressurization until atmospheric pressure. It compares the depressurization time of results from Chapter 3 (no depressurization control) with those from Chapter 4 (10, 50 and 100 bar min^{-1}). From Table A.4, the required time to depressurize the system at maximum depressurization rate, 100 bar min^{-1}, is very similar to the condition of no control, completed in less than 2 minutes.

Figure A.7. Variation of pressure versus time during pressurization and depressurization of high-pressure cell at different rates.

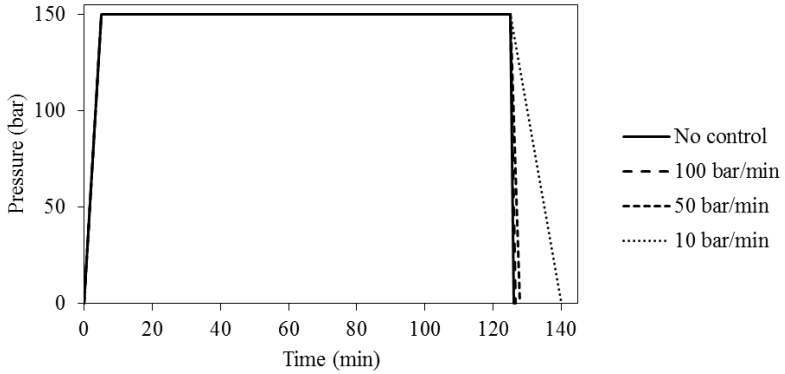

Table A.4. Time for depressurization from 150 bar to atmospheric pressure at different rates.

Depressurization rate (bar min^{-1})	Time (min)
No control	1
100	1.5
50	3
10	15

A.6 Impregnation efficiency of CEO-LLDPE films

The impregnation efficiency of experiments in Chapter 3 ranged from 45 to 47% (with 2% CEO:CO_2 mass ratio) and from 15 to 16% (with 10% CEO:CO_2 mass ratio). These mass ratios represent a proportion of CEO to LLDPE of 1:1 and 5:1. The impregnation efficiency (I%) is a relative measurement between the mass of impregnated film in relation to the initial sum of masses of film and CEO loaded in the cell ($m_{CEO,i}$, g). The impregnation efficiency was calculated according to Equation A.3.

$$I\% = \frac{m_{F,imp}}{m_{F,i} + m_{CEO,i}} \quad \text{(A.3)}$$

Experiments in Chapter 4, performed with 10% CEO:CO_2 mass ratio, presented values of impregnation efficiency between 12 and 16% (at temperature of 25 °C) and 28 to 29% (at temperature of 32 °C), as consequence of 50% reduction of total mass loaded in the high-pressure cell.

Appendix B: Experimental apparatus for high-pressure impregnation

This section describes additional information about the experimental apparatus located at LATESC as well as its operation for high-pressure impregnations. The apparatus was constructed to determine the phase equilibrium of different systems at high-pressure conditions and the present study proposed its adaptation and use for impregnation purposes. The construction and cell dimensioning of the apparatus were detailed by Comim (2012) and based on studies reported by Dariva (2000) and Lanza (2004). Table A.5 presents symbols and descriptions of valves in the experimental apparatus. These valves are also represented in Figures A.8 and A.9.

Table A.5. Description of valves used in experimental apparatus.

Symbol	Description
CV	Check valve
BV	Ball valve to isolate experimental apparatus from syringe pump
NV1	Needle valve for CO_2 load in syringe pump
NV2	Needle valve for CO_2 load in high-pressure cell (feed valve of cell)
NV3	Needle valve for pressurization of high-pressure cell using CO_2 as pneumatic fluid for displacement of cell piston (back valve of cell)
NV4	Needle valve for discharge of CO_2

Figure A.8. Schematic representation of experimental apparatus with pressure transducer connected to apparatus tubing.

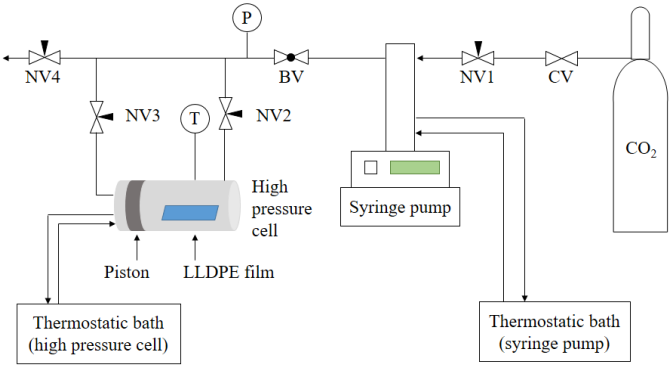

Figure A.9. Experimental apparatus with pressure transducer connected to apparatus tubing.

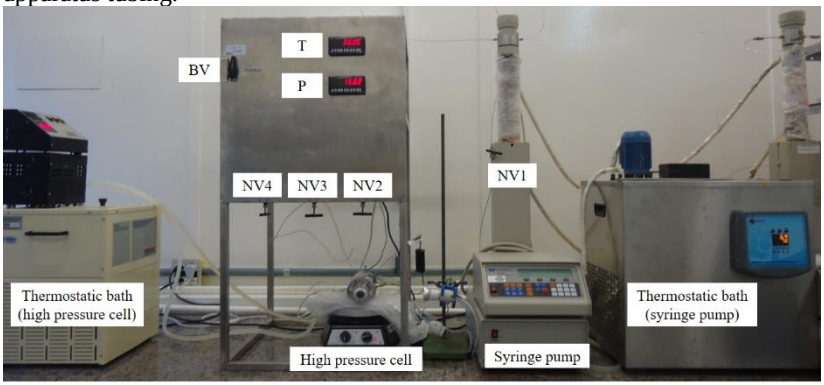

B.1 Experimental procedure for impregnation

1. Set thermostatic bath of syringe pump at 7 °C and the thermostatic bath of high-pressure cell at the temperature of operation;
2. Close the valves NV1, NV2, NV3, NV4 and BV;
3. Open CO_2 cylinder;
4. Open the NV1 to load CO_2 in syringe pump;
5. Close the CO_2 cylinder and NV1;
6. Open the BV and program the syringe pump to 100 bar;

7. Assemble the high-pressure cell initiating by cell piston adjustment. Insert the LLDPE film and the stirring bar, and finalize with the sapphire window;
8. Load the CEO in the high-pressure cell through the thermocouple connector using a syringe with needle;
9. Connect the front tubing (after NV2) and thermocouple to the cell;
10. Load the CO_2 in the high-pressure cell by opening the NV2, maintaining the CO_2 flow rate between 2 and 5 mL min^{-1};
11. Close NV2 and reduce the pressure of tubing by programming the syringe pump to 50 bar;
12. Stop the syringe pump and close BV;
13. Connect the back tubing (after NV3) to the cell and open NV3 and BV;
14. Connect the thermostatic bath to the high-pressure cell and initiate the magnetic stirring;
15. After reaching the temperature, program the syringe pump at the pressure operation;
16. Initiate counting the impregnation time.

The pressurization of cell occurs through displacement of piston. The depressurization of cell can be done with or without control of depressurization rate by means of syringe pump operation, as described in the following.

B.2 Experimental procedure for system depressurization (without control of depressurization rate)

1. Program the syringe pump to 50 bar. In this step, the piston returns to its initial position;
2. Stop the syringe pump and close BV;
3. Open NV4 to discharge CO_2 from tubing;
4. Disconnect the back tubing (after NV3) from the cell;
5. Disconnect the front tubing (after NV2) and thermocouple from the cell to remove the CO_2 contained into the cell until reaching atmospheric pressure;
6. Disconnect the thermostatic bath;
7. Open the cell and recover the CEO-impregnated LLDPE film;
8. Open BV and NV1 while keeping NV4 opened to discharge the CO_2 remaining on syringe pump and tubing.

B.3 Experimental procedure for system depressurization (with control of depressurization rate)

1. Program the syringe pump to 50 bar with a gradient of depressurization. In this step, the piston returns to its initial position;
2. Stop the syringe pump and close BV;
3. Open NV4 to discharge CO_2 from tubing;
4. Disconnect the back tubing (after NV3) from the cell and close NV3 and NV4;
5. Open BV and program the syringe pump to equilibrate with inner pressure of cell: 64 bar (for experiments at 25 °C) and 72 bar (for experiments at 32 °C), below the P_C of mixture CEO:CO_2 at 10% mass ratio (Appendix A.2);
6. Open NV2 and after reaching pressure equilibrium, program the syringe pump to 1 bar maintaining the same gradient of depressurization;
7. If the cylinder of syringe pump be full of CO_2, the pump stops depressurization. Then, close NV2 and open NV4 to discharge CO_2 of syringe pump. Close NV4 and reprogram the pump until the recorded pressure when the NV2 was closed to equilibrate with the new inner pressure of cell. Repeat steps #6 and #7, if necessary, until reaching atmospheric pressure;
8. Open NV4 to remove any CO_2 remaining on tubing;
9. Disconnect the front tubing (after NV2) and thermocouple from the cell;
10. Disconnect the thermostatic bath;
11. Open the cell and recover the CEO-impregnated LLDPE film;
12. Open NV1 while keeping NV4 opened to discharge the CO_2 remaining on syringe pump and tubing.

During impregnation experiments, the pressure transducer is connected to the apparatus tubing (Figure A.8) and shows the pressure of the system from the syringe pump to the valves. In this configuration, it is not possible to known the exact inner pressure of the cell. The pressure transducer was then connected to the cell after NV2 in order to determine the inner pressure of the cell, as presented in Figures A.10, A.11 and A.12.

Figure A.10. Schematic representation of experimental apparatus with pressure transducer connected to the high-pressure cell.

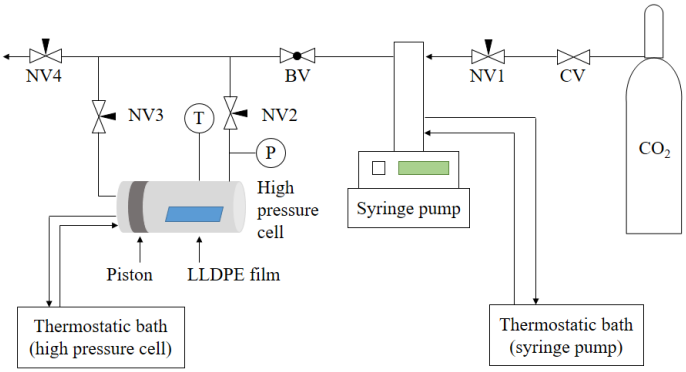

Figure A.11. Experimental apparatus with pressure transducer connected to the high-pressure cell.

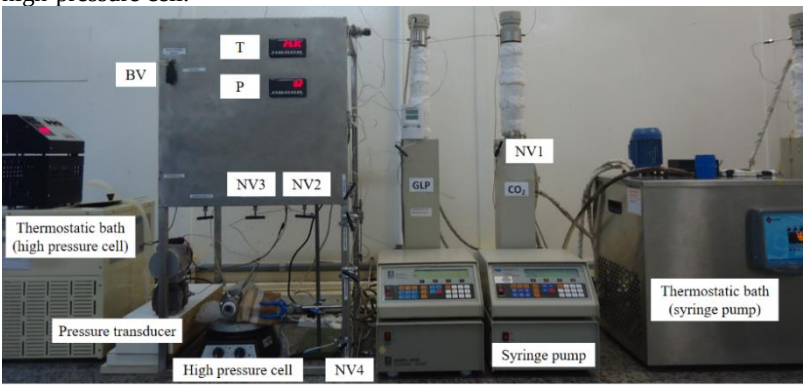

Figure A.12. Pressure transducer connected to the high-pressure cell.

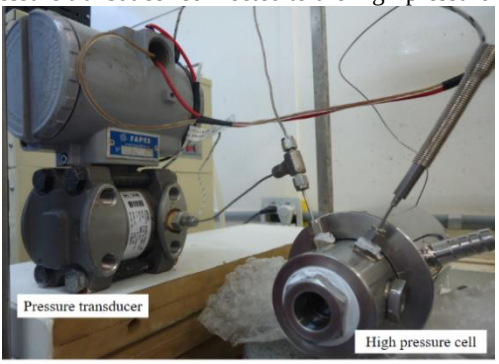

The equivalence between the measured values of pressure of transducer and syringe pump during pressurization/depressurization of the system by means of piston displacement (with back valve opened, NV3) is shown in Figure A.14 and Table A.7 (Appendix C.2). These values are important, for example, in the first part of controlled depressurization, before disconnecting the back tubing from the cell. Additionally, the equivalence between measurements of pressure by transducer and syringe pump during pressurization through CO_2 loading in high-pressure cell (with feed valve opened, NV2), without displacement of piston that remains fixed in its initial state, is presented in Figure A.15 and Table A.8 (Appendix C.3). These values are important in the second part of controlled depressurization, when the cell is directly connected to the syringe pump.

Table A.6 lists the values of measured volumes of high-pressure cell, pressure transducer and tubing that integrate the experimental apparatus (from syringe pump to cell connector of CO_2 loading), considering the two configurations of pressure transducer. It can be noted that the connection of pressure transducer to the cell increased approximately 53% of the initial volume of the system, which makes infeasible the impregnation experiments with this type of configuration. The pressure transducer has an internal membrane (mobile diaphragm filled with silicon oil), which dead volume represents over half of the cell volume. For this reason, impregnation experiments were performed with the pressure transducer connected to the apparatus tubing.

Table A.6. Measured volumes of high-pressure cell, pressure transducer and tubing of experimental apparatus.

Description (unit)	Value
1/4 in. tubes	
Wall thickness[1] (mm)	0.889
External diameter (mm)	6.40
Internal diameter[2] (mm)	4.62
1/16 in. tubes	
Wall thickness[1] (mm)	0.254
External diameter (mm)	1.50
Internal diameter[2] (mm)	0.99
Volume of tubing from syringe pump to NV2 (mL)	4.62
High-pressure cell	
Internal volume (mL)	24.55
Dead volume of cell from sapphire window to the thermocouple (mL)	3.74
Volume of tubing from NV2 to cell connector (mL)	0.40
Volume of system cell + tubing (mL)	24.95
Pressure transducer	
Internal volume (mL)	13.23
Volume of tubing from transducer to tee union and cell connector (mL)	0.10
Volume of system cell + transducer + tubing (mL)	38.28

[1] According to Swagelok specifications.
[2] Internal diameter = External diameter – (2 x wall thickness).

References

COMIM, S. R. R. Produção enzimática de poli(ε-caprolactona) em fluidos pressurizados. Tese de doutorado em Engenharia de Alimentos – Florianópolis: Universidade Federal de Santa Catarina, 2012.

DARIVA, C. Equilíbrio de fases a altas pressões em sistemas com polipropilenos: dados experimentais e modelagem SAFT. Tese de doutorado em Engenharia Química – Rio de Janeiro: Universidade Federal do Rio de Janeiro, 2000.

LANZA, M. Comportamento de fases dos óleos de oliva, soja e mamona em n-butano e propano a alta pressão. Dissertação de mestrado em Engenharia de Alimentos – Erechim: Universidade Regional Integrada do Alto Uruguai e das Missões, 2004.

Appendix C – Calibration curves

C.1 Calibration curve of thermocouple J type

Measurements for calibration of thermocouple J type were performed with distilled water using a calibrated mercury thermometer. Results are shown in Figure A.13.

Thermocouple J type: Salcas, Brazil.
Mercury thermometer: 135907/10, Incoterm, Brazil.
Thermostatic water bath: MQBTC99-20, Microquímica, Brazil.
Temperature range: 20 to 50 °C.
Heating rate: 0.25 °C min^{-1}.
Stabilization time for measurements: 10 min.

Figure A.13. Calibration curve of thermocouple J type.

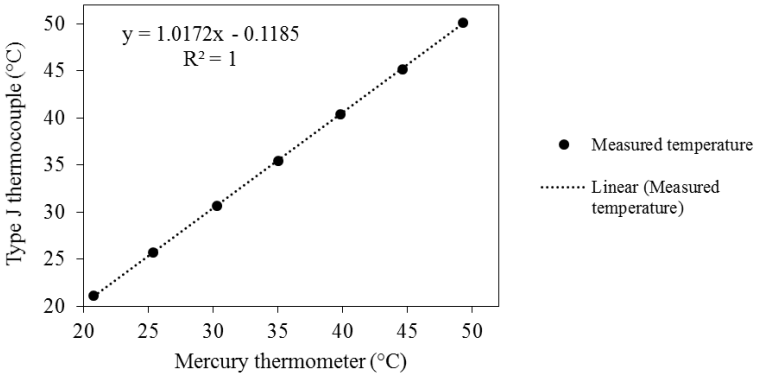

C.2 Equivalence between pressures measured by transducer and syringe pump during displacement of cell piston

The pressure transducer was connected to the cell and measurements were performed during displacement of cell piston with back valve of high-pressure cell (NV3, Figures A.8 and A.9 in Appendix B) opened. The pressure measured by transducer represents the inner pressure of the cell. The displacement of cell piston initiates at pressures above 50 bar. During pressurization, the pressure measured by the syringe pump is higher than the pressure measured by the transducer, possibly due to dissipative forces caused by piston displacement. In depressurization, the opposite effect is observed (Figure A.14). Values of measured experimental points are presented in Table A.7.

Pressure transducer: LD301, Smar, Brazil.
Syringe pump: 260HP, Teledyne Isco, USA.
Volume of CO_2 loaded in the system (cell + transducer): 23 mL.
Temperature of the cell: 25 °C.
Pressure range: 50 to 250 bar.
Pressurization/depressurization rate: 10 bar min^{-1}.
Stabilization time for measurements: 5 min.

Figure A.14. Equivalence between pressures measured by transducer and syringe pump during displacement of cell piston.

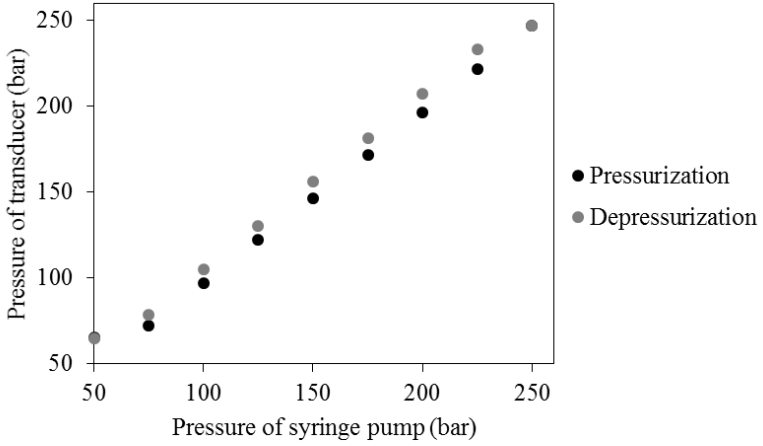

Table A.7. Pressure of transducer and syringe pump during pressurization and depressurization of the system.

Pressure of syringe pump (bar)	Pressure of transducer in pressurization (bar)	Pressure of transducer in depressurization (bar)
50	65.4	65.1
75	72.1	78.8
100	97.2	104.8
125	122.2	130.6
150	146.4	156.2
175	171.6	181.7
200	196.6	207.3
225	221.7	233.1
250	246.8	246.8

C.3 Equivalence between pressures measured by transducer and syringe pump without displacement of cell piston

The pressure transducer was connected to the cell and measurements were performed without displacement of cell piston with feed valve of high-pressure cell (NV2, Figures A.8 and A.9 in Appendix B) opened. The pressure measured by the transducer represents the inner pressure of the cell during pressurization and/or depressurization of the system, once the cell is directly connected to syringe pump by means of feed valve aperture (Figure A.15). For measurements, CO_2 was gradually loaded into the cell to reach the desired pressure. Table A.8 presents the values of measured experimental points.

Pressure transducer: LD301, Smar, Brazil.
Syringe pump: 260HP, Teledyne Isco, USA.
Temperature of the cell: 25 °C.
Pressure range: 0 to 120 bar.
CO_2 feed rate: 10 mL min^{-1}.
Stabilization time for measurements: 5 min.

Figure A.15. Equivalence between pressures measured by transducer and syringe pump without displacement of cell piston.

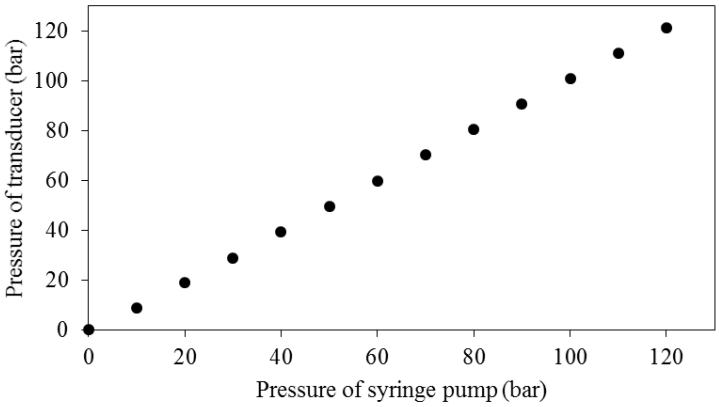

Table A.8. Pressure of transducer and syringe pump during CO_2 loading into the cell.

Pressure of syringe pump (bar)	Pressure of transducer (bar)
0	0.1
10	8.8
20	18.9
30	29.0
40	39.3
50	49.5
60	59.8
70	70.5
80	80.7
90	90.8
100	101.0
110	111.2
120	121.4

C.4 Wavelength scan of CEO and eugenol in aqueous solutions of ethanol 10%

The CEO and eugenol solutions presented maximum absorbance peak in UV region at 281 nm (Figure A.16). A good agreement between the peaks of CEO and eugenol, major compound of CEO, was observed. The absorbance peaks of β-caryophyllene and α-humulene were not detected from 200 to 900 nm. The solvent peaks were noticed below 250 nm. Theoretical and real concentrations of CEO and eugenol stock solutions (1 mg mL^{-1}) as well as their concentrations after dilution in aqueous solution of ethanol 10% (v/v) are listed in Table A.9.

UV-visible spectrophotometer: Q898U2M5, Quimis, Brazil.

Wavelength scan: 200 to 900 nm.

Figure A.16. Wavelength scan of CEO and eugenol in aqueous solutions of ethanol 10% (v/v) in UV-visible region.

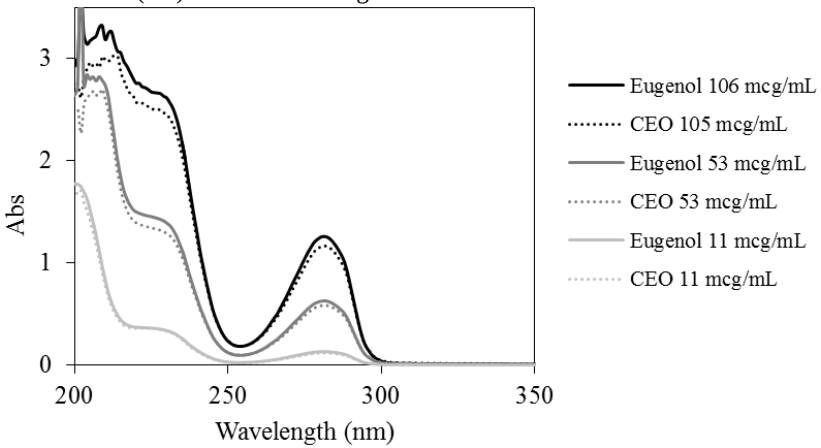

Table A.9. Theoretical and real concentrations of CEO and eugenol in aqueous solution of ethanol 10% (v/v).

Theoretical concentration ($\mu g\ mL^{-1}$)	Real concentration ($\mu g\ mL^{-1}$)	
	CEO	Eugenol
1000	1050	1060
100	105	106
50	53	53
10	11	11

C.5 Wavelength scan of CEO and eugenol in aqueous solutions of ethanol 95% (v/v)

The CEO and eugenol solutions presented maximum absorbance peak in UV region at 283 nm with good agreement between their peaks (Figure A.17). The differences in absorbance areas are related to the initial concentration of stock solutions, which values are shown in Table A.10. The absorbance peaks of β-caryophyllene and α-humulene were not detected from 200 to 900 nm. The solvent peaks were noticed below 250 nm.

UV-visible spectrophotometer: Q898U2M5, Quimis, Brazil.
Wavelength scan: 200 to 900 nm.

Figure A.17. Wavelength scan of CEO and eugenol in aqueous solutions of ethanol 95% (v/v) in UV-visible region.

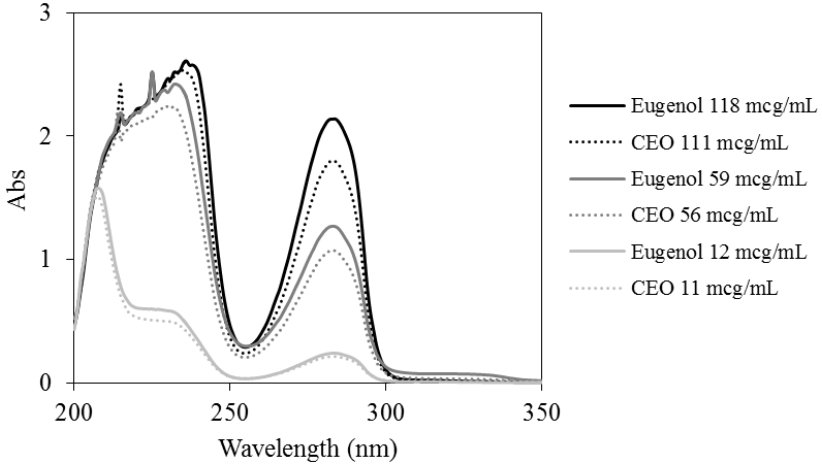

Table A.10. Theoretical and real concentrations of CEO and eugenol in aqueous solution of ethanol 95% (v/v).

Theoretical concentration ($\mu g\ mL^{-1}$)	Real concentration ($\mu g\ mL^{-1}$)	
	CEO	Eugenol
1000	1110	1180
100	111	118
50	56	59
10	11	12

C.6 Calibration curve of CEO in aqueous solution of ethanol 10% (v/v)

The calibration curve was performed with CEO stock solution in ethanol 10% (v/v) at concentration of 1050 µg mL^{-1} and results are shown in Figure A.18. Triplicate of dilutions using the same solvent ranged from 10 to 100 µg mL^{-1} with measurements at 281 nm.

UV-visible spectrophotometer: Q898U2M5, Quimis, Brazil.

Figure A.18. Calibration curve of CEO in aqueous solution of ethanol 10% (v/v).

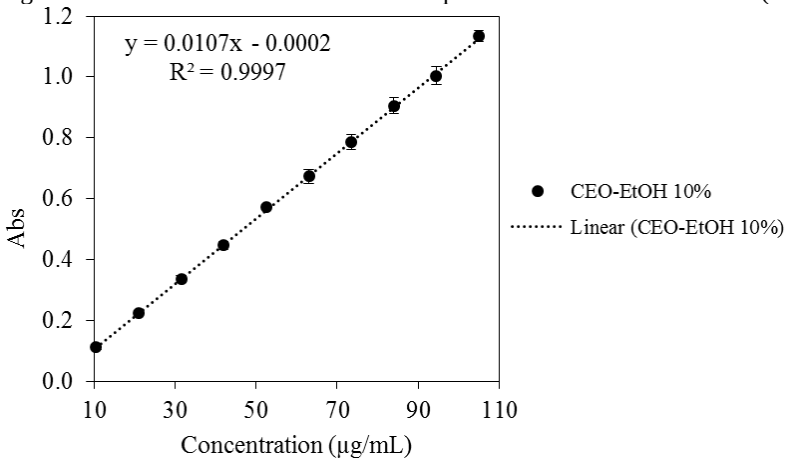

C.7 Calibration curve of CEO in aqueous solution of ethanol 95% (v/v)

The calibration curve was performed using CEO stock solution in ethanol 95% (v/v) at concentration of 1110 µg mL^{-1} and results are shown in Figure A.19. Triplicate of dilutions using the same solvent ranged from 5 to 50 µg mL^{-1} with measurements at 281 nm.

UV-visible spectrophotometer: Q898U2M5, Quimis, Brazil.

Figure A.19. Calibration curve of CEO in aqueous solution of ethanol 95% (v/v).

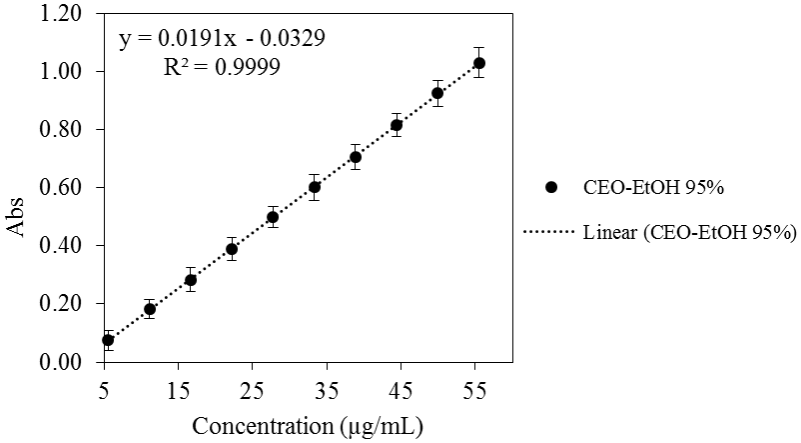

Annex – Technical information of CEO and LLDPE

FERQUIMA

LAUDO TÉCNICO

Óleo Essencial de Cravo Folha

(Eugenia caryophyllus)

Lote: 219	CAS Number: 8015-97-2
Fabricação: Junho/2014	Validade: Junho/2016

Ítens Controlados	Resultados	Especificações
Aparência	Líquido	Líquido
Cor	Amarelo	Amarelo Palha a Castanho
Impurezas	Isento	Isento
Odor	Típico - Spice	Típico - Spice
Densidade (20°C)	1,046	1,030 – 1,050
Índice de Refração (20°C)	1,536	1,520 – 1,540
Refração Ótica	-1,00°	[-2° ; 0°]
Data da Análise	21/08/2014	
Resultado	**Aprovado**	
Origem	Indonésia	
Principal componente (aprox)	Eugenol = 86 %	

Recomendações Especiais	
Manuseio	Perigos mínimos, máscara e luvas recomendável. Não ingerir. Evitar contato com a pele, olhos e mucosa. Se isso ocorrer, lavar imediatamente com água límpida em abundância. Pode causar irritação à pele sensível Em caso de derramamento, absorver o material derramado com material absorvente (areia, terra).
Incêndio	Caso haja fogo, utilizar extintor de pó químico seco e água em forma de neblina, não utilizando jatos de água para não espalhar o produto.
Explosividade	Nenhum perigo em condições normais.
Uso	Este produto destina-se ao uso industrial e como é elaborado a partir de substâncias naturais pode apresentar pequenas variações de cor e cromatografia sem causar qualquer problema na performance do produto.
Armazenamento	Armazenar em local seco, longe de umidade e do calor, protegido da luz , em recipiente original bem vedado. Não reutilizar a embalagem vazia.
Transporte	Produto não enquadrado na portaria 204/97 em vigor sobre transporte de produtos perigosos.

As informações contidas nesta publicação representam o melhor de nosso conhecimento. Entretanto, nada aqui mencionado deve ser entendido como garantia de uso. Os consumidores devem efetuar seus próprios ensaios para determinar a viabilidade da aplicação.

Engenheira Química Responsável: Alice Lasthaus CRQ: IV 04330754

Estrada Mineração Ouro Branco, 2017 • Vargem Grande. Paulista • SP • CEP: 06730-000
Tel.:**11.4159.1784 / 11.4158.3544** - Fax.:**11.4158.3420**
msn / e-mail: atendimento@ferquima.com.br
www.ferquima.com.br
FERQUIMA Ind. e Com. Ltda

Universidade Federal de Minas Gerais
Instituto de Ciências Exatas
Departamento de Química / Colegiado de Extensão
Telefax : (31) 3409-5724 – e-mail: núcleo@qui.ufmg.br

UFMG

CERTIFICADO DE ANÁLISE QUÍMICA

Solicitante: FERQUIMA IND. COM. LTDA. CNPJ: 51.699.205/0001-48

ÓLEO ESSENCIAL de CRAVO FOLHA

Nome comercial: Óleo Essencial de Cravo folha
Lote: 219 fab: jun/2014 val: jun/2016
Nomenclatura botânica: Eugenia caryophyllus
Extração: Destilação por arraste a vapor
Parte da planta: Folhas

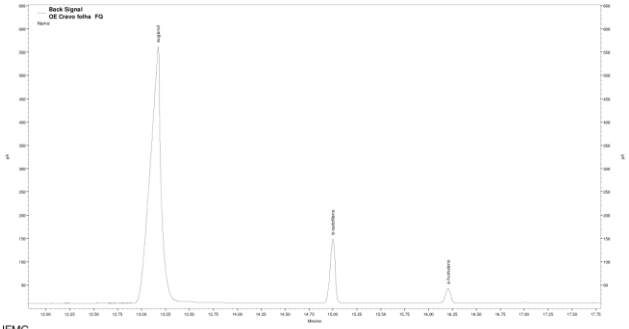

Composição Química

Pico	Constituinte ID	%
1	eugenol	86.1
2	β-cariofileno	9.8
3	α-humuleno	2.3

Dra. Vany Ferraz
Laboratório de Cromatografia
Departamento de Química – UFMG
vanyferraz@ufmg.br
Belo Horizonte, 13/06/2013

Método de análise:
Cromatografia Gasosa de Alta Resolução. Cromatógrafo a Gás AGILENT 7820A.
Coluna: HP-5 30m x 0,32mm x 0,25 µm (AGILENT). Temp.: Coluna: 70ºC (0min), 3ºC /min a 240ºC.
Injetor: 240ºC Split: 1/50. Detector FID: 250ºC. Vo l. de injeção: 1 ul (conc 1.0 % em clorofórmio)

Informação técnica

DOWLEX™ TG 2085B
Polyethylene Resin

Descrição geral

A Resina de Polietileno Linear de Baixa Densidade DOWLEX™ TG 2085B é produzida através do processo Solution. Esta resina oferece uma combinação exclusiva de excelentes propriedades mecânicas e ópticas, permitindo a redução de espessura com alta produtividade e velocidade.

Principais Características:

- Para aplicações de fina espessura e alta velocidade
- Laminação

Atende à:

- U.S. FDA 21 177 1520 (c) 3.2a

Consulte as regulamentações para obter mais detalhes.

Aditivo

- Antibloqueio: 2500 ppm
- Deslizamento: 1000 ppm
- Auxiliar de Processamento: No

Físicas	**Valor Típico**	**(Inglês)**	**Valor Típico**	**(Métrico)**	**Método**
Densidade	0,919	g/cm³	0,919	g/cm³	ASTM D792
Densidade base	0,918	g/cm³	0,918	g/cm³	Método Interno [1]
Índice de fusão (190°C/2,16 kg)	0,95	g/10 min	0,95	g/10 min	ASTM D1238
Filmes	**Valor Típico**	**(Inglês)**	**Valor Típico**	**(Métrico)**	**Método**
Espessura do filme	1,5	mil	38	µm	
Resistência à Perfuração (1,5 mil (38 µm))	109	ft·lb/in³	9,02	J/cm³	Método Interno
Módulo Secante					ASTM D882
2% Secante, DM : 1,5 mil (38 µm)	24700	psi	170	MPa	
2% Secante, DT : 1,5 mil (38 µm)	30500	psi	210	MPa	
Tensão					ASTM D882
DM : Limite de elasticidade, 1,5 mil (38 µm)	1450	psi	10,0	MPa	
DT : Limite de elasticidade, 1,5 mil (38 µm)	1450	psi	10,0	MPa	
DM : Na Ruptura, 1,5 mil (38 µm)	5370	psi	37,0	MPa	
DT : Na Ruptura, 1,5 mil (38 µm)	4640	psi	32,0	MPa	
Alongamento					ASTM D882
DM : Na Ruptura, 1,5 mil (38 µm)	830	%	830	%	
DT : Na Ruptura, 1,5 mil (38 µm)	990	%	990	%	
Resistência ao Impacto (1,5 mil (38 µm))	360	g	360	g	ASTM D1709A
Resistência ao Rasgo Elmendorf					ASTM D1922 [2]
DM : 1,5 mil (38 µm)	700	g	700	g	
DT : 1,5 mil (38 µm)	920	g	920	g	
Óticas	**Valor Típico**	**(Inglês)**	**Valor Típico**	**(Métrico)**	**Método**
Brilho (45°, 1,48 mil (37,5 µm))	57		57		ASTM D2457
Opacidade (1,48 mil (37,5 µm))	12	%	12	%	ASTM D1003

Extrusão	**Valor Típico**	**(Inglês)**	**Valor Típico**	**(Métrico)**
Temperatura de Massa	423	°F	217	°C

Formulário nº. 400-00084160pt
Rev: 2011-03-22

Notas sobre a extrusão

Condições de fabrico do filme soprado:

- Tamanho da rosca: 2,3 pol. (60 mm); L/D relação 32:1
- Abertura da matriz: 70 mil (1,8 mm)
- Temperatura de fusão: 423°F (217°C)
- Produção: 46,9 kg/h
- Diâmetro da matriz: 5,9 pol. (150 mm)
- Relação de sopro: 2.5:1
- Velocidade da rosca: 60 rpm
- Altura da linha de névoa: 19,7 pol. (50 cm)

Notas

Estas são apenas propriedades típicas e não devem ser consideradas como especificações. Os utilizadores devem confirmar os resultados efectuando os seus próprios testes.

[1] A densidade da base (do polímero) é estimada, usando a suposição de que cada 1000 ppm de Antiblock no produto acabado aumenta a densidade do polímero em 0,0006 g/cm3. A densidade da base é a densidade estimada do polímero, se ele não tiver nenhum Antiblock.

[2] Método B

Formulário nº. 400-00084160pt
Rev: 2011-03-22

Gerenciamento do Produto

A The Dow Chemical Company e suas subsidiárias (“Dow”) têm uma preocupação fundamental por todos os que produzem, distribuem e usam seus produtos, bem como pelo ambiente em que vivemos. Esta preocupação é a base de nossa filosofia de Gerenciamento do Produto, pela qual nós avaliamos as informações de segurança, saúde e meio ambiente de nossos produtos e, depois, tomamos as medidas apropriadas para proteger a saúde do funcionário e pública, assim como o nosso meio ambiente. O sucesso de nosso programa de Gerenciamento do Produto está com todas as pessoas envolvidas com os produtos da Dow — desde o conceito inicial e a pesquisa até a manufatura, uso, venda, disposição e reciclagem de cada produto.

Aviso ao Cliente

A Dow incentiva fortemente seus clientes a reverem tanto seus processos de manufatura como as aplicações dos produtos da Dow do ponto de vista da saúde humana e da qualidade do meio ambiente para assegurar que os produtos da Dow não sejam usados para o que não foram destinados ou testados. Os funcionários da Dow estão disponíveis para responder às perguntas e oferecer suporte técnico razoável. As literaturas de seus produtos, incluindo as fichas de informações de segurança de produtos químicos, devem ser consultadas antes que os produtos sejam usados. Estão disponíveis as atuais fichas de informação de segurança de produtos químicos da Dow.

Política de Aplicações Médicas

AVISO REFERENTE ÀS RESTRIÇÕES DE APLICAÇÕES MÉDICAS: A Dow não venderá ou fornecerá intencionalmente amostras de qualquer produto ou serviço (“Produto”) para qualquer aplicação comercial ou em desenvolvimento, que seja destinada para:

a. contato de longo prazo ou permanente com fluidos ou tecidos internos do corpo. “De longo prazo” é o contato que excede 72 horas contínuas ;
b. uso em próteses cardíacas, independentemente do espaço de tempo envolvido (as “próteses cardíacas” incluem, mas não estão limitadas a, cabos-eletrodo e aparelhos de marcapasso, corações artificiais, válvulas cardíacas, balão intra-aórtico e sistemas de controle, bem como dispositivos de assistência ventricular);
c. uso como componente crítico em dispositivos médicos que suportam ou sustentam a vida humana; ou
d. uso especificamente por mulheres grávidas ou em aplicações desenvolvidas especialmente para promover ou impedir a reprodução humana.

A Dow solicita que os clientes que estão considerando o uso de seus produtos em aplicações médicas, notifiquem a Dow para que possam ser conduzidas avaliações apropriadas.
A Dow não endossa ou reivindica a adequação de seus produtos para aplicações médicas específicas. É responsabilidade do fabricante de dispositivos médicos ou produtos farmacêuticos determinarem se o produto da Dow é seguro, legal e tecnicamente adequado para o uso pretendido. **A DOW NÃO OFERECE NENHUMA GARANTIA, QUER EXPRESSA OU IMPLÍCITA, REFERENTE À ADEQUAÇÃO DE QUALQUER DE SEUS PRODUTOS PARA USO EM APLICAÇÕES MÉDICAS.**

Termo de Responsabilidade

NOTA: Não serão inferidas exonerações de nenhuma patente de propriedade da Dow ou de qualquer outra empresa. Considerando-se que as condições de uso e leis aplicáveis poderem diferir de um local para outro, além de poderem sofrer alterações no decorrer do tempo, o Cliente é responsável por determinar se os produtos e as informações contidas nesse documento são apropriadas para seu uso, e garantir que seu local de trabalho e práticas de eliminação estejam em conformidade com as leis aplicáveis e outros decretos governamentais. A Dow não assume obrigações nem responsabilidades pelas informações contidas nesse documento. **NENHUMA GARANTIA É OFERECIDA POR MEIO DESTE; TODAS AS GARANTIAS IMPLÍCITAS DE COMERCIALIZAÇÃO OU ADEQUAÇÃO A UM FIM ESPECÍFICO FICAM EXPRESSAMENTE EXCLUÍDAS.**

NOTA: Se os produtos estiverem descritos como “experimentais” ou “em desenvolvimento”: (1) as especificações do produto podem não estar totalmente definidas; (2) são requeridos análise de riscos e cuidados no manuseio e uso; (3) há grande possibilidade de a Dow alterar as especificações e/ou suspender a produção; e (4) embora a Dow possa, de tempos em tempos, fornecer amostras desses produtos, ela não é obrigada a fornecer ou comercializar de outra forma tais produtos para qualquer uso ou aplicação, seja qual for.

Informações adicionais

América do Norte		**Europa/Oriente Médio**	+800-3694-6367
EUA e Canadá:	1-800-441-4369		+31-11567-2626
	1-989-832-1426	Itália:	+800-783-825
México:	+1-800-441-4369		
América Latina		**África do Sul**	+800-99-5078
Argentina:	+54-11-4319-0100		
Brasil:	+55-11-5188-9000		
Colômbia:	+57-1-219-6000	**Ásia/Pacífico**	+800-7776-7776
México:	+52-55-5201-4700		+603-7965-5392

www.dowplastics.com

Este documento é destinado para uso dentro da América Latina

Publicado em 2005-05-05

Formulário nº. 400-00084160pt
Rev: 2011-03-22